

General-order degenerate coupled-cluster theory

So Hirata^{a)}

Department of Chemistry, University of Illinois at Urbana-Champaign, Urbana, Illinois 61801,
United States

(Dated: 27 January 2026)

A size-extensive, converging, black-box coupled-cluster (Δ CC) ansatz is introduced that computes the energies and wave functions of stationary states from any degenerate or nondegenerate Slater-determinant references with any numbers of α - and β -spin electrons, any patterns of orbital occupancy, any spin multiplicities, and any spatial symmetries. For a nondegenerate determinant reference, it is identical to the single-reference, projection coupled-cluster ansatz. For degenerate determinant references, it is a natural coupled-cluster extension of degenerate Rayleigh–Schrödinger perturbation (Δ MP) theory, and is closely related to, but distinct from Li and Paldus’s state-universal multireference coupled-cluster (SUMRCC) theory. For ionized and electron-attached references, it can be viewed as a coupled-cluster Green’s function, although the present theory is convergent toward the full-configuration-interaction (FCI) limits, while Feynman–Dyson many-body Green’s function (MBGF) theory generally is not. Its single-excitation instance is a projection (nonvariational) Hartree–Fock theory for a degenerate or nondegenerate reference as per the Thouless theorem, whose practical utility seems rather limited except for core ionizations, high-spin states, and possibly electron affinities. A determinant-based, general-order algorithm is implemented, generating Δ CC energies through connected octuple excitations (Δ CCSDTQPHSO), which are compared with the results from configuration-interaction (CI), equation-of-motion coupled-cluster (EOM-CC), and SUMRCC theories up to the FCI limits as well as from Δ MP and MBGF theories up to the nineteenth order. An algebraic, optimal-scaling, order-by-order algorithm is also computer-synthesized at the levels of single excitations only (Δ CCS) and of single and double excitations (Δ CCSD). The order of performance is: Δ CC > EOM-CC > CI at the same order or Δ CC > Δ MP > MBGF at the same cost scaling.

I. INTRODUCTION

Single-reference coupled-cluster (CC) theory^{1–10} is widely regarded as the most accurate, generally applicable, size-extensive, black-box, *ab initio* method for solving the time-independent Schrödinger equations for atoms, molecules, and solids in their ground electronic states.

By “black-box,” we mean that the method requires no more than the atomic positions, number of electrons, and spin-multiplicity of a system as input and returns its unambiguous energy and wave function within the Born–Oppenheimer approximation. This is essentially the same definition of Pople’s Model Chemistry,¹¹ distinguishing its instances from those that are reserved for experts with inscrutable “chemical intuitions” in selecting multireferences, active orbitals, etc.

By “*ab initio*,” we insist on the use of the exact electronic Hamiltonian, guaranteeing the systematic convergence of the results toward the experimental data upon increasing the rank of the method and basis-set size (plus correcting for the relativistic and non-Born–Oppenheimer effects, if necessary). It imbues its instances with predictive power.^{12,13} This characteristic is not shared by empirical and semiempirical methods including density-function theory or by various machine-learning models. In fact, the latter are often parameterized by the results of high-rank CC calculations.

Since the development of its core member in 1982, i.e., coupled-cluster with connected single and double excitations (CCSD),¹⁴ following the initial reports of coupled-cluster doubles (CCD),^{15,16} CC theory has been extended to include connected triples (CCSDT),^{17,18} quadruples (CCSDTQ),¹⁹

and pentuples (CCSDTQP).²⁰ A general-order, determinant-based algorithm has been developed,^{21–23} yielding benchmark data through hextuples (CCSDTQPH), septuples (CCSDTQPHS), and octuples (CCSDTQPHSO).²⁴ They are convergent toward the exact basis-set solutions, i.e., the full-configuration-interaction (FCI) limits, at the rate that is distinctly faster than the same of configuration-interaction (CI) theory or of many-body perturbation theory (MBPT).²⁵

Further developments of CC theory followed, including the capabilities to compute the analytical derivatives of its energy with respect to various perturbations,^{26–36} leading to efficient methods to determine equilibrium structures, vibrational spectra,^{37–39} (hyper)polarizabilities,^{40–44} nuclear magnetic resonance parameters,^{45–48} and so on at unprecedented accuracy.^{12,49} CCSD under the periodic boundary conditions has been applied to infinite crystals.^{50,51} One of the weaknesses of CC theory (or of any other *ab initio* electron-correlation theories) is the slow convergence of its energies with respect to the one-electron basis-set size. This too has been overcome by the explicitly correlated ansätze^{52–58} fitted to the CCSD,^{59,60} CCSDT,⁶¹ and CCSDTQ methods,⁶¹ culminating, for instance, in the near exact (99.996–100.004%) determination of the ground-state energy of the water molecule.⁶¹

However, the most outstanding question immediately after the CCSD development has been, *how an excited state can be treated by CC theory?*⁶² Since excited-state wave functions are often dominated by two or more degenerate Slater determinants,⁶³ they are not expected to have an exponential structure from a single determinant. On the one hand, CI theory performs diagonalization of the Hamiltonian matrix in the determinant basis, naturally reporting excited-state eigenvectors that are automatically orthogonal to the ground-state eigenvector. On the other hand, CC theory is formulated as a

^{a)}Email: sohirata@illinois.edu

set of nonlinear equations to be solved for excitation amplitudes. Their numerous roots other than the one corresponding to the ground state do not admit to a simple physical interpretation as excited-state roots let alone their facile numerical determinations.^{64–68}

Nevertheless, the question has been answered decisively in the form of the development of equation-of-motion coupled-cluster (EOM-CC) theory.^{10,22,69–76} It is essentially equivalent to the coupled-cluster linear response^{77–83} or nonvariational symmetry-adapted-cluster configuration-interaction method,^{84–87} although the latter frequently invokes drastic approximations that undermine the equivalence.

EOM-CC theory gains access to excited states via the one-photon excitation processes simulated by the first-order time-dependent perturbation (linear response) theory applied to the initial ground state described by CC theory. It leads to a CI-like diagonalization procedure of a CC effective Hamiltonian matrix, whose ground-state eigenvector is decoupled from the rest. Hence, the extensive correlation energy in the ground state is captured by an extensive exponential operator, while an intensive excitation energy is described by an intensive linear operator. Two or more dominant degenerate determinants of an excited-state wave function can be completely accounted for by the linear operator.

EOM-CC with singles and doubles (EOM-CCSD) can efficiently locate all low-lying excited states of predominantly one-electron excitation character with uniform high accuracy, while it suffers from distinctly larger errors for two-electron excitations and lacks roots corresponding to three-electron and higher excitations.^{7–10,88} Since the one-electron excited states are responsible for intense peaks in one-photon electronic absorption or emission spectra, it may be said that EOM-CC theory is ideally suited for such linear spectral simulations (as opposed to nonlinear spectral simulations; see, however, Mosquera⁸⁹). By adopting as the linear operator an ionization or electron-attachment operator, EOM-CC theory can probe ionization potentials (IP-EOM-CC)^{90–94} or electron affinities (EA-EOM-CC)^{95–97} and has often been considered a coupled-cluster Green's function.^{98–104}

However, there is a more obvious and straightforward alternative answer to the above question: For a nondegenerate determinant reference — be it an excited, ionized, or electron-attached type — the target state is expressed as an exponential excitation operator acting on the reference determinant, i.e., the same as single-reference, projection (i.e., nonvariational) CC theory. There seems no reason to apprehend that it would work poorly for reference determinants that do not obey the aufbau principle. Rather, its performance may well be correlated with the presence or absence of quasidegeneracy of the reference determinant. In fact, these expectations have been borne out by recent applications of single-reference CCSD for nondegenerate excited states.^{105,106} Treating every (nondegenerate) state on an equal footing, it works as well as EOM-CCSD for predominantly one-electron excited states, distinctly better than EOM-CCSD for two-electron excited states, and it has roots for three-electron and higher single determinant references, which any truncated EOM-CC theory fails to locate at some point.

Of course, this non-aufbau CC theory does not constitute a valid black-box method because it cannot be applied to degenerate references. Damour *et al.*¹⁰⁶ adopted the two-determinant coupled-cluster singles and doubles (TD-CCSD) method of Balková, Bartlett, and coworkers^{107–112} as a degenerate counterpart applicable only to a limited class of doubly degenerate references. Clearly, this hybrid ansatz also falls short of being a unified, systematic, and general hierarchical theory.

The objective of this study is to introduce just such CC theory — degenerate coupled-cluster (Δ CC) theory — that is systematically converging, size-extensive, black-box, *ab initio*, and generally applicable to any degenerate and nondegenerate determinant references with any numbers of α - and β -spin electrons, any (aufbau or non-aufbau) patterns of orbital occupancies, any spin multiplicities, and any spatial symmetries. It adds to the arsenal of predictive electron-correlation theories based on the coupled-cluster ansatz, rivaling or in some cases even exceeding EOM-CC theory in terms of accuracy and general applicability.

For nondegenerate references, this ansatz is identical to the single-reference, projection CC ansatz, which demands the exponential wave function to satisfy the Schrödinger equation in a certain determinant space.

For degenerate references, essentially the same projection ansatz is augmented with the provision to determine a linear combination of degenerate determinants as an *effective single* reference whose exponential wave function satisfies the Schrödinger equation in a prescribed determinant space. It is based on the same logic of derivation as degenerate Rayleigh–Schrödinger perturbation (Δ MP) theory,^{113–118} and is the natural coupled-cluster extension of the latter; Δ CC theory is for Δ MP theory as CC theory is for MBPT.²⁵

Below, we will present and justify the ansatz of Δ CC theory and derive the working equations of Δ CC with singles (Δ CCS) and with singles and doubles (Δ CCSD), placing emphasis on the algebraic linkedness and thus size-extensivity of these methods. Their diagrammatic representations will then be illustrated, implying the diagrammatic linkedness and size-extensivity for the whole Δ CC hierarchy. We will proceed to delineate Δ CC theory's similarities to and differences from related theories such as Li and Paldus's state-universal multireference coupled-cluster (SUMRCC) theory,^{119–123} Balková, Bartlett, and coworkers' two-determinant coupled-cluster (TD-CC) theory,^{107–112} and degenerate Rayleigh–Schrödinger perturbation (Δ MP) theory,^{113–118} whose notorious “backward” or “folded” diagrams also manifest in Δ CC theory.

Δ CC theory can be applied to ionized or electron-attached determinant references of Koopmans and satellite types with any number of electrons removed or added. It offers an alternative viewpoint to a coupled-cluster Green's function to the ones typified by IP- and EA-EOM-CC theories. While the Feynman–Dyson perturbation expansion of many-body Green's function (MBGF) is fundamentally nonconvergent at the exact (FCI) limits except for a few Koopmans roots,¹²⁴ Δ MP theory is fundamentally convergent^{124–126} and Δ CC theory is always convergent. The proof of the latter — the *full*

Δ CC method is equivalent to FCI — is documented in this article, which is originally due to Paldus and Li,¹¹⁹ since the full Δ CC method is equal to the full SUMRCC method.¹²⁰

As per the Thouless theorem, a CCS wave function of a single Slater determinant is another single Slater determinant. Therefore, the variational CCS method is identified as the conventional, variational Hartree–Fock (HF) theory starting from any arbitrary nondegenerate reference. Here, we argue that the projection CCS method, in contrast, defines a *projection* HF theory for any nondegenerate reference, whose wave function is still a single determinant, but with different orbitals from the variational ones. Then, the Δ CCS method can be viewed as its generalization to degenerate references. We have found a few pieces of numerical evidence indicating the utility of the Δ CCS method for core ionizations, high-spin states, and possibly electron affinities.

The Δ CC methods have been implemented into two independent algorithms. One is the order-by-order implementations of the matrix-algebraic energy and t -amplitude equations at the Δ CCS and Δ CCSD levels, which have the optimal $O(n^4)$ and $O(n^6)$ dependence of the operation cost on the number of spin-orbitals (n). These equations have been derived and the corresponding codes synthesized by quantum chemists' original “artificial intelligence”¹²⁷ called TENSOR CONTRACTION ENGINE or TCE.^{128,129} The other is the determinant- or string-based algorithm,²¹ allowing general-order calculations through the full Δ CC level at an FCI computational cost at each order. Its results are compared with those of the general-order, determinant-based implementations of the CI,¹³⁰ EOM-CC,^{88,131} Δ MP,^{125,126,132} and MBGF methods¹²⁶ carried out through the FCI limits or up to the nineteenth order.

The comparison indicates the following general order of performance: Δ CC > EOM-CC > CI at the same order or Δ CC > Δ MP > MBGF at the same cost scaling.

II. THEORIES

A. Coupled-cluster (CC) ansatz (review)

Let us briefly review the ansatz of the single-reference, projection coupled-cluster (CC) theory,^{7–10} arguably the most successful electron-correlation method developed to date.

It demands that an exponential wave function $e^{\hat{T}_I}|I\rangle$ satisfy the Schrödinger equation within the space of Slater determinants reachable by $(1 + \hat{T}_I)|I\rangle$,

$$\hat{P}_I \hat{H}_I e^{\hat{T}_I}|I\rangle = \hat{P}_I e^{\hat{T}_I}|I\rangle \tilde{E}_I, \quad (1)$$

where $|I\rangle$ is the I th determinant, \hat{T}_I is an excitation operator from $|I\rangle$, \hat{P}_I is the projector onto the aforementioned space of determinants, and \tilde{E}_I is the CC energy. The number of unknowns (\tilde{E}_I plus all t -amplitudes) is equal to the number of equations. Here, Eq. (1) is not expressed in the usual, connected form, but in a disconnected (but linked) form.

The exact (*ab initio*) electronic Hamiltonian, \hat{H}_I , is independent of the reference $|I\rangle$, but in this article, it carries the

subscript I as it is brought to a normal-ordered form (indicated by “ $\{\dots\}$ ”) relative to the $|I\rangle$ vacuum,

$$\hat{H}_I = E_I^{\text{HF}} + \sum_{p,q} (f_I)_q^p \{ \hat{p}^\dagger \hat{q} \} + \frac{1}{4} \sum_{p,q,r,s} (v)_{rs}^{pq} \{ \hat{p}^\dagger \hat{q}^\dagger \hat{s} \hat{r} \}, \quad (2)$$

where the HF energy, E_I^{HF} , and Fock matrix elements, $(f_I)_q^p$, are also defined for $|I\rangle$ as

$$E_I^{\text{HF}} = E_{\text{nuc.}} + \sum_i^{\text{occ. in } |I\rangle} (h)_i^i + \frac{1}{2} \sum_{i,j}^{\text{occ. in } |I\rangle} (v)_{ij}^{ij}, \quad (3)$$

$$(f_I)_q^p = (h)_q^p + \sum_i^{\text{occ. in } |I\rangle} (v)_{qi}^{pi}. \quad (4)$$

The summation indices, i and j , run over spin-orbitals occupied by an electron in $|I\rangle$, and therefore, E_I^{HF} and $(f_I)_q^p$ are now dependent on $|I\rangle$. On the other hand, the nuclear-repulsion energy, $E_{\text{nuc.}}$, core Hamiltonian matrix elements, $(h)_q^p$, and antisymmetrized two-electron integrals, $(v)_{rs}^{pq}$, are independent of $|I\rangle$.

Single-reference CC theory is a black-box method, requiring only the nuclear-repulsion energy, reference determinant, and truncation rank of \hat{T}_I to be specified by the user. Its energy and wave function converge at the exact (FCI) results as \hat{T}_I becomes complete. It is size-extensive.

B. Degenerate coupled-cluster (Δ CC) ansatz

Degenerate coupled-cluster (Δ CC) theory is identical with the foregoing single-reference CC theory when the reference is nondegenerate, regardless of the numbers of the α - and β -spin electrons, the occupancies of spin-orbitals in the reference Slater determinant, or the definitions of the spin-orbitals.

When the reference is M -fold degenerate (as per, e.g., the Møller–Plesset zeroth-order Hamiltonian), the ansatz needs to be generalized, while encompassing the foregoing nondegenerate case without any modification. Let us first stipulate the ansatz and then give justifications.

Δ CC theory stipulates that the set of M exponential wave functions in the degenerate subspace, $\{e^{\hat{T}_I}|I\rangle\}$, together satisfy the Schrödinger equation with a matrix form of the energy in the respective spaces of determinants reachable by $\{(1 + \hat{T}_I)|I\rangle\}$,

$$\hat{P}_I \hat{H}_I e^{\hat{T}_I}|I\rangle = \hat{P}_I \sum_{J=1}^M \hat{P}_J e^{\hat{T}_J}|J\rangle E_{JI} \quad (5)$$

as well as the orthonormality of the M exponential wave functions,

$$\langle J | \hat{P}_I e^{\hat{T}_I} | I \rangle = \delta_{JI}, \quad (6)$$

where $|I\rangle$ and $|J\rangle$ are degenerate references and δ_{JI} is Kronecker's delta. Equation (6) is referred to as the “C-condition” for reasons given later. The projector \hat{P}_I spans determinants reachable by $(1 + \hat{T}_I)|I\rangle$ and they include determinants that are

degenerate with $|I\rangle$ (internal space) as well as those outside the degenerate space (external space). It is stressed that each (I th) degenerate reference has its own \hat{T}_I and \hat{P}_I operators.

Defining the M -by- M Hamiltonian and overlap matrices, \mathbf{H} and \mathbf{S} , by

$$H_{JI} = \langle J|\hat{P}_I\hat{H}_Ie^{\hat{T}_I}|I\rangle, \quad (7)$$

$$S_{JI} = \langle J|\hat{P}_Ie^{\hat{T}_I}|I\rangle, \quad (8)$$

where $|I\rangle$ and $|J\rangle$ are degenerate references, the projection of Eq. (5) onto the internal space becomes

$$\mathbf{H} = \mathbf{S}\mathbf{E}, \quad (9)$$

while Eq. (6) is written as

$$\mathbf{S} = \mathbf{1}. \quad (10)$$

The t -amplitudes in the external space are determined by solving Eq. (5). Those in the internal space are obtained by satisfying Eq. (10), whereupon $\mathbf{E} = \mathbf{H}$. The I th-state Δ CC energy \tilde{E}_I is then computed as an eigenvalue of this non-Hermitian energy matrix \mathbf{E} ,

$$\sum_{J=1}^M E_{KJ}C_{JI} = C_{KI}\tilde{E}_I. \quad (11)$$

The corresponding Δ CC wave function is given by

$$|\tilde{I}\rangle = \sum_{J=1}^M \hat{P}_Je^{\hat{T}_J}|J\rangle C_{JI}. \quad (12)$$

We shall call this Δ CC theory, where Δ denoting both a ‘difference’ between two state energies used to define the transition energy and ‘degeneracy’ of the reference determinants.

Clearly, the Δ CC ansatz reduces to the single-reference CC ansatz upon letting $M = 1$. Δ CC theory is a black-box method, requiring only the nuclear-repulsion energy, degenerate reference determinants, and truncation rank of the \hat{T}_I operators. The degenerate reference determinants are defined with any (single) set of spin-orbitals that are, typically, but not necessarily, the HF orbitals determined for any convenient state, such as a nearby, neutral, singlet, ground state (called “the orbital reference,” which is distinct from the degenerate references). The degenerate references need not have the same numbers of α - and β -spin electrons or the same spin-multiplicity as the orbital reference. They need not be the lowest-lying states, either. There is no restrictions about their spatial symmetries (such as having to belong to a different irreducible representation from the orbital reference). Δ CC theory is convergent at the exact (FCI) results for all degenerate reference states (whose degeneracy may persist or be partially or fully lifted upon correlation) as the \hat{T}_I operators become complete (see Sec. II L for a proof). It is size-extensive (see Sec. II E for a proof).

Let us justify this ansatz. Since any linear combination of degenerate eigenfunctions is also another degenerate eigenfunction, a sound ansatz should not attach particular significance to a single determinant as a reference when it is degenerate. Instead, a reference should evolve into a linear combination of all degenerate determinants as more electron correlation is included. In other words, we do not know *a priori*

the “exact” degenerate references, i.e., which linear combinations of degenerate determinants eventually map onto the *full* Δ CC wave functions (see Sec. III L). We determine them via Eq. (11), which would then approach the exact degenerate references as the \hat{T}_I operators become more complete. This is also consistent with degenerate Rayleigh–Schrödinger perturbation theory (to which Δ CC theory is intimately related; see Sec. II H), which updates the degenerate references at each perturbation order via diagonalization of an “energy matrix” akin to the above \mathbf{E} . The diagonalization ensures that the wave functions of Eq. (12) be biorthogonal to one another in the internal space.

Each degenerate determinant is entitled to its own set of t -amplitudes (i.e., no “internal contraction” scheme is adopted). This is a natural generalization of the single-reference CC ansatz to degenerate references, where the only essential difference is the need for determining the linear combinations of degenerate references in the latter case. In terms of the physics of electron correlation also, it does not make much sense for two reference determinants, even if they are degenerate, to share the same set of excitation amplitudes. It also goes against degenerate Rayleigh–Schrödinger perturbation theory, in which perturbation corrections to the wave functions differ from one degenerate reference to another. These justify Eqs. (5) and (12) in which $|J\rangle$ is acted on by its own, independent $e^{\hat{T}_J}$ operator.

Equation (10) ensures that there be no conflict within the degenerate subspace, i.e., that $e^{\hat{T}_J}|J\rangle$ does not overlap with any other degenerate reference determinant $|I\rangle$, when $I \neq J$. If $|I\rangle$ were spanned by $e^{\hat{T}_J}|J\rangle$, the exact Δ CC wave function cannot be written uniquely in the form of Eq. (12), and its convergence toward FCI with increasing the rank of \hat{T} is no longer assured. This condition is essentially the same as “the C-conditions” of Li and Paldus in their state-universal multireference coupled-cluster (SUMRCC) theory,^{119–123} to which Δ CC theory is closely related. However, there is an important distinction between these two theories, which will be discussed in Sec. II F. Until the convergence of iterative algorithms to satisfy Eqs. (5) and (6), $\mathbf{S} \neq \mathbf{1}$ and the energy matrix that enters Eq. (5) needs to be evaluated by $\mathbf{E} = \mathbf{S}^{-1}\mathbf{H}$ (not by $\mathbf{E} = \mathbf{H}$).

Perhaps the thorniest issue of the Δ CC ansatz embodied by Eqs. (5) and (6) is whether or not to include the second projector \hat{P}_J . It has been concluded that limiting the scope of the action of $e^{\hat{T}_J}$ by \hat{P}_J in Eq. (5) is consistent with the same in Eq. (6) and therefore more agreeable. This choice furthermore allows the use of the same, uniform formula and computer code to evaluate $\hat{P}_Je^{\hat{T}_J}|J\rangle$ at a given order of \hat{T}_J , explicitly maintaining the black-box nature of the method. However, it also seems possible to define an alternative black-box ansatz without the second project \hat{P}_J , which we may revisit in a future investigation.

C. Δ CCS

As the first concrete example of Δ CC theory, let us consider the degenerate coupled-cluster singles (Δ CCS) method. Since degenerate references are often singly excited from one another and Δ CC theory must take into account coupling among these degenerate references as well as electron correlation in each reference, the lowest meaningful instance should be Δ CCS rather than the degenerate coupled-cluster doubles (Δ CCD) method. We shall thus consider the energy and amplitude equations of Δ CCS, which have been derived and partially typeset by TCE.^{128,129}

Here, \hat{P}_I is the projector onto the set of all singly excited determinants from $|I\rangle$, i.e., $\{I_h^p\}$. The left-hand side of Eq. (5) is expanded as

$$\begin{aligned} \langle I_{h_1}^{p_2} | \hat{H}_I e^{\hat{T}_I} | I \rangle &= (f_I)_{h_1}^{p_2} - (f_I)_{h_1}^{h_3} (t_I)_{h_3}^{p_2} + (f_I)_{h_1}^{p_2} (t_I)_{h_1}^{p_3} \\ &\quad - (t_I)_{h_4}^{p_3} (v)_{h_1 p_3}^{h_4 p_2} - (t_I)_{h_1}^{p_3} (t_I)_{h_4}^{p_2} (f_I)_{h_4}^{h_4} \\ &\quad + (t_I)_{h_3}^{p_2} (t_I)_{h_5}^{p_4} (v)_{h_1 p_4}^{h_5 h_3} + (t_I)_{h_1}^{p_3} (t_I)_{h_5}^{p_4} (v)_{p_4 p_3}^{h_5 p_2} \\ &\quad - (t_I)_{h_3}^{p_2} (t_I)_{h_1}^{p_4} (t_I)_{h_6}^{p_5} (v)_{p_5 p_4}^{h_6 h_3} \\ &\quad + (t_I)_{h_1}^{p_2} \langle I | \hat{H}_I e^{\hat{T}_I} | I \rangle \end{aligned} \quad (13)$$

with

$$\begin{aligned} \langle I | \hat{H}_I e^{\hat{T}_I} | I \rangle &= E_I^{\text{HF}} + (f_I)_{h_1}^{h_1} (t_I)_{h_1}^{p_2} + \frac{1}{2} (t_I)_{h_2}^{p_1} (t_I)_{h_4}^{p_3} (v)_{p_3 p_1}^{h_4 h_2} \\ &= H_{II}, \end{aligned} \quad (14)$$

where Einstein's convention of implied summations over repeated indices is employed, and p and h as in $(t_I)_h^p$ stand for a virtual and occupied spin-orbital, respectively, in the I th degenerate reference determinant. These are essentially the same as the so-called T_1 -amplitude and energy equations, respectively, of single-reference CCS except for the last term of Eq. (13), which is unlinked. However, this term will be canceled by the unlinked contribution in the right-hand side of Eq. (5), leaving a fully linked t -amplitude equation (see below).

Equation (14), which is connected and thus linked, gives the diagonal elements of \mathbf{H} of Eq. (7). When $|I_{h_1}^{p_2}\rangle$ in the internal space, i.e., it is degenerate with $|I\rangle$, Eq. (13) defines the off-diagonal elements of \mathbf{H} ; for $|J\rangle$ that differs from $|I\rangle$ by more than one spin-orbital, $H_{JI} = 0$. Once the C-conditions [Eq. (6) or (10)] are satisfied, the last term of Eq. (13) vanishes, making it also connected and therefore linked. When $|I_{h_1}^{p_2}\rangle$ in the external space, Eq. (13) becomes the left-hand side of the t -amplitude equation [Eq. (5)], which is *not* linked.

The left-hand side of Eq. (6) is expanded as

$$\langle I_{h_1}^{p_2} | e^{\hat{T}_I} | I \rangle = (t_I)_{h_1}^{p_2}, \quad (15)$$

$$\langle I | e^{\hat{T}_I} | I \rangle = 1. \quad (16)$$

When $|I_{h_1}^{p_2}\rangle$ is in the internal space, Eqs. (15) and (16) together define \mathbf{S} of Eq. (8). When $|J\rangle$ is more than one-spin-orbital different from $|I\rangle$, $S_{JI} = 0$. These equations also define factors appearing in the right-hand side of the t -amplitude equation [Eq. (5)].

The right-hand side of the t -amplitude equation in the external space [Eq. (5)] then becomes

$$\begin{aligned} \langle I_{h_1}^{p_2} | \hat{H}_I e^{\hat{T}_I} | I \rangle &= \langle I_{h_1}^{p_2} | e^{\hat{T}_I} | I \rangle E_{II} \\ &\quad + \sum_{J \neq I} \sum_{h_3}^{\text{occ. in } |J\rangle} \sum_{p_4}^{\text{vir. in } |J\rangle} \langle I_{h_1}^{p_2} | J_{h_3}^{p_4} \rangle \langle J_{h_3}^{p_4} | e^{\hat{T}_J} | J \rangle E_{JI}, \end{aligned} \quad (17)$$

where $\langle I_{h_1}^{p_2} | J_{h_3}^{p_4} \rangle$ and $\langle I_{h_1}^{p_2} | J \rangle$, called parities, take the value of 0 or ± 1 . All the other Dirac brackets, $\langle \dots \rangle$, have already been expanded above.

Once the C-conditions [Eq. (6)] are satisfied, $\mathbf{E} = \mathbf{S}^{-1} \mathbf{H} = \mathbf{H}$ and thus $E_{II} = H_{II}$. Therefore, upon solution of the Δ CCS equations, the first term in the right-hand side of Eq. (17), which is unlinked, cancels out the sole unlinked term in the left-hand side, i.e., the last term of Eq. (13), ensuring the linkedness of the equation and thus the size-extensivity of Δ CCS. The last term of Eq. (17) may *appear* unlinked, but it is not; since $J \neq I$, $|J\rangle$ is a single excitation from $|I\rangle$, and hence $E_{JI} = H_{JI} = \langle I_h^p | \hat{H}_I e^{\hat{T}_I} | I \rangle$ is an open diagram designating an intensive excitation amplitude (not an extensive energy). Hence, the last term is disconnected, but linked. This linked-disconnected term can, however, be depicted as a “backward” diagram of Sandars^{114,117} or “folded” diagram of Brandow^{113,115–117} in degenerate many-body perturbation theories, which is connected by warped lines. See Sec. II E for more.

In an iterative algorithm to solve the Δ CCS equations, we first determine \mathbf{H} and \mathbf{S} using Eqs. (13)–(16) within the internal space (i.e., spanned by all degenerate references). Then, we form $\mathbf{E} = \mathbf{S}^{-1} \mathbf{H}$, whereafter the t -amplitude equation [Eq. (17)] is solved in the external space. The details of this last step differ between the determinant-based, general-order algorithm and algebraic, optimal-scaling algorithm (see Sec. III).

D. Δ CCSD

Next, let us consider the degenerate coupled-cluster singles and doubles (Δ CCSD) method. Its projector \hat{P}_I spans the zero, singly, and doubly excited states from $|I\rangle$, leading to an energy equation and two sets of t -amplitude equations.

The projection onto the doubly excited determinants from $|I\rangle$ is expanded by TCE (Refs. 128 and 129) as

$$\begin{aligned}
\langle I_{h_1 h_2}^{p_3 p_4} | \hat{H}_I e^{\hat{T}_I} | I \rangle = & (v)_{h_1 h_2}^{p_3 p_4} - \hat{A} \left[(t_I)_{h_5}^{p_3} (v)_{h_1 h_2}^{h_5 p_4} \right] + \hat{A} \left[(t_I)_{h_2}^{p_5} (v)_{h_1 h_2}^{p_3 p_4} \right] - \hat{A} \left[(f_I)_{h_1}^{h_5} (t_I)_{h_5 h_2}^{p_3 p_4} \right] - \hat{A} \left[(f_I)_{h_5}^{p_4} (t_I)_{h_1 h_2}^{p_5 p_3} \right] + \frac{1}{2} (t_I)_{h_5 h_6}^{p_3 p_4} (v)_{h_1 h_2}^{h_5 h_6} \\
& + \hat{A} \left[(t_I)_{h_6 h_2}^{p_5 p_3} (v)_{h_1 p_5}^{h_6 p_4} \right] + \frac{1}{2} (t_I)_{h_1 h_2}^{p_5 p_6} (v)_{p_5 p_6}^{p_3 p_4} + (t_I)_{h_5}^{p_3} (t_I)_{h_6}^{p_4} (v)_{h_1 h_2}^{h_5 h_6} - \hat{A} \left[(t_I)_{h_2}^{p_5} (t_I)_{h_6}^{p_3} (v)_{h_1 p_5}^{h_6 p_4} \right] + (t_I)_{h_1}^{p_5} (t_I)_{h_2}^{p_6} (v)_{p_5 p_6}^{p_3 p_4} \\
& - \hat{A} \left[(f_I)_{h_6}^{h_5} (t_I)_{h_5 h_2}^{p_3 p_4} (t_I)_{h_1}^{p_6} \right] + \hat{A} \left[(f_I)_{h_6}^{p_5} (t_I)_{h_1 h_2}^{p_6 p_3} (t_I)_{h_5}^{p_4} \right] + \frac{1}{2} \hat{A} \left[(t_I)_{h_5 h_6}^{p_3 p_4} (t_I)_{h_2}^{p_7} (v)_{h_1 p_7}^{h_5 h_6} \right] - \hat{A} \left[(t_I)_{h_6 h_2}^{p_5 p_3} (t_I)_{h_7}^{p_4} (v)_{h_1 p_5}^{h_6 h_7} \right] \\
& - \hat{A} \left[(t_I)_{h_5 h_2}^{p_3 p_4} (t_I)_{h_7}^{p_6} (v)_{h_1 p_6}^{h_5 h_7} \right] - \hat{A} \left[(t_I)_{h_6 h_2}^{p_5 p_3} (t_I)_{h_1}^{p_7} (v)_{p_5 p_7}^{h_6 p_4} \right] - \frac{1}{2} \hat{A} \left[(t_I)_{h_1 h_2}^{p_5 p_6} (t_I)_{h_7}^{p_3} (v)_{p_5 p_6}^{h_7 p_4} \right] + \hat{A} \left[(t_I)_{h_1 h_2}^{p_5 p_3} (t_I)_{h_7}^{p_6} (v)_{p_5 p_6}^{h_7 p_4} \right] \\
& + \frac{1}{2} \hat{A} \left[(t_I)_{h_1 h_2}^{p_5 p_4} (t_I)_{h_7 h_8}^{p_6 p_3} (v)_{p_5 p_6}^{h_7 h_8} \right] + \frac{1}{4} (t_I)_{h_1 h_2}^{p_5 p_6} (t_I)_{h_7 h_8}^{p_3 p_4} (v)_{p_5 p_6}^{h_7 h_8} - \frac{1}{2} \hat{A} \left[(t_I)_{h_5 h_1}^{p_3 p_4} (t_I)_{h_8 h_2}^{p_6 p_7} (v)_{p_6 p_7}^{h_5 h_8} \right] - \hat{A} \left[(t_I)_{h_6 h_1}^{p_5 p_4} (t_I)_{h_8 h_2}^{p_7 p_3} (v)_{p_5 h_8}^{h_6 h_7} \right] \\
& + \hat{A} \left[(t_I)_{h_2}^{p_5} (t_I)_{h_6}^{p_3} (t_I)_{h_7}^{p_4} (v)_{h_1 p_5}^{h_6 h_7} \right] - \hat{A} \left[(t_I)_{h_1}^{p_5} (t_I)_{h_2}^{p_6} (t_I)_{h_7}^{p_3} (v)_{p_5 p_6}^{h_7 p_4} \right] + \frac{1}{2} (t_I)_{h_1}^{p_5} (t_I)_{h_2}^{p_6} (t_I)_{h_7 h_8}^{p_3 p_4} (v)_{p_5 p_6}^{h_7 h_8} \\
& + \hat{A} \left[(t_I)_{h_1}^{p_5} (t_I)_{h_6}^{p_4} (t_I)_{h_8 h_2}^{p_7 p_3} (v)_{p_5 p_7}^{h_6 h_8} \right] + \hat{A} \left[(t_I)_{h_1}^{p_5} (t_I)_{h_7}^{p_6} (t_I)_{h_8 h_2}^{p_3 p_4} (v)_{p_5 p_6}^{h_7 h_8} \right] + \frac{1}{2} (t_I)_{h_5}^{p_3} (t_I)_{h_6}^{p_4} (t_I)_{h_1 h_2}^{p_7 p_8} (v)_{p_7 p_8}^{h_5 h_6} \\
& - \hat{A} \left[(t_I)_{h_5}^{p_4} (t_I)_{h_7}^{p_6} (t_I)_{h_1 h_2}^{p_8 p_3} (v)_{p_6 p_8}^{h_5 h_7} \right] + (t_I)_{h_1}^{p_5} (t_I)_{h_2}^{p_6} (t_I)_{h_7}^{p_3} (t_I)_{h_8}^{p_4} (v)_{p_5 p_6}^{h_7 h_8} + \hat{A} \left[(t_I)_{h_1}^{p_3} \langle I | \hat{H}_I e^{\hat{T}_I} | I \rangle \right] + (t_I)_{h_1 h_2}^{p_3 p_4} \langle I | \hat{H}_I e^{\hat{T}_I} | I \rangle, \quad (18)
\end{aligned}$$

where $\hat{A}[\dots]$ is the anti-symmetrizer⁸ and the remaining Dirac brackets are further expanded below. This equation is the same as the T_2 -amplitude equation of single-reference CCSD apart from the last two terms, which are disconnected. The last term is wholly unlinked, while the penultimate term contains an unlinked term with the rest being linked-disconnected (see below).

The projection onto the singly excited determinants leads to

$$\begin{aligned}
\langle I_{h_1}^{p_2} | \hat{H}_I e^{\hat{T}_I} | I \rangle = & (f_I)_{h_1}^{p_2} - (f_I)_{h_1}^{h_3} (t_I)_{h_3}^{p_2} + (f_I)_{p_3}^{p_2} (t_I)_{h_1}^{p_3} - (t_I)_{h_4}^{p_3} (v)_{h_1 p_2}^{h_4 p_2} + (f_I)_{p_4}^{h_3} (t_I)_{h_3 h_1}^{p_4 p_2} + \frac{1}{2} (t_I)_{h_4 h_5}^{p_3 p_2} (v)_{h_1 p_3}^{h_4 h_5} + \frac{1}{2} (t_I)_{h_5 h_1}^{p_3 p_4} (v)_{p_3 p_4}^{h_5 p_2} \\
& - (t_I)_{h_1}^{p_3} (t_I)_{h_4}^{p_2} (f_I)_{p_3}^{h_4} - (t_I)_{h_3}^{p_2} (t_I)_{h_5}^{p_4} (v)_{h_1 p_4}^{h_3 h_5} - (t_I)_{h_1}^{p_3} (t_I)_{h_5}^{p_4} (v)_{p_3 p_4}^{h_5 p_2} - \frac{1}{2} (t_I)_{h_4 h_5}^{p_3 p_2} (t_I)_{h_1}^{p_6} (v)_{p_3 p_6}^{h_4 h_5} - \frac{1}{2} (t_I)_{h_5 h_1}^{p_3 p_4} (t_I)_{h_6}^{p_2} (v)_{p_3 p_4}^{h_5 h_6} \\
& + (t_I)_{h_4 h_1}^{p_3 p_2} (t_I)_{h_6}^{p_5} (v)_{p_3 p_5}^{h_4 h_6} - (t_I)_{h_1}^{p_3} (t_I)_{h_4}^{p_2} (t_I)_{h_6}^{p_5} (v)_{p_3 p_5}^{h_4 h_6} + (t_I)_{h_1}^{p_2} \langle I | \hat{H}_I e^{\hat{T}_I} | I \rangle. \quad (19)
\end{aligned}$$

This is identified as the disconnected form of the T_1 -amplitude equation of single-reference CCSD, whose last term is disconnected and unlinked.

The projection onto $|I\rangle$ is isomorphic to the energy equation of single-reference CCSD,

$$\begin{aligned}
\langle I | \hat{H}_I e^{\hat{T}_I} | I \rangle = & E_I^{\text{HF}} + (f_I)_{p_2}^{h_1} (t_I)_{h_1}^{p_2} + \frac{1}{4} (t_I)_{h_3 h_4}^{p_1 p_2} (v)_{p_1 p_2}^{h_3 h_4} \\
& + \frac{1}{2} (t_I)_{h_2}^{p_1} (t_I)_{h_4}^{p_3} (v)_{p_1 p_3}^{h_2 h_4} = H_{II}, \quad (20)
\end{aligned}$$

which is connected and thus linked. It gives the diagonal elements of \mathbf{H} .

When $|I_{h_1 h_2}^{p_3 p_4}\rangle$ and $|I_{h_1}^{p_2}\rangle$ are in the internal space, Eqs. (18) and (19) define the off-diagonal elements of \mathbf{H} ; for $|J\rangle$ that is more than two-spin-orbital different from $|I\rangle$, $H_{JI} = 0$. Otherwise they become the left-hand sides of the t -amplitude equations [Eq. (5)] in the external space.

The matrix elements entering the C-conditions [Eq. (6)] and the right-hand side of the t -amplitude equations [Eq. (5)] are given by

$$\langle I_{h_1 h_2}^{p_3 p_4} | e^{\hat{T}_I} | I \rangle = (t_I)_{h_1 h_2}^{p_3 p_4} + \hat{A} \left[(t_I)_{h_1}^{p_3} (t_I)_{h_2}^{p_4} \right], \quad (21)$$

$$\langle I_{h_1}^{p_2} | e^{\hat{T}_I} | I \rangle = (t_I)_{h_1}^{p_2}, \quad (22)$$

$$\langle I | e^{\hat{T}_I} | I \rangle = 1. \quad (23)$$

When $|I_{h_1 h_2}^{p_3 p_4}\rangle$ and $|I_{h_1}^{p_2}\rangle$ are in the internal space, these define the elements of \mathbf{S} ; for $|J\rangle$ that is more than two-spin-orbital different from $|I\rangle$, $S_{JI} = 0$.

The right-hand sides of the t -amplitude equations in the external space [Eq. (5)] now read

$$\begin{aligned}
\langle I_{h_1 h_2}^{p_3 p_4} | \hat{H}_I e^{\hat{T}_I} | I \rangle = & \langle I_{h_1 h_2}^{p_3 p_4} | e^{\hat{T}_I} | I \rangle E_{II} \\
& + \sum_{J \neq I} \sum_{h_5}^{\text{occ. in } |J\rangle} \sum_{p_6}^{\text{vir. in } |J\rangle} \langle I_{h_1 h_2}^{p_3 p_4} | J_{h_5}^{p_6} \rangle \langle J_{h_5}^{p_6} | e^{\hat{T}_J} | J \rangle E_{JI} \\
& + \sum_{J \neq I} \sum_{h_5 < h_6}^{\text{occ. in } |J\rangle} \sum_{p_7 < p_8}^{\text{vir. in } |J\rangle} \langle I_{h_1 h_2}^{p_3 p_4} | J_{h_5 h_6}^{p_7 p_8} \rangle \langle J_{h_5 h_6}^{p_7 p_8} | e^{\hat{T}_J} | J \rangle E_{JI}, \quad (24)
\end{aligned}$$

$$\begin{aligned}
\langle I_{h_1}^{p_2} | \hat{H}_I e^{\hat{T}_I} | I \rangle = & \langle I_{h_1}^{p_2} | e^{\hat{T}_I} | I \rangle E_{II} \\
& + \sum_{J \neq I} \sum_{h_3}^{\text{occ. in } |J\rangle} \sum_{p_4}^{\text{vir. in } |J\rangle} \langle I_{h_1}^{p_2} | J_{h_3}^{p_4} \rangle \langle J_{h_3}^{p_4} | e^{\hat{T}_J} | J \rangle E_{JI} \\
& + \sum_{J \neq I} \sum_{h_3 < h_4}^{\text{occ. in } |J\rangle} \sum_{p_5 < p_6}^{\text{vir. in } |J\rangle} \langle I_{h_1}^{p_2} | J_{h_3 h_4}^{p_5 p_6} \rangle \langle J_{h_3 h_4}^{p_5 p_6} | e^{\hat{T}_J} | J \rangle E_{JI}, \quad (25)
\end{aligned}$$

where parities, $\langle I_{h_1 h_2}^{p_3 p_4} | J_{h_5 h_6}^{p_7 p_8} \rangle$, $\langle I_{h_1 h_2}^{p_3 p_4} | J_{h_5}^{p_6} \rangle$, $\langle I_{h_1 h_2}^{p_3 p_4} | J \rangle$, $\langle I_{h_1}^{p_2} | J_{h_3 h_4}^{p_5 p_6} \rangle$, $\langle I_{h_1}^{p_2} | J_{h_3}^{p_4} \rangle$, and $\langle I_{h_1}^{p_2} | J \rangle$, take the value of 0, or ± 1 , and all the other Dirac brackets have already been defined in terms of t -amplitudes and molecular integrals.

Substituting Eq. (19) into Eq. (18), we find that the last two terms of the latter, which are disconnected, contain the unlinked contribution of

$$\hat{A} \left[(t_I)_{h_1}^{p_3} (t_I)_{h_2}^{p_4} \langle I | \hat{H}_I e^{\hat{T}_I} | I \rangle \right] + (t_I)_{h_1 h_2}^{p_3 p_4} \langle I | \hat{H}_I e^{\hat{T}_I} | I \rangle. \quad (26)$$

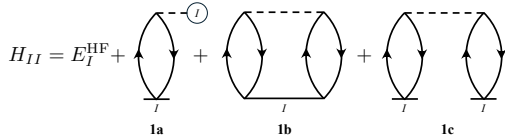


FIG. 1. The diagonal energy, H_{II} , of Δ CCSD [Eq. (20)]. The dashed line with circled I denotes $(f_I)_{\text{in}}^{\text{out}}$, while the dashed line translates to $(v)_{\text{left out, right out}}^{\text{left in, right in}}$. The solid line with I designates $(t_I)_{\text{in}}^{\text{out}}$ or $(t_I)_{\text{left out, right out}}^{\text{left in, right in}}$.

When $|I_{h_1 h_2}^{p_3 p_4}\rangle$ is in the internal space, this sum will be zero because of the C-conditions [see Eqs. (6) and (21)]. When $|I_{h_1 h_2}^{p_3 p_4}\rangle$ is in the external space, this sum will be canceled by the first term in the right-hand side of Eq. (24) because the latter can be written as

$$\langle I_{h_1 h_2}^{p_3 p_4} | e^{\hat{T}_I} | I \rangle E_{II} = \left((t_I)_{h_1 h_2}^{p_3 p_4} + \hat{A} \left[(t_I)_{h_1}^{p_3} (t_I)_{h_2}^{p_4} \right] \right) H_{II}, \quad (27)$$

which is equal to Eq. (26). Likewise, the last term of Eq. (19), which is unlinked, will be zero if $|I_{h_1}^{p_2}\rangle$ is in the internal space by virtue of the C-conditions [Eqs. (6) and (22)]; if $|I_{h_1}^{p_2}\rangle$ is in the external space, this term will be canceled by the first term in the right-hand side of Eq. (25), which is unlinked. After these systematic cancellations, only linked terms remain, proving the size-extensivity of Δ CCSD.

Note that the disconnected, but linked contributions in the penultimate term of Eq. (18) persist, as do all the other linked-disconnected terms in the right-hand sides of Eqs. (24) and (25). While the t_J -amplitudes ($J \neq I$) define the latter, the t_I -amplitudes appear in the linked-disconnected contributions in Eq. (18), and hence they are not expected to cancel each other, which we must evaluate. Generally, the t -amplitude equations of Δ CC theory are disconnected at least initially, but always linked, although some (not all) of these linked-disconnected terms can be drawn as the connected backward or folded diagrams (see below). (Other authors seem to adopt different definitions^{117,120} of “connectedness,” but our final conclusions about size-extensivity are always the same.)

E. Size-extensivity

The foregoing proofs of the size-extensivity of Δ CCS and Δ CCSD can be generalized to all orders. We shall analyze the linkedness of diagrams of the energy and t -amplitude equations, Eq. (5), under the assumption that the C-condition, Eq. (6), is satisfied ($S = \mathbf{1}$). Then, E_{II} in Eq. (5) can be read as H_{II} because $E = S^{-1}H = H$. By demonstrating the *diagrammatic* linkedness for Δ CCSD, we can infer that the same logic applies to Δ CC theory of all orders.

It may be recalled that an unlinked, thus size-extensivity-violating, diagram is defined as a disconnected diagram with at least one of the disconnected subdiagrams being closed.^{8,133} Conversely, a disconnected diagram made of any number of open subdiagrams only is still linked (which we call linked-disconnected¹²⁵), and it does not imply the violation of size-extensivity.^{8,133}

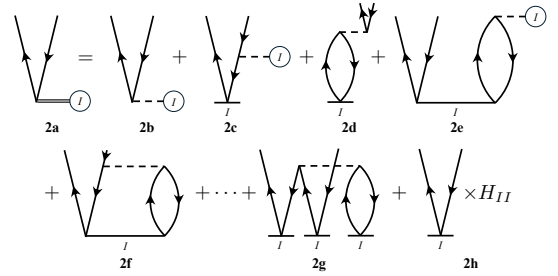


FIG. 2. The left-hand side, $\langle I_i^a | \hat{H}_I e^{\hat{T}_I} | I \rangle$, of the t -amplitude equation of Δ CCSD [Eq. (19)] in the external single-excitation space ($\epsilon_a - \epsilon_i \neq 0$). The double line with I (2a) designates the CC effective Hamiltonian $(\hat{H}_I e^{\hat{T}_I})_{\text{in}}^{\text{out}}$, which is unlinked through diagram 2h.

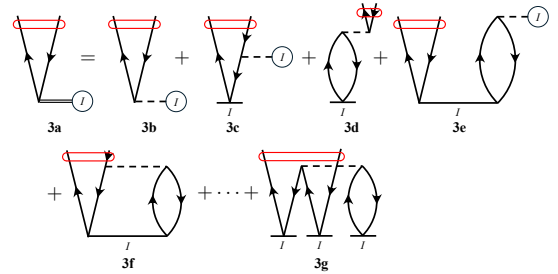


FIG. 3. The left-hand side, $\langle I_i^a | \hat{H}_I e^{\hat{T}_I} | I \rangle$, of the t -amplitude equation of Δ CCSD [Eq. (19)] in the internal single-excitation space, i.e., the off-diagonal energy, H_{II} , with $|J\rangle = |I_i^a\rangle$. The red oblong denotes the fictitious resolvent line that demands $\epsilon_a - \epsilon_i = 0$. The double line with I (3a) now designates the connected CC effective Hamiltonian $(\hat{H}_I e^{\hat{T}_I})_{\text{in}}^{\text{out}}$. See Fig. 10.2 of Shavitt and Bartlett⁸ for a complete list of diagrams.

The diagrams (in the Shavitt–Bartlett style⁸) representing the diagonal element H_{II} of Δ CCSD are given in Fig. 1, which are connected and thus linked.

The left-hand side of the t -amplitude equation of Δ CCSD [Eq. (19)] in the external single-excitation space, $\langle I_i^a | \hat{H}_I e^{\hat{T}_I} | I \rangle$, is drawn in Fig. 2, where we revert to the convention that i, j, k , etc. refer to occupied spin-orbitals and a, b, c , etc. to virtual (unoccupied) ones. It consists of open, connected, and thus linked diagrams except for the last one (2h), which is unlinked. This unlinked diagram will be canceled by the identical one (9b) appearing in the right-hand side, leaving a fully linked t -amplitude equation (see below). In this figure is also introduced a new vertex (2a), represented by a double-line with a circled “ I ”. It defines the one-electron part of the CC effective Hamiltonian operator $\hat{H}_I e^{\hat{T}_I}$ and is unlinked. It is the sum of the one-electron part of the usual single-reference CC effective Hamiltonian, $(\hat{H}_I e^{\hat{T}_I})_C$, which is connected as indicated by the subscript “C,” plus the last, unlinked diagram (2h).

Figure 3 draws the same matrix element, $\langle I_i^a | \hat{H}_I e^{\hat{T}_I} | I \rangle$, in the internal single-excitation space. It defines the off-diagonal element, H_{II} , where $|J\rangle = |I_i^a\rangle$ with $\epsilon_a - \epsilon_i = 0$. This figure appears almost the same as Fig. 2 with two crucial differences. First, the dangling lines are intersected by a fictitious resolvent line (red oblong), whose fictitious denominator is zero. This

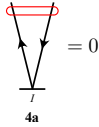


FIG. 4. The C-condition, $S_{JI} = 0$, of ACCSD [Eq. (22)], where $|J\rangle = |I_i^a\rangle$ with $\epsilon_a - \epsilon_i = 0$.

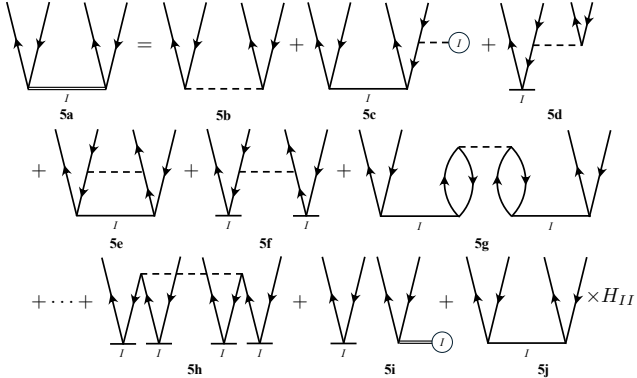


FIG. 5. The left-hand side, $\langle I_{ij}^{ab} | \hat{H}_I e^{\hat{T}_I} | I \rangle$, of the t -amplitude equation of ACCSD [Eq. (18)] in the external double-excitation space ($\epsilon_a + \epsilon_b - \epsilon_i - \epsilon_j \neq 0$). The double line with I (5a) designates the CC effective Hamiltonian $(\hat{H}_I e^{\hat{T}_I})_{\text{left out, right out}}$, which is unlinked through diagrams 5i and 5j.

resolvent is “fictitious” because it does nothing mathematically except to restrict the ranges of orbital indices to the ones that satisfy $\epsilon_a - \epsilon_i = 0$. Second, the last, unlinked diagram (2h) of Fig. 2 vanishes in Fig. 3 by virtue of the C-conditions [Eqs. (6) and (22)], which is diagrammatically depicted as Fig. 4. As a result, its double-line vertex with “ I ” (3a) now denotes the one-electron part of the connected, and thus linked CC effective Hamiltonian operator $(\hat{H}_I e^{\hat{T}_I})_C$.

Figure 5 illustrates the t -amplitude equation in the external double-excitation space, i.e., $\langle I_{ij}^{ab} | \hat{H}_I e^{\hat{T}_I} | I \rangle$ with $\epsilon_a + \epsilon_b - \epsilon_i - \epsilon_j \neq 0$. The last diagram (5j) is wholly unlinked, while the penultimate diagram (5i) is partially unlinked because of the unlinked diagram 2h of Fig. 2. The rest are linked. The sum of the last two diagrams (5i+5j) is reorganized in Fig. 6. It consists of a linked-disconnected diagram (6a) and an unlinked product (6b). The latter will be canceled by the same (13b).

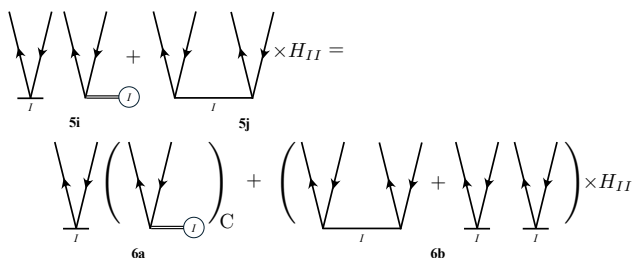


FIG. 6. The sum of the last two diagrams (5i+5j) of Fig. 5 can be reorganized as above, where $(\dots)_C$ is the connected part of Fig. 2, i.e., all of its diagrams except for the last (2h).

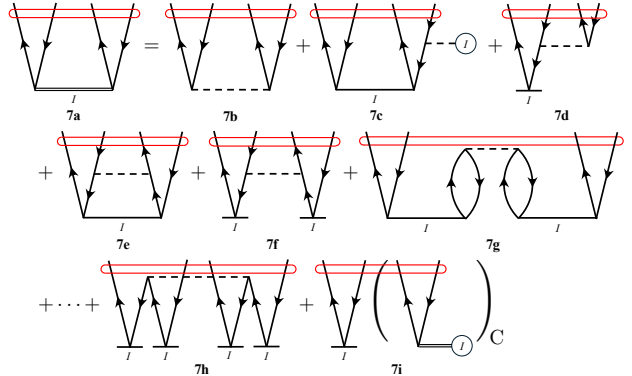


FIG. 7. The left-hand side, $\langle I_{ij}^{ab} | \hat{H}_I e^{\hat{T}_I} | I \rangle$, of the t -amplitude equation of ACCSD [Eq. (18)] in the internal double-excitation space, i.e., the off-diagonal energy, H_{JI} , with $|J\rangle = |I_{ij}^{ab}\rangle$. The red oblong denotes the fictitious resolvent line that demands $\epsilon_a + \epsilon_b - \epsilon_i - \epsilon_j = 0$. The double line with I (7a) designates the CC effective Hamiltonian $(\hat{H}_I e^{\hat{T}_I})_{\text{left out, right out}}$, which is linked. See Figs. 9.2 and 10.3 of Shavitt and Bartlett⁸ for a complete list of diagrams.

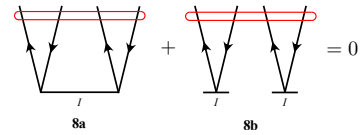


FIG. 8. The C-condition, $S_{JI} = 0$, of ACCSD [Eq. (21)], where $|J\rangle = |I_{ij}^{ab}\rangle$ with $\epsilon_a + \epsilon_b - \epsilon_i - \epsilon_j = 0$.

in the right-hand side of the t -amplitude equation (see below). Upon the cancellation, the t -amplitude equation will be fully linked (though partially disconnected) in the single- and double-excitation spaces.

Figure 7 is the same as Fig. 5, but in the internal double-excitation space, defining the off-diagonal element, H_{JI} , with $|J\rangle = |I_{ij}^{ab}\rangle$ with $\epsilon_a + \epsilon_b - \epsilon_i - \epsilon_j = 0$. Unlinked contributions akin to the last product (6b) of Fig. 6, do not exist in this figure because of the C-conditions [Eqs. (6) and (21)], which can be diagrammatically depicted as Fig. 8. The double-line vertex with label “ I ” (7a) thus denotes the two-electron part of the CC effective Hamiltonian $(\hat{H}_I e^{\hat{T}_I})_{\text{linked}}$, which is linked (partially linked-disconnected) in the internal space.

Let us move onto the right-hand sides of the t -amplitude equations. The one in the external single-excitation space, Eq. (25), is diagrammatically represented in Fig. 9. It corresponds to Eq. (25) term-by-term. The first term (9b) is unlinked and cancels the whole unlinked contribution in the corresponding left-hand side of the t -amplitude equation, i.e., the last term of Eq. (19) or diagram 2h of Fig. 2. This leaves the t -amplitude equation in the single-excitation space fully linked. However, this is not obvious because the rest of the diagrams (9c and 9d) in Fig. 9 do not even have the correct topology; they have too many dangling lines as compared with the left-hand side (9a).

We shall illustrate how these dangling lines are contracted with one another so that the diagrams are transformed into ones with the correct topology. Let us take the first prod-

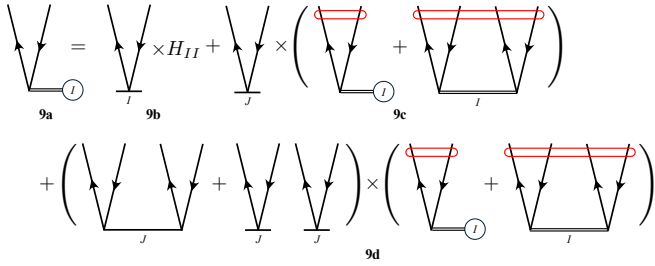


FIG. 9. The right-hand side of the t -amplitude equation of Δ CCSD [Eq. (25)] in the external single-excitation space ($\epsilon_a - \epsilon_i \neq 0$). Diagram **9b** is unlinked, and will cancel the sole unlinked term (**2h**) in the left-hand side of the t -amplitude equation. Subsequent diagrams have the wrong topology because some dangling lines are yet to be contracted (see the following figures and corresponding discussions in the main text).

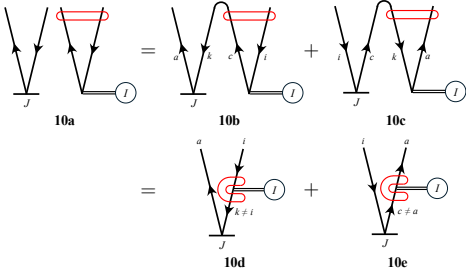


FIG. 10. The first product of **9c** in Fig. 9, which has the wrong topology, is first transformed into the sum of two “backward” or “folded” diagrams with the correct topology by contracting excess dangling lines with warped lines with dual hole/particle attribute. They are then transformed into the sum of two connected diagrams, which are isomorphic with single-reference CC diagrams. The line directions in diagrams **10d** and **10e** report the hole/particle distinction relative to the $|J\rangle$ vacuum.

uct of **9c** as an example (Fig. 10). This diagram represents $\langle I_{h_1}^{p_2} | J_{h_3}^{p_4} \rangle \langle J_{h_3}^{p_4} | e^{\hat{T}_J} | J \rangle \langle J | \hat{H}_I e^{\hat{T}_I} | I \rangle$ [the second term of Eq. (25)], where $|J\rangle$ and $|I\rangle$ are degenerate. Since $\langle I_{h_1}^{p_2} | J_{h_3}^{p_4} \rangle = \pm 1$, it is either that (i) $|J\rangle = \pm |I_i^c\rangle$ with $\epsilon_c - \epsilon_i = 0$ (but $c \neq i$) and $|I_i^a\rangle = \pm |J_k^a\rangle$ with $c = k$ but $k \neq i$ or that (ii) $|J\rangle = \pm |I_k^a\rangle$ with $\epsilon_a - \epsilon_k = 0$ (but $a \neq k$) and $|I_i^a\rangle = \pm |J_i^c\rangle$ with $c = k$ but $c \neq a$. In case (i), the virtual orbital (particle line) of the linked CC effective Hamiltonian $(\hat{H}_I e^{\hat{T}_I})_{\text{linked}}$ (double-line) vertex labeled c is identified as the occupied orbital (hole line) of the t_J vertex labeled k , and hence they should be one warped line. The contraction of these two lines results in diagram **10b**, an example of the “backward” diagram of Sandars^{114,117} or the “folded” diagram of Brandow^{113,115–117} in degenerate many-body perturbation theories (hereafter a folded diagram). Case (ii) corresponds to folded diagram **10c**, where the occupied k orbital of the $(\hat{H}_I e^{\hat{T}_I})_{\text{linked}}$ (double-line) vertex turns out to be the same as the virtual c orbital of the t_J vertex. So each warped line changes its hole/particle attribute as it goes from one vertex/vacuum to another vertex/vacuum.

At this stage, the two diagrams **10b** and **10c** have the correct topology as they are upward open with two dangling lines, and can thus be left as they are. They are also connected and thus

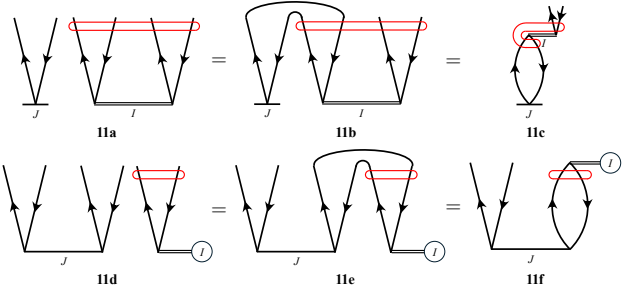


FIG. 11. Two other nontopological diagrams of Fig. 9 are transformed into the diagrams with the correct topology. They are connected and thus linked, and are isomorphic with single-reference CC diagrams.

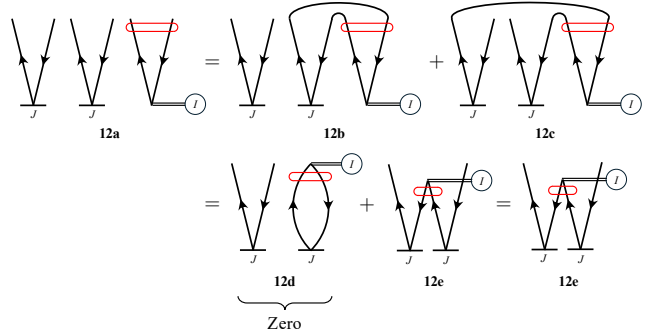


FIG. 12. Another nontopological diagram of Fig. 9 is transformed into the sum of two diagrams with the correct topology. The unlinked diagram is zero by virtue of the C-conditions (Fig. 4), leaving only the connected and thus linked diagram, which is isomorphic with a single-reference CC diagram.

linked.

It is also possible to flip the warped lines on the CC effective Hamiltonian (double-line) vertexes to arrive at diagrams **10d** and **10e**, which are isomorphic with the usual single-reference CC diagrams. It is more appropriate to change the line directions of the Hamiltonian (double-line) vertexes than of the excitation vertexes. In these diagrams, the hole/particle attribute of each line becomes unambiguous and is relative to the $|J\rangle$ vacuum. The red oblongs of fictitious resolvents, imposing line-index restrictions arising from the degeneracy of $|J\rangle$ and $|I\rangle$, become “C” shaped tubes. In diagram **10d**, this restricts the summation over index k to those that satisfy $\epsilon_k = \epsilon_i$ but $k \neq i$. In diagram **10e**, the fictitious resolvent demands $\epsilon_a = \epsilon_c$ but $c \neq a$.

Two other diagrams with incorrect topology in Fig. 9 are shown in Fig. 11. Two dangling lines of each disconnected subdiagram must be contracted with one another by warped lines to form folded diagrams with the correct topology. They are connected and thus linked. They can furthermore be transformed to diagrams isomorphic with the usual single-reference CC diagrams by shifting the double-line vertexes upward and straightening the warped lines. The hole/particle attributes are now relative to the $|J\rangle$ vacuum.

A three-part disconnected diagram in Fig. 9 is reproduced in Fig. 12. The correct topology can be restored by contract-

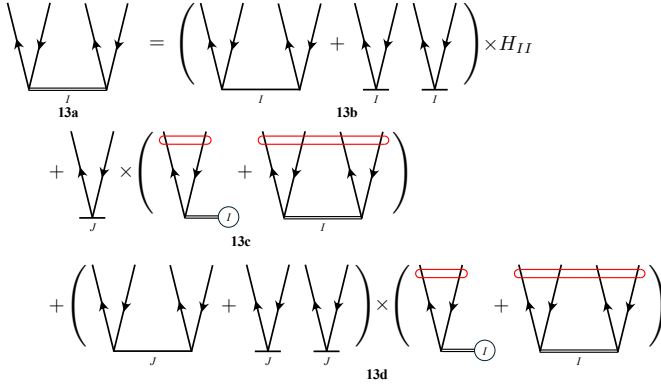


FIG. 13. The right-hand side of the t -amplitude equation of Δ CCSD [Eq. (24)] in the external double-excitation space ($\epsilon_a + \epsilon_b - \epsilon_i - \epsilon_j \neq 0$). Product **13b** is unlinked, and will cancel the whole unlinked contribution in the left-hand side of the t -amplitude equation (product **6b** of Fig. 6). Subsequent nontopological diagrams will be transformed into linked diagrams with the correct topology (see the following figures and corresponding discussions in the main text).

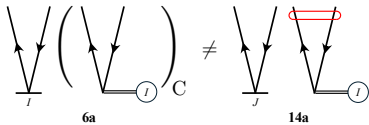


FIG. 14. A linked-disconnected diagram in product **13c** of Fig. 13 differs from and, therefore, does not cancel the linked-disconnected diagram **6a** of Fig. 6 with the same topology in the left-hand side of the t -amplitude equation. The Δ CC t -amplitude equations are generally disconnected, but always linked.

ing the two dangling lines of the double-line vertex with the two dangling lines of one t_J vertex (**12b** or **12d**) or one dangling line each from the two t_J vertexes (**12c** or **12e**). Folded diagram **12b** or **12d** is unlinked, while the other (**12c** or **12e**) is connected and linked. However, the unlinked diagram (**12b** or **12d**) is zero by virtue of the C-conditions [Eqs. (6) and (22) or Fig. 4]. Therefore, the right-hand side of the t -amplitude remains linked.

The diagrammatic representation of the right-hand side of the t -amplitude equation in the external double-excitation space is shown in Fig. 13. It is the literal diagrammatic translation of Eq. (24). The first product (**13b**) is unlinked, and it cancels exactly the whole unlinked contribution in the left-hand side, i.e., Eq. (26) or the last product (**6b**) in Fig. 6. Upon this cancellation, the t -amplitude equation in the external double-excitation space is fully linked.

The first product of **13c**, reproduced as diagram **14a** in Fig. 14, is linked-disconnected with the correct topology (upward open with four dangling lines). It does not cancel a similar linked-disconnected diagram (**6a**) in the left-hand side of the t -amplitude equation (Fig. 6) because diagram **6a** is made of the t_I and $(\hat{H}_I e^{\hat{T}_I})_C$ vertexes of the $|I\rangle$ vacuum, while diagram **14a** involves the t_J and internal $(\hat{H}_I e^{\hat{T}_I})_C$ vertexes. In short, the Δ CC equations are not necessarily connected, but always linked.

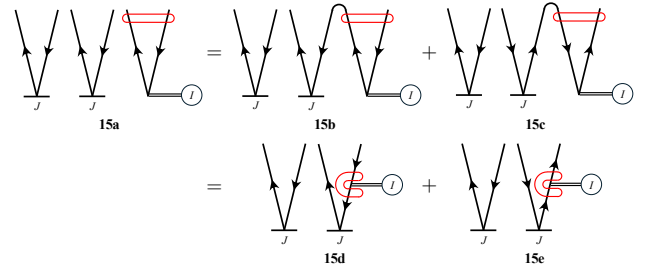


FIG. 15. Another nontopological diagram in Fig. 13 is transformed into linked-disconnected diagrams.

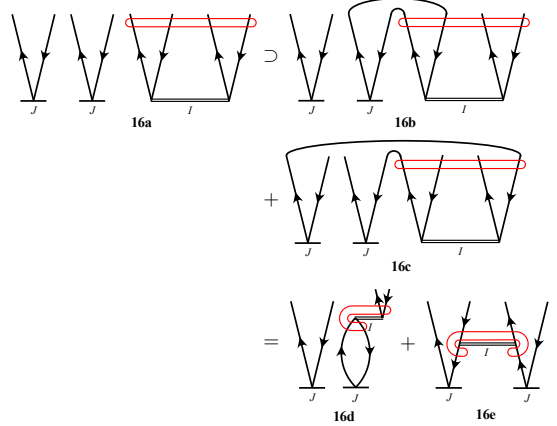


FIG. 16. Yet another nontopological diagram in Fig. 13 is transformed into the sum of linked-disconnected (**16d**) and connected (**16e**) diagrams. There are other contraction patterns (not shown).

The subsequent products in Fig. 13 have the wrong topologies with too many dangling lines only because excess lines are not contracted yet. A three-part disconnected diagram (**15a**) in Fig. 15 can be contracted to form two topologically correct, linked-disconnected diagrams. They are linked and do not violate size-extensivity.

Yet another three-part disconnected diagram (**16a**) of Fig. 16 can be contracted in various ways, all leading to linked diagrams, although some are disconnected.

To summarize, the only unlinked contributions in the left-hand sides of the t -amplitude equations in the external space are the ones that contain the factor of H_{II} , i.e., a closed disconnected part. They are canceled exactly by the same unlinked contributions in the right-hand sides of the respective equations. An off-diagonal element H_{JI} ($J \neq I$) is an open diagram, and any term containing it as a factor is generally linked. When the H_{JI} diagram itself has an unlinked contribution, the latter is always zero by virtue of the C-conditions. It can be readily inferred that these systematic cancellations and disappearances of unlinked terms apply to Δ CC theory of all orders. However, linked-disconnected diagrams persist in Δ CC theory, in contrast to the single-reference CC ansatz, where the sum of linked-disconnected diagrams is factored by the t -amplitude equation of a lower order and is hence zero, rendering the single-reference CC energy and amplitude equations fully connected.

F. Relationship to Li–Paldus multireference coupled-cluster theory

Li and Paldus proposed a state-universal multireference coupled-cluster (SUMRCC) theory with a general, incomplete model space.^{119–123} Here, an incomplete model space refers to any arbitrary set of Slater determinants, whereas a complete model space is the full-configuration-interaction determinant basis spanned by a set of “active” spin-orbitals. Li–Paldus SUMRCC theory is a generalization of the Jeziorski–Monkhorst SUMRCC theory,¹³⁴ the latter being limited to a complete model space.

There are other Hilbert-space multireference coupled-cluster theories, e.g., the state-specific Brillouin–Wigner coupled-cluster theory of Hubač, Pittner, and coworkers,^{135–139} and the state-specific multireference coupled-cluster theory of Mukherjee and coworkers.^{140–144} They are less closely related to the present ΔCC theory. For an excellent overview of these and various other multireference coupled-cluster theories, see Evangelista *et al.*¹⁴⁵ All of them require the user to specify active orbitals and/or multireferences based on their intuition, and are not a black-box method.

A complete set (in the usual sense of the words; not implying a complete model space) of M degenerate reference determinants is a special case of an incomplete model space. Therefore, Li–Paldus SUMRCC theory can serve as a degenerate coupled-cluster theory. Its ansatz then demands that the t -amplitudes satisfy the projected Schrödinger equation,

$$\hat{P}_I \hat{H}_I e^{\hat{T}_I} |I\rangle = \hat{P}_I \sum_{J=1}^M e^{\hat{T}_J} |J\rangle E_{JI} \quad (28)$$

with

$$H_{JI} = \langle J | \hat{H}_I e^{\hat{T}_I} | I \rangle, \quad (29)$$

under the so-called “C-conditions,”

$$S_{JI} = \langle J | e^{\hat{T}_I} | I \rangle = \delta_{JI}, \quad (30)$$

where $\mathbf{E} = \mathbf{S}^{-1} \mathbf{H}$ and the notations of symbols are the same as in Sec. II B. The energies are then obtained as the eigenvalues of the \mathbf{E} matrix. This ansatz bears striking similarity with that of ΔCC theory, and motivations or justifications for these equations are essentially the same as those for the ΔCC equations given in Sec. II B. For instance, the C-conditions are introduced to avoid one-to-many mapping of the references to the exact wave functions, which, if not avoided, would spoil the convergence to exactness.

However, ΔCC and Li–Paldus SUMRCC theories have one crucial difference: Many of the \hat{P}_I operators in the ansatz of ΔCC theory [Eqs. (5)–(8)] are absent in the above equations for Li–Paldus SUMRCC theory for degenerate references. These projectors are there to ensure that ΔCC theory treats all degenerate references on an equal footing, whereas Li–Paldus SUMRCC theory takes into account the correlation effects in the internal space more fully than in the external space. Consequently, the number and types of the terms in the formalism

of Li–Paldus SUMRCC theory vary depending on the details of degenerate references, while they are uniform in ΔCC theory. Consequently, Li–Paldus SUMRCC theory may not be written in a closed matrix-algebraic (as opposed to symbolic or string-based) form with a fixed number of terms, not being able to fulfill our desideratum of a black-box method. In ΔCC theory, in contrast, its diagrammatic formalism and matrix-algebraic algorithm are independent of the references.

Let us take the CCS instances of the two theories as an example to illustrate this important difference. When $|J\rangle = |I_{ij}^{ab}\rangle$, $E_{JI} = 0$ in ΔCCS because \hat{P}_I erases the configuration interaction across a double excitation, whereas in Li–Paldus SUMRCCS it is nonzero and captures a major double-excitation correlation effect within the internal space. Hence, Li–Paldus SUMRCCS is more accurate than ΔCCS at a commensurately elevated cost. The effective excitation rank of Li–Paldus SUMRCCS is ambiguous and in between the CCS and CCSD levels in this example of degenerate references. In contrast, ΔCCS treats correlation effects from all determinants — internal or external — more uniformly at the CCS level. Furthermore, Li–Paldus SUMRCCS formula for E_{JI} has to transmogrify depending the excitation rank of $|J\rangle$ relative to $|I\rangle$.

In summary, Li–Paldus SUMRCC theory of a given rank is always more accurate than ΔCC theory of the same rank simply because the former takes into account higher-order Hamiltonian and overlap matrix elements, although both are convergent at exactness (Sec. II L). The former is also commensurately more expensive. Li–Paldus SUMRCC theory is size-extensive as proven by the original authors¹²³ (see also a related, elegant proof by Jeziorski and Monkhorst¹³⁴) and so is ΔCC theory. ΔCC theory is a black-box method, while Li–Paldus SUMRCC theory is not.

G. Relationship to two-determinant coupled-cluster theory

The single-reference CC ansatz (Sec. II A) was generalized to doubly degenerate references by Balková, Bartlett, and their coworkers under the name: two-determinant coupled-cluster theory or TD-CC for short.^{107–112} Its instance including the single and double excitations, i.e., TD-CCSD, was adopted as a “ΔCCSD” method for doubly degenerate references in the performance survey conducted by Damour *et al.*¹⁰⁶

This TD-CC ansatz and the present ΔCC theory are both size-extensive, black-box, degenerate coupled-cluster theories, but they differ in two respects. First, the former (TD-CC) adopts a specific pair of degenerate determinants as references, which form an open-shell singlet state, while the latter (ΔCC) can handle any and all degenerate and nondegenerate references. Second, TD-CC theory is based on the SUMRCC ansatz of Meissner *et al.*,¹⁴⁶ which is, in turn, distinguished from Li–Paldus SUMRCC theory by the absence and presence, respectively, of the C-condition. Neither the SUMRCC theory of Meissner *et al.*¹⁴⁶ nor TD-CC theory is expected to converge at FCI upon increasing the excitation rank. Since ΔCC theory also employs the C-condition, it is one-step more removed from TD-CC theory than from Li–Paldus SUMRCC

theory.

H. Relationship to degenerate Rayleigh–Schrödinger perturbation theory

Single-reference Rayleigh–Schrödinger perturbation theory^{8,25} stipulates its n th-order correction to the I th-state energy to be

$$E_I^{(n)} = \langle I^{(0)} | \hat{V} | I^{(n-1)} \rangle, \quad (31)$$

where the Hamiltonian is partitioned into the zeroth-order Hamiltonian and perturbation operator as $\hat{H} = \hat{H}_0 + \hat{V}$, and $|I^{(n)}\rangle$ is the n th-order correction to the I th-state wave function and $|I^{(0)}\rangle = |I\rangle$ (a single Slater determinant). The $|I^{(n)}\rangle$ is obtained recursively as

$$|I^{(n)}\rangle = \hat{R}_I \left(\hat{V} |I^{(n-1)}\rangle - \sum_{i=1}^{n-1} |I^{(n-i)}\rangle E_I^{(i)} \right), \quad (32)$$

where the resolvent, $\hat{R}_I = (E_I^{(0)} - \hat{H}_0)^{-1}$, is understood to project out all determinants that lead to a division by zero (the summation in the above is also understood to vanish when $n = 1$). Here, we confine ourselves to the Møller–Plesset partitioning of the Hamiltonian. This single-reference n th-order Møller–Plesset perturbation (MP n) theory¹⁴⁷ is convergent at exactness (FCI) as $n \rightarrow \infty$ unless divergent. It is equivalent to the n th-order MBPT or MBPT(n) for $n \geq 2$,^{8,25} although the latter is formulated with linked diagrams only and explicitly size-extensive.^{8,148–153}

This ansatz was generalized by Hirschfelder and Certain¹¹⁸ to degenerate references. Several other groups developed essentially the same theory under different names.^{113–117,154} We called this theory (with the same Møller–Plesset partitioning) Δ MP n ,^{125,126} where n is the perturbation order and Δ carries the dual meaning of ‘difference’ and ‘degeneracy’.

The perturbative corrections to the degenerate state energies constitute an M -by- M non-Hermitian¹¹⁷ matrix of the form,

$$E_{JI}^{(n)} = \langle J^{(0)} | \hat{V} | I^{(n-1)} \rangle, \quad (33)$$

of which the perturbation corrections to the wave functions are given recursively by

$$|I^{(n)}\rangle = \hat{R}_I \left(\hat{V} |I^{(n-1)}\rangle - \sum_{i=1}^{n-1} \sum_{J=1}^M |J^{(n-i)}\rangle E_{JI}^{(i)} \right), \quad (34)$$

where the resolvent, $\hat{R}_I = (E_I^{(0)} - \hat{H}_0)^{-1}$, in this case, projects out all degenerate reference determinants that would cause a division by zero, and thus plays a somewhat analogous role as the C-conditions of Δ CC theory [Eq. (6)]. The n th-order perturbation correction to the I th-state energy is an eigenvalue of the matrix $\mathbf{E}^{(n)}$:

$$\sum_{J=1}^M E_{KJ}^{(n)} C_{JI} = C_{KI} \tilde{E}_I^{(n)}, \quad (35)$$

which mirrors the Δ CC energy of Eq. (11).

Δ MP n theory reduces to MP n theory when $M = 1$. Δ MP n theory is convergent at exactness for all degenerate reference states as $n \rightarrow \infty$ unless divergent.¹¹⁸ The initial degeneracy may persist or be partially or fully lifted with increasing n .¹¹⁸ It can be applied to any degenerate or nondegenerate determinant references with any numbers of α - and β -spin electrons, any spin multiplicities, and any spatial symmetries, without any modification to its algebraic working equations. It is size-extensive.¹¹⁷

It is evident that Δ CC theory is a faithful coupled-cluster extension of Δ MP n theory outlined above; Δ CC theory is to Δ MP n theory as (single-reference) CC theory is to (single-reference) MP n theory.

Δ MP n theory applies Rayleigh–Schrödinger perturbation theory to all degenerate references simultaneously, forming the energy matrix $\mathbf{E}^{(n)}$.¹¹⁸ The diagonalization of this matrix then determines the linear combinations of the degenerate determinants, which converge at the projection of the exact wave functions onto the degenerate-determinant space as $n \rightarrow \infty$. Hence, the motivations and justifications of the Δ MP n ansatz are identical to those of Δ CC theory, both of which are black-box methods. The energy corrections, $\tilde{E}_I^{(n)}$, thus defined satisfies the canonical definition of converging, size-extensive perturbation theory, i.e.,

$$\tilde{E}_I^{(n)} = \frac{1}{n!} \left. \frac{\partial^n E_I}{\partial \lambda^n} \right|_{\lambda=0}, \quad (36)$$

where E_I is the exact I th-state energy and $\hat{H} = \hat{H}_0 + \lambda \hat{V}$. The compliance to this canonical definition implies its size-extensivity,⁸ without needing a formal proof of the linked-diagram theorem.^{8,148–153} It may be said that other numerous postulates of degenerate perturbation theories are fundamentally inferior to this *canonical* Δ MP ansatz based on Eq. (36). By extension, Δ CC theory introduced here is also the *canonical* degenerate coupled-cluster theory because it is an infinite diagram resummation of Δ MP theory.

Just like Δ CC theory, but unlike Li–Paldus SUMRCC theory, the highest excitation rank taken into account from each degenerate reference is the same in Δ MP theory. For example, the first-order correction to $|I^{(0)}\rangle$ is limited to one- and two-electron excitations from $|I^{(0)}\rangle$,

$$\begin{aligned} |I^{(1)}\rangle = & \sum_i^{\text{occ. in } |I\rangle} \sum_a^{\text{vir. in } |I\rangle} |I_i^a\rangle \frac{\langle i | \hat{f}_i | a \rangle}{\epsilon_i - \epsilon_a} \\ & + \sum_{i < j}^{\text{occ. in } |I\rangle} \sum_{a < b}^{\text{vir. in } |I\rangle} |I_{ij}^{ab}\rangle \frac{\langle ij | ab \rangle}{\epsilon_i + \epsilon_j - \epsilon_a - \epsilon_b}, \end{aligned} \quad (37)$$

regardless of the details of the degenerate reference determinants such as the degrees of spin-orbital differences, where ϵ_p is the p th spin-orbital energy of the orbital reference. Consequently, the first iterative cycle (indicated by superscript “[1]”) of the Δ CCSD calculation with zero initial t -amplitudes yields the Δ MP1 wave functions for all degenerate references,

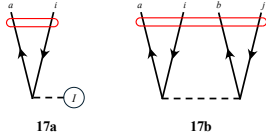


FIG. 17. The off-diagonal first-order correction to energy, $E_{JI}^{(1)}$, is represented by diagram 17a when $|J\rangle = |I_i^a\rangle$ or by diagram 17b when $|J\rangle = |I_{ij}^{ab}\rangle$. The dashed line with circled I denotes $(f_I)_{in}^{out} - \epsilon_{out}\delta_{out,in}$, while the dashed line translates to $(v)_{left\ in,\ right\ out}^{left\ out,\ right\ in}$. The red oblongs denote fictitious resolvent lines with zero fictitious denominator, i.e., $\epsilon_a - \epsilon_i = 0$ in 17a or $\epsilon_a + \epsilon_b - \epsilon_i - \epsilon_j = 0$ in 17b.

i.e.,

$$(t_I^{[1]})_i^a = \frac{\langle i|\hat{f}_I|a\rangle}{\epsilon_i - \epsilon_a}, \quad (38)$$

$$(t_I^{[1]})_{ij}^{ab} = \frac{\langle ij|ab\rangle}{\epsilon_i + \epsilon_j - \epsilon_a - \epsilon_b}, \quad (39)$$

as well as the Δ MP2 energies *if and only if* the $\hat{T}_I^2/2!$ contribution to the energy is neglected; note that $(t_I^{[1]})_i^a$ is generally nonzero when the I th determinant is not the orbital reference. Therefore, Δ MP2 energy is recovered in the first iterative cycle (with zero initial t -amplitudes and zero $(t_I^{[1]})_i^a$ -amplitudes) of Δ CCSD. This familiar relationship between CCSD and MP2 is maintained between Δ CCSD and Δ MP2.

Let us further examine the relationship diagrammatically. The Møller–Plesset partitioning of the Hamiltonian means

$$\hat{H}_0 = E_{II}^{(0)} + \sum_p \epsilon_p \{ \hat{p}^\dagger \hat{p} \}, \quad (40)$$

$$\begin{aligned} \hat{V} = E_{II}^{(1)} + \sum_{p \neq q} & \left((f_I)_q^p - \epsilon_p \delta_{pq} \right) \{ \hat{p}^\dagger \hat{q} \} \\ & + \frac{1}{4} \sum_{p,q,r,s} (v)_{rs}^{pq} \{ \hat{p}^\dagger \hat{q}^\dagger \hat{s}^\dagger \hat{r} \}, \end{aligned} \quad (41)$$

where

$$E_{II}^{(0)} = E_{\text{nuc.}} + \sum_i^{\text{occ. in } |I\rangle} \epsilon_i, \quad (42)$$

$$E_{II}^{(1)} = E_I^{\text{HF}} - E_{II}^{(0)}. \quad (43)$$

The off-diagonal first-order corrections to energy, $E_{JI}^{(1)} = \langle J|\hat{V}|I\rangle$, are diagrammatically depicted in Fig. 17. Note that $E_{JI}^{(n)}$ with $J \neq I$ is an open diagram and also linked, despite its designation as an “energy,” and hence any term containing it as a factor does not immediately imply the violation of size-extensivity.

Likewise, the first-order corrections to the I th reference wave function, $|I^{(1)}\rangle = \hat{R}_I \hat{V} |I^{(0)}\rangle$, are represented by diagrams in Fig. 18. These two figures look identical except for the resolvent lines. The diagrams in Fig. 17 have fictitious resolvent lines (the red oblongs) which do nothing mathematically, but indicate that the corresponding fictitious denominators are zero because of the degeneracy of $|J\rangle$ and $|I\rangle$. The diagrams in

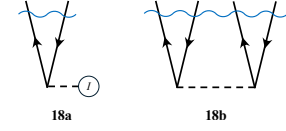


FIG. 18. The first-order correction to the I th reference wave function, $|I^{(1)}\rangle$. Its projection onto the single-excitation space is represented by diagram 18a, while its projection onto the double-excitation space by diagram 18b. The blue wiggly lines denote resolvent lines.

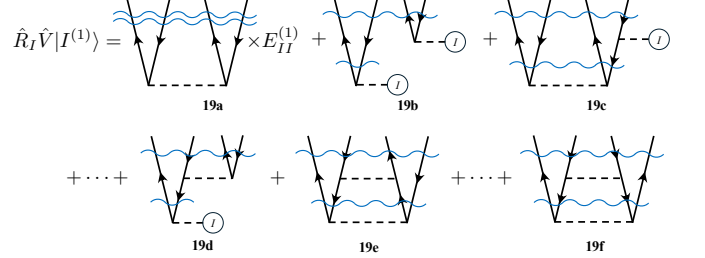


FIG. 19. The diagrammatic representation of the principal part of the second-order correction to the I th reference wave function, i.e., the first term of Eq. (44), in the double-excitation space. Diagram 19a is unlinked.

Fig. 18 have actual resolvent lines (the blue wiggly lines) due to \hat{R}_I .

The second-order correction to the I th reference wave function is then written as

$$|I^{(2)}\rangle = \hat{R}_I \hat{V} |I^{(1)}\rangle - \hat{R}_I \sum_{J=1}^M |J^{(1)}\rangle E_{JI}^{(1)}. \quad (44)$$

The diagrammatic representation of the first term (the principal part) of the right-hand side is given in Fig. 19 in the case of its projection onto the double-excitation space. The first diagram (19a) is unlinked, while all the others are linked. The second term (the renormalization part) of the right-hand side in the double-excitation space is diagrammatically depicted in

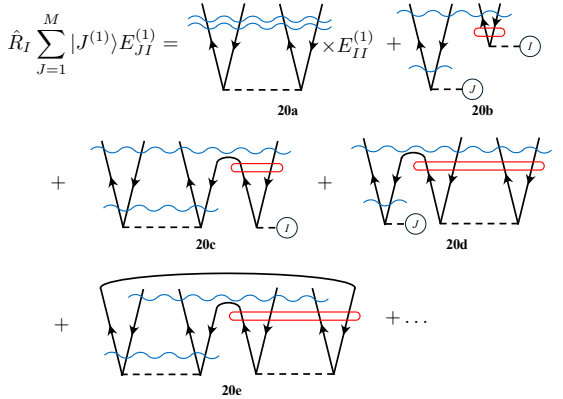


FIG. 20. The diagrammatic representation of the renormalization part of the second-order correction to the I th reference wave function, i.e., the second term of Eq. (44), in the double-excitation space. Diagram 20a is unlinked.

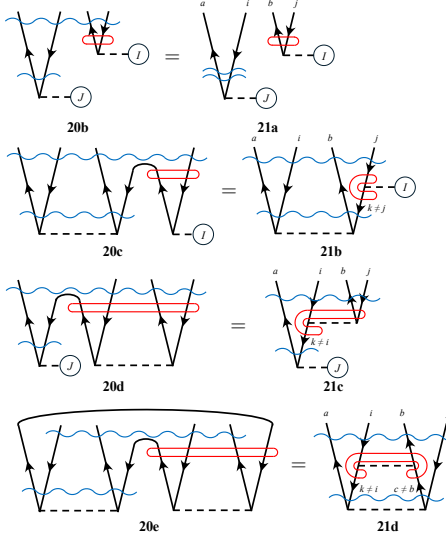


FIG. 21. A transformation of the folded diagrams with warped lines in Fig. 20 into Δ CC-like diagrams with lines straightened.

Fig. 20. Its first diagram (**20a**) is unlinked and identical to diagram **19a**, cancelling each other out. The same cancellation occurs in the single-excitation space, leaving only linked diagrams in Eq. (44) and proving the size-extensivity of Δ MP2 wave function and Δ MP3 energy.

Figure 20 has many folded diagrams,^{113–117} where the two upward open subdiagrams of $|J^{(1)}\rangle$ and $E_{JI}^{(1)}$ are linked by common indices represented by warped lines. Each warped line is a hole line (occupied orbital) for one disconnected subdiagram (before the linking), but is also a particle line (virtual orbital) for the other. The disconnected part corresponding to $E_{JI}^{(1)}$ is acted on by the fictitious resolvent line (the red oblong), restricting the index ranges to those whose corresponding fictitious denominators are zero. The other disconnected part representing $|J^{(1)}\rangle$ is intersected by an actual resolvent line (the blue wiggly line), whose denominator is never zero. The whole diagram is again intersected at the top by another actual resolvent line of \hat{R}_I .

These folded diagrams can be transformed into diagrams isomorphic with usual single-reference MBPT diagrams, with the warped lines straightened. One way to do this is to lift the $E_{JI}^{(1)}$ subdiagram part with fictitious resolvent line and changing the direction of the warped line anchored to it, as shown in Fig. 21. We then arrive at diagrams that resemble Δ CC diagrams shown in Sec. II E, in which the fictitious resolvent lines are now warped into ‘‘C’’ shaped tubes. The line directions now indicate the hole/particle distinction relative to the $|J\rangle$ vacuum. This diagrammatic correspondence suggests that Δ CC theory is an infinite diagram resummation of Δ MP theory just as CC theory is of MBPT.

Alternatively, the $|J^{(1)}\rangle$ subdiagram can be lifted and the direction of the warped line anchored to it can be reversed, as shown in Fig. 22. The warped line is now straightened and its direction unambiguously indicates the hole/particle distinction relative to the $|I\rangle$ vacuum, at the expense of making the bottom resolvent line warped into the ‘‘C’’ shape. In each

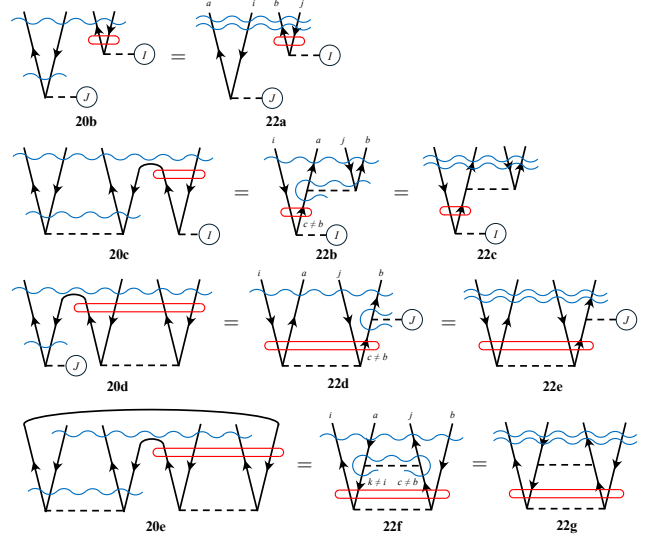


FIG. 22. An alternative transformation of the folded diagrams with warped lines in Fig. 20 into diagrams with lines straightened, and then into the so-called ‘‘renormalization diagrams’’¹⁵⁵ with resolvent lines shifted up.

diagram, the warped resolvent line can be shifted up, piling on the top resolvent line by virtue of the zero orbital-energy differences represented by the fictitious resolvent lines. For example, in diagram **20b** of Fig. 21, the bottom actual resolvent line is associated with $(\epsilon_i - \epsilon_a)^{-1}$. This is equal to $(\epsilon_i + \epsilon_j - \epsilon_a - \epsilon_b)^{-1}$ represented by one of the two longer resolvent lines in diagram **22a** by virtue of the fictitious resolvent line demanding $\epsilon_j - \epsilon_b = 0$. Likewise, the warped resolvent line $(\epsilon_c + \epsilon_j - \epsilon_a - \epsilon_b)^{-1}$ of diagram **22b** can straighten, move up, and pile onto the top resolvent line $(\epsilon_i + \epsilon_j - \epsilon_a - \epsilon_b)^{-1}$ because of the fictitious resolvent line $\epsilon_i - \epsilon_c = 0$ to become diagram **22c**. We thus arrive at the diagrams that are isomorphic with the ‘‘renormalization diagrams’’ (so called because they too originate from the renormalization term of the Rayleigh–Schrödinger recursion) of finite-temperature many-body perturbation theory,¹⁵⁵ in which resolvent lines corresponding to a zero denominator are shifted up.

I. Relationship to equation-of-motion coupled-cluster theory

There is no simple relationship between Δ CC and equation-of-motion coupled-cluster (EOM-CC) theories^{10,22,69–76} as they are based on different design philosophies. In EOM-CC theory, the I th-state energy, \tilde{E}_I , is obtained by solving the following equation for the linear operator \hat{C}_I :

$$\hat{P}_0 \hat{H} e^{\hat{T}_0} \hat{C}_I |0\rangle = \hat{P}_0 e^{\hat{T}_0} \hat{C}_I |0\rangle \tilde{E}_I \quad (45)$$

or equivalently,

$$\hat{P}_0 (e^{-\hat{T}_0} \hat{H} e^{\hat{T}_0}) \hat{C}_I |0\rangle = \hat{P}_0 \hat{C}_I |0\rangle \tilde{E}_I, \quad (46)$$

where $|0\rangle$ is typically, but not necessarily, the neutral, singlet, ground-state determinant, which is nondegenerate, and

\hat{P}_0 is the projector onto the determinant space spanned by $(1 + \hat{T}_0)|0\rangle$. The amplitudes of \hat{T}_0 are, in turn, pre-determined by single-reference CC theory by solving the following equation for \hat{T}_0 :

$$\hat{P}_0(e^{-\hat{T}_0}\hat{H}e^{\hat{T}_0})|0\rangle = \hat{P}_0|0\rangle\tilde{E}_0, \quad (47)$$

which is equivalent to Eq. (1) for $I = 0$. Since \hat{T}_0 and \hat{C}_I commute, acting \hat{C}_I from the left on both sides of Eq. (47) and subtracting it from Eq. (46), we arrive at an equation-of-motion method with the CC effective Hamiltonian, $e^{-\hat{T}_0}\hat{H}e^{\hat{T}_0}$,

$$\hat{P}_0\left[\left(e^{-\hat{T}_0}\hat{H}e^{\hat{T}_0}\right), \hat{C}_I\right]|0\rangle = \hat{P}_0\hat{C}_I|0\rangle\tilde{\omega}_I, \quad (48)$$

where $\tilde{\omega}_I = \tilde{E}_I - \tilde{E}_0$.

At this point, there is considerable latitude in choosing the form of \hat{C}_I . When \hat{C}_I is an excitation operator of the same rank as \hat{T}_0 , Eq. (48) is connected (and thus linked), postulating a size-extensive and intensive method for the excitation energy from the ground to the I th excited state.^{22,69–76} When \hat{C}_I is an ionization or electron-attachment operator, this ansatz defines ionization-potential (IP) or electron-attachment (EA) EOM-CC theory.^{90–97} The \hat{C}_I can be a double-ionization operator, postulating the double-ionization-potential (DIP) EOM-CC theory.^{156–159} The double-electron-attachment (DEA) EOM-CC theory^{158,160,161} has also been introduced. The \hat{C}_I can even incorporate a spin-flip operation, leading to various spin-flip EOM-CC theories,^{162–164} which have been shown to have superior performance. To maintain the size-extensivity and intensivity, the rank of \hat{C}_I needs to be chosen carefully.¹³³

The size-extensive and intensive ansatz of EOM-CC theory (i.e., the ranks of \hat{T}_0 and \hat{C}_I are the same) is naturally derived by the first-order time-dependent perturbation (linear response) theory applied to single-reference CC theory.^{77,81–83} In this picture, $e^{\hat{T}_0}$ describes the electron correlation in, typically, a neutral, singlet, nondegenerate ground state, whose wave function has an exponential structure, while \hat{C}_I takes care of an excitation process, dominated by just a few destination determinants, which are often degenerate and automatically linearly combined in a spin- and spatial-symmetry-adapted manner.

In Δ CC theory, in contrast, massive electron rearrangements caused by excitations, ionizations, electron attachments, spin flips, etc. are described by a reference wave function, which needs not be any more complicated than a single determinant or a linear combination of degenerate determinants with appropriate electron occupancies. Electron correlation thereof is then a small perturbation captured by an exponential operator.

Generally, Δ CC and EOM-CC theories are complementary to each other as follows (see also Sec. IV):

(1) *Accuracy*: Δ CC theory treats each state on an equal footing and is applicable to all possible states in one and the same uniform formalism. It is only slightly dependent on the spin-orbitals used to define determinants (i.e., the orbital reference), but otherwise it does not rely on any particular state or the fidelity of its description. EOM-CC theory, on the other hand, relies on the accurate CC description of the nondegen-

erate ground state and reaches excited or other states by simulated one-photon absorption, ionization, etc. processes. As a result, EOM-CC theory cannot describe multi-electron processes as accurately as one-electron processes and does not even have roots with excitation ranks exceeding the truncation order of \hat{C}_I . The accuracy of Δ CC theory is much more uniform and primarily determined by how dominant the reference determinants are in the exact wave functions, i.e., the degree of strong correlation or presence of intruder states.^{165,166}

(2) *Applicability*: Δ CC theory can home in on any state out of order with any numbers of α - and β -spin electrons, spin multiplicities, or spatial symmetries. In contrast, EOM-CC theory can determine the energies of several lowest-lying states using a trial-vector algorithm,^{167–170} which is robust and extremely efficient. The latter algorithm may, nonetheless, miss some lower-lying states with high spin multiplicities depending on the initial guesses, and has difficulty homing on in high-lying states such as core excitations/ionizations. However, most applications of EOM-CC theory are spectral simulation of one-photon absorption, ionization, etc., and its selective superior performance for excitations/ionizations with sizable one-photon transition probabilities may be deemed a practical advantage. EOM-CC theory also naturally defines oscillator strengths for the transitions from the ground state, which may prove more cumbersome with Δ CC theory, where the wave functions of two different references are not necessarily orthogonal to each other.

(3) *Computational Cost*: Δ CC theory solves nonlinear t -amplitude equations for any state, and suffers from convergence difficulties far more frequently than EOM-CC theory, whose algorithms are exceedingly stable. Δ CC theory also encounters complex energies⁶⁴ more often than EOM-CC theory. The latter can have complex energies in principle, but almost never does in practice. Δ CC theory has the same cost scaling per state as EOM-CC theory of the same rank, e.g., $O(n^4)$ for CCS, $O(n^6)$ for CCSD, etc., where n is the number of spin-orbitals. However, the prefactor of the cost function of Δ CC theory is much greater than that of EOM-CC theory at least in the primitive optimal-scaling algorithm of the former implemented in this study.

(4) *Development Cost*: In the existing paradigm, one must separately develop the CC theory series through a high rank for ground states, the EOM-CC series for excited states,^{75,76} the IP-EOM-CC series for ionized states, the EA-EOM-CC series for electron-attached states, the DIP-EOM-CC series for doubly ionized states, and so on. For Δ CC theory, in contrast, just one formulation and code at a given rank suffice in all possible cases. Streamlined formulations, advanced optimizations, and proven algorithms already available for single-reference CC theory are likely reusable in efficient and robust Δ CC implementations. In this sense, Δ CC theory may prove economical in terms of the development cost. Recall that the cost of *ab initio* theory developments has become so great that expert systems (a type of artificial intelligence) have been invoked for decades.^{127,128}

J. Relationship to Green's function theory

Several groups have argued that a coupled-cluster version of one-particle many-body Green's function (MBGF) theory^{125,126,171–185} is IP- and EA-EOM-CC theories.^{98–104} Here, we propose an alternative viewpoint in which an equally natural coupled-cluster extension of MBGF theory is Δ CC theory.

The Δ MP n energy differences (as described in Sec. II H) between the nondegenerate neutral and ionized (or electron-attached) states are equal to the n th-order MBGF or MBGF(n) method in the diagonal, frequency-independent approximation to the self-energy for $n \leq 3$.^{125,126,174,186} At $n = 4$, Δ MP n and MBGF(n) begin to diverge from each other with the difference being the so-called semireducible and linked-disconnected diagram contributions.^{125,126} As $n \rightarrow \infty$, Δ MP n converges at exact IPs and EAs (unless it diverges) for both Koopmans and non-Koopmans (satellite) states, as the semireducible and linked-disconnected diagrams recuperate the effects of off-diagonal elements and frequency-dependence of the self-energy, respectively. As $n \rightarrow \infty$, MBGF(n) with the nonapproximated (beyond the perturbation approximation) self-energy also converges at exactness for most Koopmans states.^{125,126} Surprisingly, for most other states, MBGF(n) converges at wrong limits.¹²⁴ The root cause of this nonconvergence has been identified¹²⁴ as the nonanalyticity of Green's functions, which, therefore, cannot be expanded in a converging power series in many frequency domains. In this sense, the Feynman–Dyson perturbative MBGF theory is fundamentally flawed, whereas Δ MP n is sound and robust as it directly expands energies and wave functions (instead of Green's functions), which are analytic.

One route to generalizing a perturbation theory to a coupled-cluster theory is to perform an infinite partial resummation of diagrams. Summing all ladder and ring diagrams of MBPT leads to D-MBPT(∞) of Bartlett and Shavitt,^{187,188} which is identified as the linearized coupled-cluster doubles (LCCD) method.⁸ Summing all ladder and ring diagrams of Δ MP n theory for IPs and EAs defines the Tamm–Danoff approximation (TDA) and random-phase approximation (RPA), which can then be viewed as coupled-cluster theory for IPs and EAs.

As discussed in Sec. II H, in the first iterative cycle, an Δ CCSD calculation with zero initial t -amplitudes and zero $(t_I^{[1]})_i^a$ -amplitudes gives the Δ MP1 t -amplitudes and Δ MP2 ionization or electron-attachment energy for a nondegenerate or degenerate, ionized or electron-attached reference(s). The latter is equal to the MBGF(2) result in the diagonal, frequency-independent approximation. This relationship supports the notion that Δ CC theory is a coupled-cluster extension of MBGF theory; the Δ CC self-energy diagram is an infinite partial resummation of the Δ MP n self-energy diagrams, while the latter are obtained by cutting one line (or a loop) of the Δ MP n energy diagrams in a non-HF reference.¹²⁶ (Such infinite diagram resummations seem difficult without first imposing the frequency-independent approximation, but it does not spoil the convergence to exactness.)

The self-energy of Δ CC theory is diagonal, decoupling the

IP and EA sectors. It is also frequency-independent, while the MBGF self-energy is frequency-dependent. Δ CC theory as a CC Green's function may thus be criticized for not meeting the mathematical definition of a Green's function or not possessing the physical meanings and properties of a Feynman propagator.¹⁸⁹ However, both Δ CC and Δ MP n theories are convergent at exactness (unless divergent) for all states, while MBGF is fundamentally nonconvergent for most states,¹²⁴ the latter owing to its very reliance on the nonanalytic Green's function. In this sense, Δ CC and Δ MP n theories (as well as IP- and EA-EOM-CC theories) are superior to MBGF, and there may not be any practical advantage of placing the former in the framework of Green's function theory.

K. Relationship to Hartree–Fock theory

According to the Thouless theorem,¹⁹⁰ a coupled-cluster-singles (CCS) wave function is a single Slater determinant,

$$|\Psi\rangle = e^{\hat{T}_1} |\Phi\rangle, \quad (49)$$

where both $|\Psi\rangle$ and $|\Phi\rangle$ designate a Slater determinant composed of a respective set of orthogonal spin-orbitals, and \hat{T}_1 is the one-electron excitation operator. When $|\Phi\rangle$ is normalized, $|\Psi\rangle$ is not; instead, $|\Psi\rangle$ is intermediately normalized, i.e., $\langle \Psi | \Phi \rangle = 1$.

One can define a generalized Hartree–Fock theory for a nondegenerate reference in at least two ways. One is to vary spin-orbitals that constitute $|\Phi\rangle$ or, equivalently, to vary \hat{T}_1 for a fixed $|\Phi\rangle$, so that its expectation value of \hat{H} is minimized,

$$\min \frac{\langle \Phi | e^{\hat{T}_1^\dagger} \hat{H} e^{\hat{T}_1} | \Phi \rangle}{\langle \Phi | e^{\hat{T}_1^\dagger} e^{\hat{T}_1} | \Phi \rangle}. \quad (50)$$

The latter is identified as postulating the variational coupled-cluster (VCC) method^{191–200} limited to singles (VCCS) (see also Refs.^{69,201,202}). However, because this VCC ansatz cannot be easily extended to VCCSD and higher owing to its nonterminating working equations,^{191–200} we shall not consider it in this article, except to show in Appendix that the nonterminating equations is nevertheless tractable at the VCCS level.

The other is to demand that the CCS wave function satisfy the Schrödinger equation within the determinant space spanned by $(1 + \hat{T}_1)|\Phi\rangle$:

$$\langle \Phi | \hat{H} e^{\hat{T}_1} | \Phi \rangle = \langle \Phi | E e^{\hat{T}_1} | \Phi \rangle, \quad (51)$$

$$\langle \Phi_i^a | \hat{H} e^{\hat{T}_1} | \Phi \rangle = \langle \Phi_i^a | E e^{\hat{T}_1} | \Phi \rangle, \quad \forall a, \forall i, \quad (52)$$

which is identified as the projection CCS method. This is distinct from the usual, variational HF theory unless the orbital reference is already a HF solution (in which case, $\hat{T}_1 = 0$ is a trivial solution). The projection CCS energy is bounded from below by the corresponding, variational HF energy.⁶⁹ It has the advantage of being straightforwardly extensible to CCSD and higher. If we adopt this projection CCS as a generalized, *projection* HF theory, Δ CCS (Sec. II C) is its natural extension to degenerate references. Its performance will be discussed in Sec. IV.

The sum of the zeroth- and first-order energies [Eqs. (42) and (43)] of single-reference Møller-Plesset perturbation theory recovers the HF energy expression or the expectation value of the Hamiltonian in a single Slater determinant. Therefore, it may be argued that the Δ MP1 method is another projection HF theory for degenerate and nondegenerate references. It is a “projection” HF theory because the orbitals in the reference determinants are predetermined and not varied. We shall examine its performance in Sec. IV.

On the other hand, it does not seem appropriate to view Li and Paldus’s SUMRCCS as any kind of HF theory because it fully accounts for correlation effects due to two-electron and higher-order excitations within the internal space, while a HF theory is not supposed to take into account correlation effects beyond classical Coulomb and exchange effects.

L. Relationship to the full-configuration-interaction method

The t -amplitudes of the single-reference *full* CC method can be restored uniquely and unambiguously from the excitation amplitudes (c -amplitudes) of FCI. This process is called the cluster analysis, and its feasibility decides whether a CC theory forms a converging series toward FCI. It has been established by Li and Paldus^{119,120} that the cluster analysis is feasible for their SUMRCC theory, which is predicated by the C-conditions that prevents multiple roots from corresponding to one state.

Since the *full* Δ CC method is identical to Li and Paldus’s *full* SUMRCC method (their truncated instances are different), Δ CC theory also constitutes a converging series of approximations toward FCI. They both rely on the C-condition. The crucial difference is, as discussed in Sec. II F, that Δ CC theory is a black-box method limited to degenerate references, while Li-Paldus SUMRCC theory admits a general incomplete model space as its reference, but its precise algebraic or diagrammatic formalisms vary depending on the reference and are known only at runtime.

Below, we document the cluster analysis of the *full* Δ CC method.^{119,120} Let $|\Psi_I\rangle$ be the exact (FCI) wave function for the I th state,

$$|\Psi_I\rangle = \sum_J^{\text{int.}} |J\rangle C_{JI} + \sum_A^{\text{ext.}} |A\rangle C'_{AI}, \quad (53)$$

where $|J\rangle$ and $|A\rangle$ designate an internal and external determinant, respectively, and \mathbf{C} and \mathbf{C}' are FCI coefficients. Writing the inverse of the M -by- M matrix \mathbf{C} (where M is the degree of degeneracy) as \mathbf{C}^{-1} , we have

$$\begin{aligned} \sum_I^{\text{int.}} |\Psi_I\rangle (\mathbf{C}^{-1})_{IJ} &= |J\rangle + \sum_I^{\text{int.}} \sum_A^{\text{ext.}} |A\rangle (\mathbf{C}')_{AI} (\mathbf{C}^{-1})_{IJ} \\ &= |J\rangle + \sum_A^{\text{ext.}} |A\rangle \langle A| \hat{C}_1 + \hat{C}_2 + \dots |J\rangle, \end{aligned} \quad (54)$$

where \hat{C}_n is the n -electron excitation operator, whose amplitudes are given by $\mathbf{C}'\mathbf{C}^{-1}$. The matrix \mathbf{C} is invertible if the FCI

wave functions are correctly one-to-one mapped onto determinants, and the correct mapping is facilitated by trial-vector algorithms.^{167–170}

On the other hand, as per Eq. (12), the full Δ CC wave function is written as

$$\begin{aligned} |\Psi_I\rangle &= \sum_J^{\text{int.}} e^{\hat{T}_J} |J\rangle C_{JI} \\ &= \sum_J^{\text{int.}} |J\rangle C_{JI} + \sum_J^{\text{int.}} (\hat{T}_J + \hat{T}_J^2/2! + \dots) |J\rangle C_{JI}, \end{aligned} \quad (55)$$

in which \hat{P}_J is absent because we are considering the *full* Δ CC method. Comparing this equation with Eq. (53), we see that the \mathbf{C} of the former (Δ CC) is the same as the \mathbf{C} of the latter (FCI) *if and only if* the C-conditions [Eq. (6)] are imposed.

This last point will become clearer when the above equation is multiplied by \mathbf{C}^{-1} from the right, leading to

$$\begin{aligned} \sum_I^{\text{int.}} |\Psi_I\rangle (\mathbf{C}^{-1})_{IJ} &= |J\rangle + \sum_A^{\text{ext.}} |A\rangle \langle A| \hat{T}_J + \hat{T}_J^2/2! + \dots |J\rangle \\ &\quad + \sum_{K \neq J}^{\text{int.}} |K\rangle \langle K| \hat{T}_J + \hat{T}_J^2/2! + \dots |J\rangle \quad (56) \\ &= |J\rangle + \sum_A^{\text{ext.}} |A\rangle \langle A| \hat{T}_J + \hat{T}_J^2/2! + \dots |J\rangle, \end{aligned} \quad (57)$$

where the C-condition, $\langle K| \hat{T}_J + \hat{T}_J^2/2! + \dots |J\rangle = \delta_{KJ}$, has been used in the last equality. The final expression mirrors the last line of Eq. (54), implying

$$\hat{C}_1 + \hat{C}_2 + \hat{C}_3 + \dots = \hat{T}_J + \hat{T}_J^2/2! + \hat{T}_J^3/3! + \dots \quad (58)$$

Decomposing \hat{T}_J by excitation ranks,

$$\hat{T}_J \equiv \hat{T}_1 + \hat{T}_2 + \hat{T}_3 + \dots, \quad (59)$$

we determine the exact t -amplitudes from FCI’s c -amplitudes recursively,

$$\hat{T}_1 = \hat{C}_1, \quad (60)$$

$$\hat{T}_2 = \hat{C}_2 - \hat{T}_1^2/2!, \quad (61)$$

$$\hat{T}_3 = \hat{C}_3 - \hat{T}_2 \hat{T}_1 - \hat{T}_1^3/3!, \quad (62)$$

and so on.

This proves the equivalence of the FCI and full Δ CC methods and hence the exact convergence of the Δ CC theory hierarchy. The foregoing proof is originally due to Paldus and Li.¹¹⁹

III. COMPUTER IMPLEMENTATIONS

A. Determinant-based, general-order algorithm

In a determinant- or string-based algorithm,^{21,130} a Slater determinant is computationally represented by a pair of α -

and β -strings of bits, with the n th bit storing the α - or β -spin electron occupation number of the n th spin-orbital. A wave function, which is a linear combination of these determinants, can then be specified by an array of expansion coefficients indexed by these string pairs. The action of any quantum-mechanical operator such as \hat{H}_I , \hat{T}_I , $e^{\hat{T}_I}$, and \hat{P}_I on a wave function is described computationally by faithfully executing the second-quantized definition of the operator as a series of bit manipulations.

In this way, virtually any *ab initio* electron-correlation theory that has a well-defined determinantal ansatz can be implemented in a general-order algorithm by making relatively simple modifications to a string-based FCI program.¹³⁰ The computational cost is also that of a FCI calculation regardless of the order of the hierarchical theory, and its intended utility is to provide benchmark data for the smallest systems that help characterize the theory's behavior and performance or verify efficient implementations. General-order CI,¹³⁰ CC,^{21–23} EOM-CC,^{22,88,131} MBPT,¹³² ΔMP,¹²⁵ and MBGF^{125,126} have been developed by this strategy. For pioneering symbolic implementations of multireference coupled-cluster programs, see Janssen and Schaefer,²⁰³ Li and Paldus,²⁰⁴ Abrams and Sherrill,²⁰⁵ Lyakh *et al.*,²⁰⁶ and Evangelista *et al.*¹⁴⁵

ΔCC theory has a well-defined determinantal ansatz and can thus be implemented into a general-order, determinant-based algorithm largely reusing computational kernels of the determinant-based CC program²¹ as part of POLYMER.²⁰⁷ A general-order Li–Paldus SUMRCC algorithm can be realized simultaneously in the same program.²⁰⁷ The iterative procedure of the n th-order ΔCC method for M -fold degenerate references is as follows:

(1) Generate initial guesses of t -amplitudes for all degenerate references ($1 \leq I \leq M$). (In our implementation, they are either zero or the exact values recovered from FCI as per Sec. II L.)

(2) Form $e^{\hat{T}_I}|I\rangle$ for all degenerate references as linear combinations of determinants.²¹

(3) Form $\hat{H}_I e^{\hat{T}_I}|I\rangle$ for all degenerate references as linear combinations of determinants.²¹ (While the appearance of the normal-ordered \hat{H}_I differs from one degenerate reference to another, its content is the same, and just one common subroutine that acts the *ab initio* \hat{H} on a wave function suffices.)

(4) Build the M -by- M matrices \mathbf{H} and \mathbf{S} of Eqs. (7) and (8) in the internal space. Their elements across two determinants differing by more than n spin-orbitals are zeroed by the \hat{P}_I operators in Eqs. (7) and (8). (In the Li–Paldus SUMRCC methods, no elements need to be zeroed.)

(5) Invert \mathbf{S} by the LU decomposition, and then form $\mathbf{E} = \mathbf{S}^{-1}\mathbf{H}$. (Even though $\mathbf{S} = \mathbf{1}$ at the convergence, this is not the case during the iterative process and it must not be assumed that $\mathbf{E} = \mathbf{H}$.) Determine and print the eigenvalues of \mathbf{E} . (Complex eigenvalues are detected occasionally in cases of convergence difficulties.)

(6) Compute the residuals, i.e., the differences between the left- and right-hand sides of Eq. (5) in the external space or those of Eq. (6) in the internal space, both computable by the quantities obtained in steps (2) and (3). The \hat{P}_J operator sets $e^{\hat{T}_I}|J\rangle$ to zero if the external determinant is more than n spin-

orbitals different from $|J\rangle$. (In the Li–Paldus SUMRCC methods, this zeroing is suppressed.)

If the residuals are less than a preset threshold, the convergence is achieved and the program halts; otherwise, update the t -amplitudes for all degenerate references and go back to step (2).

The standard MBPT-style update, which adds the residuals (divided by the zeroth-order energy differences) to the most recent t -amplitudes in the external (internal) space, works reasonably well, but not as well as the same in the single-reference CC methods for the ground states. In cases of convergence difficulty, the direct inversion in the iterative subspace (DIIS)²⁰⁸ is found effective. In the full ΔCC method, which is equivalent to the full Li–Paldus SUMRCC method, when the exact t -amplitudes are used as initial guesses, convergence is achieved instantly.

B. Algebraic, optimal-scaling, order-by-order algorithm

Optimal-scaling algorithms of ΔCCS and ΔCCSD are implemented based on the algebraic equations given in Secs. II C and II D. The equations have been derived by TCE,^{128,129} and further transformed into computational sequences consisting of unary matrix additions and binary matrix multiplications after the optimizations known as the strength reduction and factorization.^{128,129} These optimizations define the so-called “intermediates,” lowering the size-dependence of costs of ΔCCS and ΔCCSD to the optimal $O(n^4)$ and $O(n^6)$, respectively, with the number of spin-orbitals (n), not counting the $O(n^5)$ integral-transformation step.

Note that the t -amplitude equations in Secs. II C and II D are purposefully left disconnected or even unlinked, the cancellation of the latter occurring numerically. This algorithm choice has been made because the presence of these unlinked terms has no impact on the size-dependence of cost, while the removal of disconnected terms is neither possible nor necessary. (These “disconnected” terms are linked, and do not violate size-extensivity. Li and Paldus consider them “connected,” and so the distinction seems nonessential. See Fig. 14 and its associated discussion in the main text.)

These computational sequences are then converted by debug-mode TCE to the FORTRAN90 subroutines as part of POLYMER²⁰⁷ that evaluate the right-hand sides of the energy and t -amplitude equations. In this pilot implementation, our primary concerns have been the correctness of the formulas and computer codes, and hence the codes do not exploit spin, spatial, or index-permutation symmetries. They are also for serial executions only, and while their size-dependence of cost is optimal, their wall-clock-time execution speeds are slow, leaving room for improvement. (On the other hand, the FORTRAN77 subroutines of the CC and EOM-CC methods synthesized by production-mode TCE as part of NWChem²⁰⁹ take advantage of all of these symmetries, strength reduction, factorization, and intermediate reuse as well as load-balanced parallelism. They are fully optimized, scalable, and fast.^{76,128} We have not explored production-mode TCE for the ΔCC methods in this study.)

```

DO i=1,no(I)
DO a=1,nv(I)
  i1(mo(i,I),mv(a,I))=fi(mo(i,I),mv(a,I))
ENDDO
ENDDO
DO i=1,no(I)
DO a=1,nv(I)
  DO b=1,nv(I)
    DO j=1,no(I)
      i1(mo(i,I),mv(a,I))=i1(mo(i,I),mv(a,I)) +
        +(1/2)*t1i(mv(b,I),mo(j,I))*v(mo(j,I),mo(i,I),mv(b,I),mv(a,I))
    ENDDO
  ENDDO
ENDDO
i0(1)=EHFI
DO a=1,nv(I)
  DO i=1,no(I)
    i0(1)=i0(1)+t1i(mv(a,I),mo(i,I))*i1(mo(i,I),mv(a,I))
  ENDDO
ENDDO
DO a=1,nv(I)
  DO b=1,nv(I)
    IF (a > b) CYCLE
    DO i=1,no(I)
      DO j=1,no(I)
        IF (i > j) CYCLE
        i0(1)=i0(1)+t2i(mv(a,I),mv(b,I),mo(i,I),mo(j,I)) +
          +v(mo(i,I),mo(j,I),mv(a,I),mv(b,I))
      ENDDO
    ENDDO
  ENDDO
ENDDO
ENDDO

```

FIG. 23. The FORTRAN90 pseudocode for the diagonal Δ CCSD energy for the I th degenerate reference determinant [Eq. (20)]. The element of array $i0(1)$ returns the energy, array $i1$ stores an intermediate formed by the strength reduction and factorization, arrays $t1_I$ and $t2_I$ are, respectively, single- and double-excitation t -amplitudes, variable EHF_I and array f_I are the I -dependent HF energy and Fock matrix, and array v is the anti-symmetrized two-electron integrals. Variables $n_o(I)$ and $n_v(I)$ are the numbers of occupied and virtual spin-orbitals in the I th determinant, while arrays $m_o(i,I)$ and $m_v(a,I)$ store the lists of occupied and virtual spin-orbitals of the I th determinant. The actual code is synthesized by TCE.

Overall, the iterative procedure of the algebraic Δ CCS and Δ CCSD algorithms is essentially the same as the determinant-based algorithm outlined above since the disconnected and unlinked terms are left intact in the algebraic formulas. Only minor differences exist in the way in which the matrix elements and residuals are evaluated in the correctly scaling subroutines synthesized by TCE. Below, we document the iterative procedure of the algebraic algorithm, taking the Δ CCSD method for M -fold degenerate references as an example. (Li-Paldus SUMRCC theory cannot be implemented in this manner.)

(1) For each (I th) degenerate reference, store the numbers [$n_o(I)$ and $n_v(I)$] and lists [$m_o(i,I)$ for $i = 1, \dots, n_o(I)$ and $m_v(a,I)$ for $a = 1, \dots, n_v(I)$] of occupied and virtual spin-orbitals.

(2) For each (I th and J th) degenerate reference pair, evaluate and store the (nonzero) parities, i.e., $\langle I_{ij}^{ab}|J_{kl}^{cd}\rangle$, $\langle I_{ij}^{ab}|J_k^c\rangle$, $\langle I_{ij}^{ab}|J\rangle$, $\langle I_i^a|J_{kl}^{cd}\rangle$, $\langle I_i^a|J_k^c\rangle$, and $\langle I_i^a|J\rangle$. See Eqs. (24) and (25).

(3) For each (I th) degenerate reference, evaluate and store the I -dependent HF energy, E_I^{HF} , and Fock matrix elements, $(f_I)_q^p$, by Eqs. (3) and (4).

(4) Generate initial guesses of t -amplitudes for all degenerate references ($1 \leq I \leq M$). They are zero in the present implementation.

(5) For each (I th) degenerate reference, evaluate the diagonal Δ CCSD energy $\langle I|\hat{H}_I e^{\hat{T}_I}|I\rangle$ [Eq. (20)] using the TCE-synthesized subroutine with E_I^{HF} and $(f_I)_q^p$ formed in step (3).

(Figure 23 illustrates the structure of the pilot code synthesized by TCE for the diagonal Δ CCSD energy. While TCE correctly identifies a common factor as the intermediate $(i_1)_a^i$ and its synthesized code has the correct cost scaling, the nested loops over gapped lists of occupied or virtual spin-orbitals pose a practical efficiency bottleneck.)

(6) For each (I th) degenerate reference, form the left-hand sides of the t -amplitude equations, i.e., Eqs. (18) and (19), using the TCE-synthesized subroutines. Populate the off-diagonal elements of \mathbf{H} with them, while its diagonal elements have been computed in step (5).

(7) For each (I th) degenerate reference, form the exponential wave functions, i.e., Eqs. (20) and (21), using the TCE-synthesized subroutines. Populate the off-diagonal elements of \mathbf{S} with them, while its diagonal elements are unity. Invert \mathbf{S} by the LU decomposition, and form $\mathbf{E} = \mathbf{S}^{-1} \mathbf{H}$. Determine and print the eigenvalues of \mathbf{E} .

(8) For each (I th) degenerate reference, evaluate the right-hand sides of the t -amplitude equations, i.e., Eqs. (24) and (25), using parities determined in step (2) and the exponential wave functions and \mathbf{E} formed in step (7). Compute the residuals. They are the differences between the left- and right-hand sides of the t -amplitude equations in the external space, i.e., Eq. (18) minus Eq. (24) or Eq. (19) minus Eq. (25); they are $\mathbf{S} - \mathbf{1}$ in the internal space.

If the residuals are less than a preset threshold, the convergence is achieved. Otherwise, update the t -amplitudes for all degenerate references in the same way as the determinant-based algorithm, and go back to step (5).

IV. NUMERICAL TESTS

The Δ CC methods through the FCI limit have been applied to the same group of small molecules as that previously used in the general-order CC,²¹ EOM-CC,⁸⁸ and IP- and EA-EOM-CC benchmarks.¹³¹ They are compared with the general-order CI, EOM-CC, and Li-Paldus SUMRCC methods through the FCI limits as well as with the general-order Δ MP (Ref. 125) and Feynman-Dyson MBGF methods^{124,126} through the nineteenth order. The CI and (EOM-)CC methods are characterized by the truncation order (k) of the cluster and linear excitation operators, specified by suffixes: S ($k = 1$), SD (2), SDT (3), SDTQ (4), SDTQP (5), SDTQPH (6), SDTQPHS (7), and SDTQPHSO (8).²⁴ See Refs. 21, 88, 124, and 131 for the geometries, basis sets, whether the frozen-core and/or frozen-virtual approximations are invoked, and other technical details.

In all cases, the orbital reference is the determinant with an equal number of α - and β -spin electrons obeying the aufbau principle, whose orbitals are determined by the spin-restricted HF method. The zeroth-order energy ($E_{II}^{(0)}$) of the I th determinant, by which the degeneracy is judged, is the sum of the occupied HF orbital energies.

When evaluating the performance, the computational cost and its size-dependence should be factored in. Although the costs of the determinant-based algorithms scale exponentially with the number of spin-orbitals (n) regardless of the method's

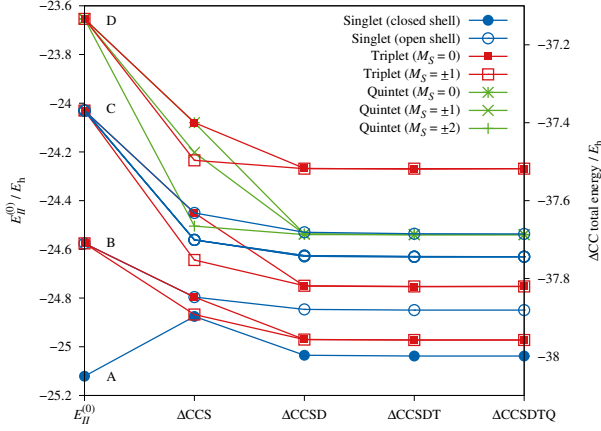


FIG. 24. The total energies of the ground and excited states of CH^+ ($r_{\text{CH}} = 1.131 \text{ \AA}$) obtained by the ΔCC methods and 6-31G** basis set with the highest virtual and lowest occupied orbitals kept frozen.⁸⁸ The determinant references with the numbers of the α - and β -spin electrons being (3, 3), (4, 2), or (5, 1) are used, leading to roots corresponding to the total magnetic spin quantum numbers of $M_S = 0, 1$, or 2, respectively. The zeroth-order energies ($E_H^{(0)}$) of the reference determinants refer to the left axis, while the rest of the data to the right axis. The references are labeled “A” through “D.”

rank, the intrinsic size-dependencies of the costs are as follows: ACCS scales as $O(n^4)$, ACCSD as $O(n^6)$, ACCSDT as $O(n^8)$, or k th-order ΔCC as $O(n^{2k+2})$. The CI, EOM-CC, and Li–Paldus SUMRCC methods scale identically as the ΔCC method of the same rank. The $\Delta\text{MP}2$, $\Delta\text{MP}3$, and $\Delta\text{MP}4$ methods scale as $O(n^4)$, $O(n^6)$, and $O(n^7)$, respectively, in the thoroughly optimized algorithms.⁸ An MBGF method has the same scaling as the ΔMP method of the same perturbation order. The $O(n^5)$ integral-transformation step is excluded from the cost.

All calculations were performed with the POLYMER program.²⁰⁷ The numerical data are available as supplementary material.

A. Excited states

1. CH^+

The CH^+ molecule has six electrons, of which four are correlated in the frozen-core approximation adopted here. The ΔCC energies of several low-lying states obtained with (degenerate) determinant references with the number of the α - and β -spin electrons being (3, 3), (4, 2), or (5, 1) are shown in Fig. 24.

The ground-state wave function has the dominant single determinant labeled “A” in Fig. 24, which is used as the orbital reference. Its occupancy diagram shown in Fig. 25 obeys the aufbau principle. Therefore, for the ground state, ΔCC theory is equal to single-reference CC theory with the restricted HF reference. Both states’ energies are practically exact at the ACCSD level. They maintain the expected degeneracy accurately even when the roots come from different sectors.

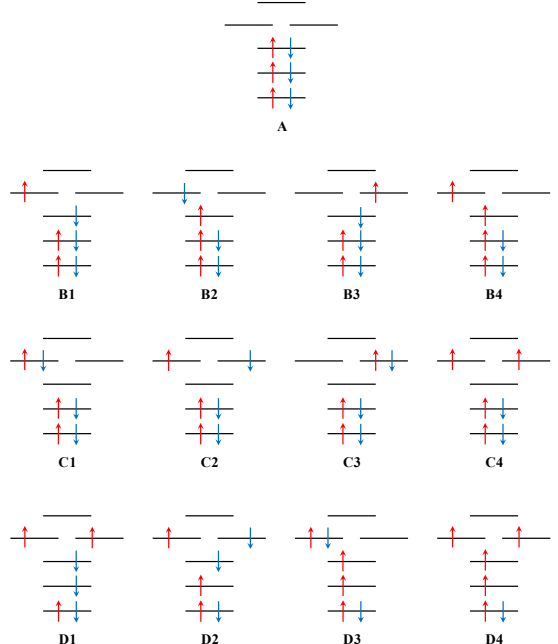


FIG. 25. Occupancy diagrams of some low-lying determinant references of CH^+ . Labels “A” through “D” correspond to $E_H^{(0)}$ of Fig. 24. They are not exhaustive.

CCSD is already nearly exact.

Since the lowest-unoccupied molecular orbital (LUMO) is doubly degenerate, the second lowest-lying determinants already have a high degree of degeneracy. They are four-fold degenerate in the (3,3) sector or eight-fold degenerate in the combined (3,3), (4,2), and (2,4) sectors. Some of these degenerate references are shown in Fig. 25 with label “B.” Occupancy diagrams B1, B2, and B3 are three of the four degenerate references in the (3,3) sector, whereas diagram B4 is one of the two in the (4,2) sector. For the lowest excited states already, the use of ΔCC (not CC) theory is essential, although determinants of different sectors do not couple with one another, and can thus be handled by separate ΔCC calculations.

As seen in Fig. 24, the eight-fold degeneracy of references B is lifted as they split into a degenerate pair of triplets (the red squares) and doubly degenerate open-shell singlets (the blue, open circles). The triplets can be reached from the reference determinants in the (3,3) sector, and they have the total magnetic spin quantum number (M_S) of zero (the red, filled squares) and may be called “low spin.” Those that come from the references in the (4,2) or (2,4) sector (the red, open squares) have $M_S = 1$ or -1 , respectively, and may be called “high spin.”

In accordance with Hund’s rule, the triplets lie lower than the singlets. Both states’ energies are practically exact at the ACCSD level. They maintain the expected degeneracy accurately even when the roots come from different sectors.

TD-CCSD (Ref. 107–112) is designed to describe open-shell singlets such as the one encountered here (the blue, open circles). This state’s reference determinants are, however, nominally four-fold degenerate in the (3,3) sector, exceeding

the two-determinant limit of the TD-CC ansatz. Since two out of the four-fold degeneracy originates from the degeneracy of the LUMOs, which are orthogonal to each other, TD-CCSD can still handle these states. However, the Δ CCSD method, which is distinct from TD-CCSD and more general, can treat them equally well without any special considerations needed for the degree or nature of the degeneracy of the references.

Only at the Δ CCS level is the degeneracy of the triplets non-physically lifted. Their energies are also less converged. The loss of degeneracy is due to the fact that configurations B1 and B2 in Fig. 24 differ by two spin-orbitals and their coupling is not accounted for by the Δ CCS method limited to singles. The high-spin ($M_S = \pm 1$) state (the red, open square) is more accurately described by Δ CCS than the low-spin ($M_S = 0$) state (the red, filled square). This is because the high-spin configuration B4 dominates in the ground-state wave function in the (4,2) sector, which can therefore be handled well by single-reference CC theory. Its degenerate counterpart in the (3,3) sector, in contrast, is an excited state whose wave function has equal contributions from the low-spin configurations B1 and B2, which couple with each other. Hence, this is a manifestation of the well-known observation that high-spin states tend to be dominated by single determinants, and thus constitute a more convenient reference, which underlies the ingenious spin-flip methods of Krylov and coworkers.^{162–164,210,211} Δ CC theory too can take advantage of this phenomenon by simply adopting a high-spin reference, free of any additional formulation or coding work.

References labeled “C” are four-fold degenerate in the (3,3) sector, nondegenerate in each of the (4,2) and (2,4) sectors, and altogether six-fold degenerate. Upon inclusion of electron correlation, they split into doubly degenerate open-shell singlets and a nondegenerate open-shell singlet (the blue, open circles) as well as triplets (the red squares). The same observations as above for the states labeled by B apply: For all states, the Δ CCSD energies are nearly exact. A nonphysical lifting of degeneracy of the triplets occurs at the Δ CCS level, and their energies from the high-spin references are more accurate.

References labeled “D” are ten-fold degenerate in the (3,3) sector, six-fold generate in each of the (4,2) and (2,4) sectors, and nondegenerate in each of the (5,1) and (1,5) sectors; altogether 24-fold degenerate. Only the triplets (the red squares) and quintets (the green crosses) spawned from them are plotted in Fig. 24. Once again, their states’ degeneracies are spuriously lifted at the Δ CCS level, and the greater the $|M_S|$, the more accurate their split energies. The Δ CCS energies of the highest-spin references are nearly as accurate as the Δ CCSD energies. This is understandable because the quintet state is the ground state in the (5,1) sector, whose wave function is dominated by the single determinant D4 of Fig. 25. This determinant has so few β -spin occupied orbitals and so few α -spin virtual orbitals that there is expected to be little electron correlation. Δ CCS only needs to describe the orbital relaxation from reference A to D4, which it does accurately.

Figure 26 compares the vertical excitation energies of the same molecule⁸⁸ obtained by the CI, EOM-CC, Δ CC, and Li–Paldus SUMRCC methods through the FCI limits as well as by the Δ MP method through the sixth order. The refer-

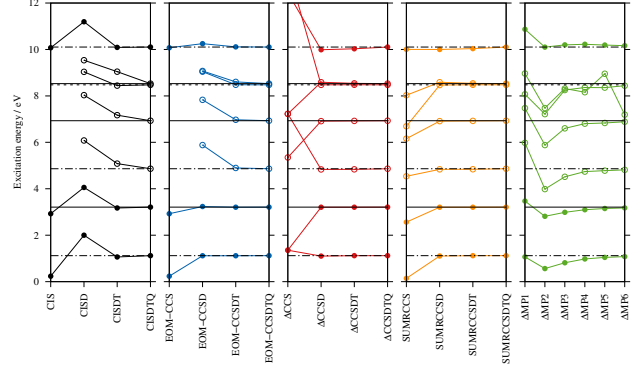


FIG. 26. Same as Fig. 24, but for the vertical excitation energies computed by the CI, EOM-CC, Δ CC, Li–Paldus SUMRCC, and Δ MP methods using low-spin ($M_S = 0$) reference determinants.⁸⁸ The solid, dotted-dashed, and dashed horizontal lines indicate the exact (FCI) values for singlet, triplet, and quintet states, respectively. Filled circles correspond to predominantly one-electron excitations and open circles to predominantly two-electron excitations.

ences are low-spin determinants. Filled circles plot the excitations to states with predominantly one-electron character, while the open circles correspond to those with predominantly two-electron character. The ground-state wave function is 92.2% zero-electron character. See Table 2 of Ref. 88 for the precise percentage weights of the singles and doubles in their FCI wave functions.

Going from CISD to EOM-CCSD, the errors for the one-electron excitations (filled circles) decrease from 0.8–0.9 eV to invisibly small (< 0.03 eV). For the two-electron excitations (open circles), CIS and EOM-CCS, which are one and the same method, lack corresponding roots, while CISD and EOM-CCSD do have roots that suffer from comparable, substantial errors of approximately 1 eV. EOM-CCSDT is nearly exact for both types of excitations (errors less than 0.04 eV). In general, the k th-order EOM-CC is always superior to the k th-order CI, and is quantitative for excitations of up to $(k-1)$ -electron character. The accuracy is independent of the spin multiplicities of the initial or final states. These performance characteristics are well known.^{7,8,10,88}

Going from EOM-CC to Δ CC, we make the following observations: Unlike EOM-CCS, Δ CCS has roots for all states regardless of their excitation character. However, its results are rather erratic, posing a considerable challenge when assigning energies to states especially for highly degenerate references. Errors in the excitation energies are substantial and do not correlate with the excitation character. Hence, the practical utility of Δ CCS seems rather limited, but see below for exceptions.

Once we raise the rank to Δ CCSD, the theory’s accuracy and thus utility improve dramatically. It has roots for all states and the excitation energies are nearly exact for both one- and two-electron excitations (errors less than 0.03 eV), as foreshadowed by Fig. 24. Unlike EOM-CCSD, which has errors

approaching 1 eV for two-electron excitations (and lacks roots for three-electron excitations; see below), Δ CCSD displays uniform high accuracy for any state insofar as the state's wave function is dominated by a linear combination of degenerate determinants.

Only when a wave function has a noticeable contribution from an energetically nearby determinant (the situation that may be variously referred to as strong correlation, quasidegeneracy, intruder states,^{165,166} etc.) does a higher-order Δ CC method become necessary to maintain accuracy. Hence, the performance expectation of Δ CC theory is the same as that of single-reference CC theory for nondegenerate ground states, which is well documented.^{7,8,10}

The performance of Δ CC and Li–Paldus SUMRCC theories are essentially the same except for the lowest-rank members: SUMRCCS has roots for all excitations and its excitation energies are better than the Δ CCS roots, though not necessarily superior to the CIS or EOM-CCS roots when the latter exist. The similarity in performance of higher-rank members originates from the same in their ansätze, and a closer inspection shows that SUMRCC is slightly more accurate than Δ CC of the same rank at a commensurately elevated cost because the latter erases some higher-order excitation amplitudes by projectors. This slight accuracy boost of SUMRCC comes at the cost of losing the black-box nature of the method.

The Δ MP n results are plotted in the rightmost subgraph. They are convergent toward the respective, correct, exact limits unless they are divergent. The Δ MP1 method has roots for two-electron excitations and is distinctly superior to Δ CCS, but not necessarily to CIS, EOM-CCS, or SUMRCCS. The Δ MP2 method is poor, apparently giving unbalanced descriptions of the initial and final states. The Δ MP3 method and onward tend to correct the errors of the Δ MP2 excitation energies in a monotonic, but slowly convergent manner. Since Δ MP3 is a $O(n^6)$ procedure, it should be compared with CISD, EOM-CCSD, and Δ CCSD, which are also the $O(n^6)$ methods. The performance of these methods is in the order: Δ CCSD > EOM-CCSD > Δ MP3 > CISD. When an emphasis is placed on two-electron excitations, the order changes to: Δ CCSD \gg Δ MP3 > EOM-CCSD \approx CISD.

Lastly, some remarks on the convergence of the iterative solution algorithms of the Δ CC t -amplitude equations (Sec. III) may be in order. Without DIIS, Δ CC calculations tend to fail for many references. With DIIS, the Δ CC calculations for degenerate references B and C of Fig. 24 converge at a similar rate as the single-reference CC calculations for the ground state (A). For the ten-fold degenerate references D, the convergence difficulty has been encountered even with DIIS, but not uniformly; the convergence is slow for some roots, while rapid for others. Convergence difficulties are sometimes accompanied by complex energies.^{64,165,166} However, overall, Δ CC theory is generally well behaved and a practically viable method.

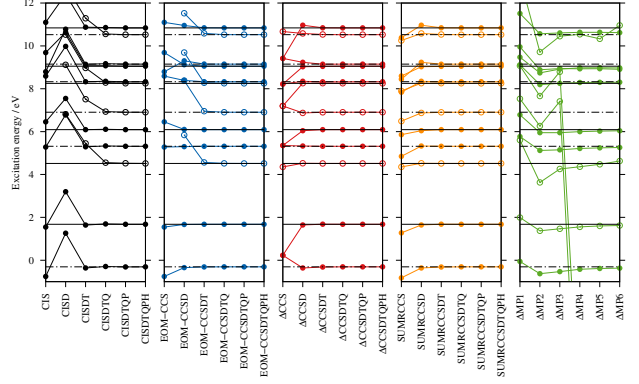


FIG. 27. The vertical excitation energies of CH_2 ($r_{\text{CH}} = 1.102 \text{ \AA}$ and $a_{\text{HCH}} = 104.7^\circ$) (relative to its singlet ground state) calculated by the CI, EOM-CC, Δ CC, Li–Paldus SUMRCC, and Δ MP methods and 6-31G* basis set with the highest virtual and lowest occupied orbitals kept frozen in the low-spin reference determinants.⁸⁸ The solid and dotted-dashed horizontal lines indicate the exact (FCI) values for singlet and triplet states, respectively. Filled circles correspond to predominantly one-electron excitations and open circles to predominantly two-electron excitations.

2. CH_2

The vertical excitation energies of the CH_2 molecule,⁸⁸ a twelve-electron system in the frozen core and virtual approximation, are computed by Δ CC and other methods, using the singlet HF reference (note that the ground state is triplet). The results are shown in Fig. 27. They reinforce the general performance trends observed for CH^+ in Sec. IV A 1.

CIS = EOM-CCS lack two-electron excitation roots (open circles), but they are impressively accurate for one-electron excitations (filled circles). CISD overestimates excessively all shown excitation energies (errors of ≈ 1.5 eV), suggesting that it may be treating the ground state favorably at the expense of excited states. EOM-CCSD does not have this problem and is nearly exact for one-electron excitations. However, for two-electron excitations, it has errors sometimes in excess of 1 eV.

Δ CCS has roots for all excited states, but its excitation energies do not seem useful (and are challenging to assign for highly degenerate references). Δ CCSD is as accurate as EOM-CCSD for one-electron excitations and distinctly superior to the latter for two-electron excitations. Δ CCSD is practically converged at the FCI limits for all shown excitation energies, and is, therefore, an attractive alternative to EOM-CCSD. Its relative pros and cons are listed in Sec. III.

The Li–Paldus SUMRCC methods behave nearly identically as the Δ CC methods except at the singles-only level. The fact that black-box Δ CC theory produces essentially the same accurate results (except at the Δ CCS level) as the more general, but expert method like Li–Paldus SUMRCC theory underscores the practical utility of the former.

Δ MP1 has roots for all excitations, whose numerical values seem reasonable if not superior to CIS = EOM-CCS. Δ MP2

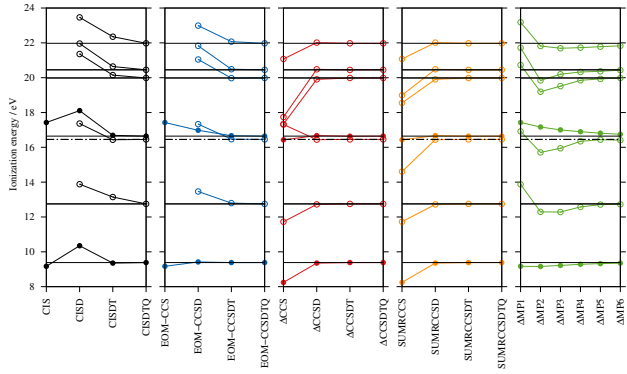


FIG. 28. The vertical ionization energies of BH ($r_{\text{BH}} = 1.232 \text{ \AA}$) calculated by the CI, EOM-CC, Δ CC, Li-Paldus SUMRCC, and Δ MP methods and 6-31G** basis set with the highest virtual and lowest occupied orbitals kept frozen in the low-spin reference determinants.¹³¹ The solid and dotted-dashed horizontal lines indicate the exact (FCI) values for doublet and quartet states, respectively. Filled circles correspond to Koopmans ionization potentials and open circles to satellite ionization transitions.

tends to underestimate all excitation energies, which are corrected systematically by Δ MP3 and onward except for at least two sets of two-electron excitations where the perturbation series quickly diverge. In fact, it almost appears a rule than an exception that perturbation series that initially converge turn to diverge eventually,²¹² making it crucial to perform infinite diagram resummation as realized in the form of Δ CC theory.

B. Ionized states

1. BH

The BH molecule is a four-electron system in the frozen core and virtual approximation. Its vertical ionization energies have been computed by the hole-particle CI, IP-EOM-CC, Δ CC, and Li-Paldus SUMRCC methods through the FCI limits as well as by the Δ MP method up to the sixth order. The results are shown in Fig. 28.

Here, CIS = IP-EOM-CCS use the 1h (one hole) operator as the linear ionization operator, CISD and IP-EOM-CCSD employ the 2h-1p (two-hole-one-particle) operator, CISDT and IP-EOM-CCSDT the 3h-2p operator, etc. These combinations ensure the size-extensivity and intensivity of the methods¹³³ and are the standard choice. For the Δ CC and Δ MP methods, such considerations are unnecessary, and the same formalisms and codes handle any states with any numbers of α - and β -spin electrons; they only need a reference determinant as input. See the last paragraph of Sec. II for more on this point.

There are two Koopmans ionization potentials (IPs) (the filled circles) shown in Fig. 28: the first IP at 9.4 eV and the second IP at 16.6 eV. The singles weights of the correspond-

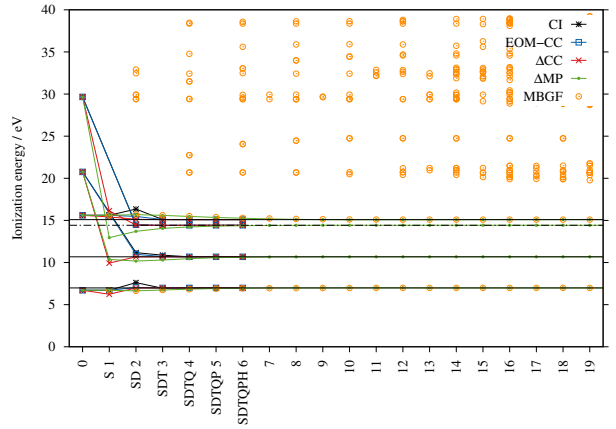


FIG. 29. The vertical ionization energies of BH ($r_{\text{BH}} = 1.232 \text{ \AA}$) using the minimal (STO-3G) basis set with all electrons correlated in the low-spin reference determinants.¹²⁴ The horizontal axis gives the truncation order of excitation operators or the perturbation order. The CI, EOM-CC, Δ CC, and Δ MP data are shown for the two lowest Koopmans ionization potentials and two doubly degenerate satellite ionization transitions in between. The solid and dotted-dashed horizontal lines indicate the corresponding exact (FCI) data for doublet and quartet states, respectively. The MBGF data plot all roots of the inverse Dyson equation with the frequency-dependent, nondiagonal (thus nonapproximated) self-energy.

ing ionized wave functions are, respectively, 93% and only 76%.¹³¹ The rest of the IPs are satellites (the open circles) and their corresponding ionized wave functions have 94% or more two-electron character.

The CIS = IP-EOM-CCS = Δ MP1 roots exist only for the Koopmans IPs and their results correspond to the HF orbital energies (the signs reversed) as per the Koopmans theorem. The agreement is excellent for the first IP owing to the well-known systematic cancellation of correlation and orbital relaxation errors.¹⁸⁶ The agreement is less good for the second IP likely because of its noticeable two-electron character. The 2h-1p CISD method is poor with errors in excess of 1 eV for all shown IPs. IP-EOM-CCSD erases these large error nearly completely for the first IP, but it brings about only modest improvements for the satellite IPs and second Koopmans IP. The destination states have, respectively, dominant and appreciable two-electron character.

Δ CC theory displays remarkable performance for all IPs. Their results are practically converged at the Δ CCSD level (errors less than 0.08 eV). The same goes to the results of the Li-Paldus SUMRCC calculations beyond singles.

The Δ MP series seems convergent for all IPs. We shall explore higher-order Δ MP methods in what follows.

Figures 29–32 extend the analysis on the BH molecule's IPs to higher-order Δ MP and MBGF calculations through the nineteenth order. (This is an all-electron calculation with the minimal basis set and differs from the preceding one.)

It may be recalled^{124–126} that the Δ MP n method is equivalent to the MBGF(n) method in the diagonal, frequency-independent approximation to the self-energy for $n \leq 3$. The Δ MP series is convergent at the FCI limits (unless divergent).

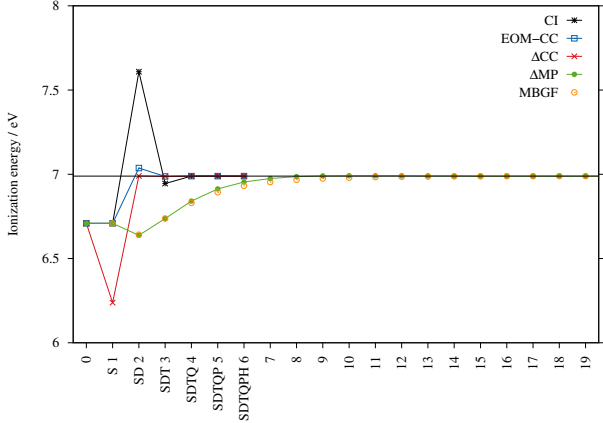


FIG. 30. The enlargement of Fig. 29 around the first Koopmans state.

The MBGF series with the nonapproximated self-energy converges at the FCI limits for some Koopmans states, but for most other states, surprisingly, it has a zero radius of convergence; even when MBGF converges, it often does so at wrong limits.¹²⁴

Figure 29 confirms these. For the two Koopmans and two satellite states considered, with increasing n , the ΔMP_n results (the green dots) quickly snap onto the horizontal lines indicating the FCI data. In contrast, the plots of the IPs obtained by higher-order MBGF with nonapproximated self-energy (the orange, open circles) fall upon the FCI lines of the two Koopmans states only, but not of the two satellite states. The roots for the latter converge at wrong limits around or above 20 eV, exposing a severe, fundamental flaw of Feynman–Dyson MBGF.¹²⁴

Figure 30 zooms in on the first Koopmans IP around 7 eV. For this root, both the ΔMP_n and MBGF(n) methods converge at the FCI limit upon increasing n . The rate of convergence is slightly faster for ΔMP , again, questioning the relative merits of the two similar methods.^{124–126,186} CIS = EOM-CCS yield the same value as the ΔMP_1 or the MBGF(1) method, obeying the Koopmans theorem. ACCS is distinctly worse than the other four methods. However, ACCSD is nearly exact, slightly more accurate than IP-EOM-CCSD and distinctly better than 2h-1p CISD, ΔMP_3 , or MBGF(3), which are all $O(n^6)$ procedures. IP-EOM-CCSDT catches up with ACCSDT, but the 3h-2p CISDT, ΔMP_5 , and MBGF(5) methods still fall short.

Figure 31 focuses on the second Koopmans IP around 15.1 eV and its nearby satellite ionization transition at 14.4 eV. For the former, the performance of the methods is in the order: ACC > IP-EOM-CC > CI and ACC > $\Delta MP \approx$ MBGF. For the latter, which is a two-electron process, CIS = IP-EOM-CCS do not even have the corresponding root. CISD is accurate, which is accidental because CISDT has a greater error. IP-EOM-CCSD has a slightly visible error, but IP-EOM-CCSDT is essentially converged. In contrast, ACCSD is nearly exact. The ΔMP series is monotonically convergent, and its rate is not particularly slower than those for the Koopmans IPs. On the other hand, as discussed above, the corresponding MBGF roots are nowhere near the exact value and outside this graph.

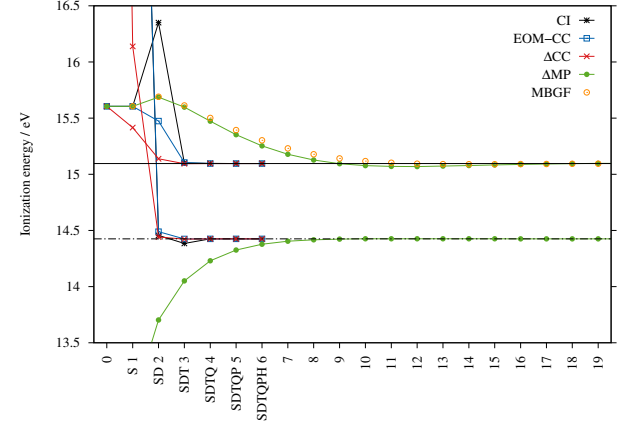


FIG. 31. The enlargement of Fig. 29 around the second Koopmans state. The MBGF roots for the nearby satellite state at 14.4 eV are nonconvergent¹²⁴ and outside this graph.

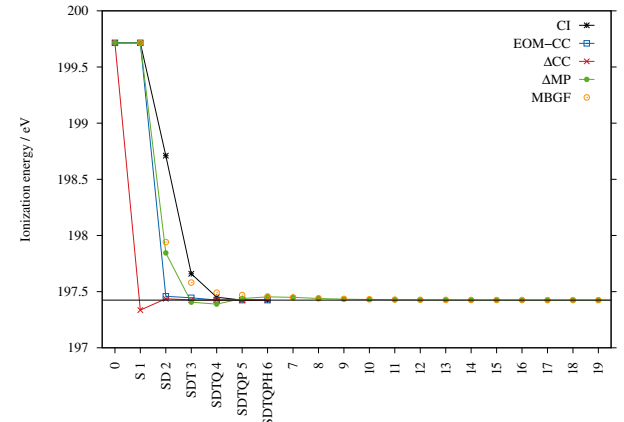


FIG. 32. The enlargement of Fig. 29 around the third Koopmans (or core-ionized) state.

In Fig. 32, we now turn to the core ionization, i.e., the third Koopmans IP. There has been much attention to such ionizations occurring in the extreme ultraviolet range,²¹³ as they can report element-specific dynamical information about spin and oxidation states of transition metals in a molecule. The Koopmans approximation, i.e., CIS = IP-EOM-CCS = ΔMP_1 = MBGF(1), is poor, as orbital relaxation effects are large. ACCS works remarkably well in this case. It may be because the one-electron excitation operator takes into account the relaxation effects, while correlation effects are small because core orbitals are so far removed from other orbitals. However, whether this is merely accidental remains to be established by a more systematic study. IP-EOM-CCSD and ACCSD are essentially converged, while CI is much less accurate. ΔMP and MBGF series both converge at the FCI limits, with ΔMP_3 being near exact.

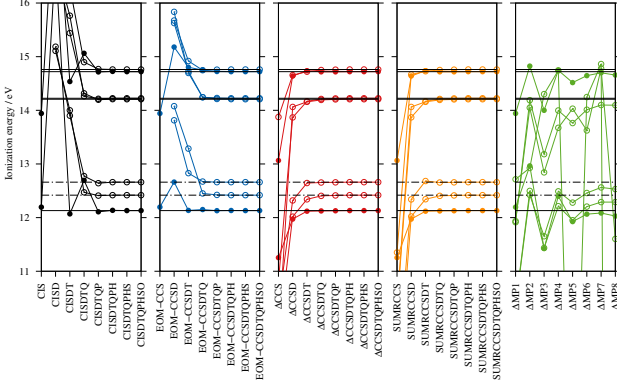


FIG. 33. The vertical ionization energies of C_2 ($r_{\text{CC}} = 1.262 \text{ \AA}$) calculated by the CI, EOM-CC, Δ CC, Li-Paldus SUMRCC, and Δ MP methods and 6-31G basis set with the two highest virtual and two lowest occupied orbitals kept frozen in the low-spin reference determinants.¹³¹ The solid and dotted-dashed horizontal lines indicate the exact (FCI) values for doublet and quartet states, respectively. Filled circles correspond to Koopmans states and open circles to satellite states.

2. \mathbf{C}_2

The C_2 molecule's ground-state wave function has a large multi-determinant character. Consequently, even its Koopmans ionization transitions have appreciable three-electron character.¹³¹ The CI series does not converge until we reach CISDTQ, and even IP-EOM-CC theory struggles until we invoke IP-EOM-CCSDT for Koopmans IPs (Ref. 131) or IP-EOM-CCSDTQ for satellite ionization transitions. In contrast, Δ CCSD is already usefully accurate for the first and second Koopmans IPs with errors of 0.16 and 0.08 eV, respectively (as compared with 0.53 and 0.46 eV at IP-EOM-CCSD or 4.68 and 3.50 eV at 2h-1p CISD). Δ CCSDT is near exact for these states (errors less than 0.02 eV).

For satellite states, Δ CCSDT is quantitative with errors less than 0.08 eV and Δ CCSDTQ is essentially exact. In comparison, IP-EOM-CCSDT has errors up to 0.87 eV.

As before, Li-Paldus SUMRCC theory displays similar behavior and performance as Δ CC theory. For this challenging multi-determinant problem, the difference seems smaller (and, in fact, Δ CCS works slightly better than SUMRCCS).

The Δ MP series are wildly oscillatory. Their plots provide a contrast to the rapid and much smoother convergence of the Δ CC plots, underscoring the importance and power of the infinite diagram resummation in the latter.

C. Electron-attached states

1. CH^+

Figure 34 plots the vertical electron affinities (EAs) of CH^+ computed by the hole-particle CI, EA-EOM-CC, Δ CC, Li-

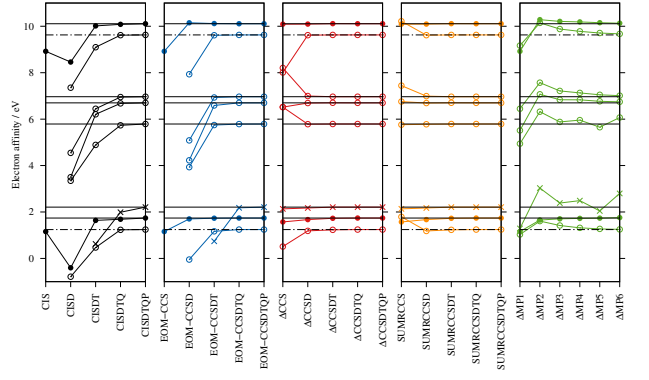


FIG. 34. The vertical electron affinities of CH^+ ($r_{\text{CH}} = 1.120 \text{ \AA}$) calculated by the CI, EOM-CC, Δ CC, Li-Paldus SUMRCC, and Δ MP methods and 6-31G* basis set with the highest virtual and lowest occupied orbitals kept frozen in the low-spin reference determinants.¹³¹ The solid and dotted-dashed horizontal lines indicate the exact (FCI) values for doublet and quartet states, respectively. Filled circles correspond to Koopmans states, open circles to 2p-1h satellite states, and crosses to the 3p-2h satellite state.

Paldus SUMRCC, and Δ MP methods. There are two Koopmans electron affinities (the filled circles) in the shown energy range. The rest are satellite electron-attachment transitions, and one of them is the 3p-2h type (the crosses), while four are the 2p-1h type (the open circles).

For the Koopmans EAs, CIS = EA-EOM-CCS = Δ MP1 yield the HF orbital energy (the sign reversed) as per the Koopmans theorem. The results are rather poor because unlike in IPs, correlation and orbital-relaxation errors do not cancel with each other, but rather they pile up.¹⁸⁶ CISD has errors approaching 2 eV, while EA-EOM-CCSD is nearly converged. Δ CCS and Li-Paldus SUMRCCS are impressively accurate and Δ CCSD and Li-Paldus SUMRCCSD are essentially exact. Δ MP2 is also accurate. These may suggest that there is little correlation but considerable orbital relaxation upon electron attachment.

CIS fails to locate the roots corresponding to the 2p-1h satellite states. CIS and CISD also lack the root for the 3p-2h state. EA-EOM-CCSD do have the 2p-1h roots, but their EAs are in error by nearly 2 eV and are not useful. EA-EOM-CCSDT nearly completely corrects these errors. EA-EOM-CCSDT is still erroneous by 1.5 eV for the 3p-2h satellite electron attachment, and it takes EA-EOM-CCSDTQ for its prediction to be quantitative (error of 0.03 eV). These performance trends are expected.^{7,8,10,131}

In contrast, Δ CC and Li-Paldus SUMRCC series are practically converged at the CCSD level. For the 3p-2h state, which poses a considerable difficulty for EA-EOM-CC, even Δ CCS and Li-Paldus SUMRCCS are quantitative (errors of 0.07 eV) and almost as accurate as EA-EOM-CCSDTQ. This is because the state's wave function is dominated by doubly degenerate 3p-2h determinants and is straightforward to describe. The Δ MP series are also generally rapidly convergent except for a few signs of oscillatory divergence. For this par-

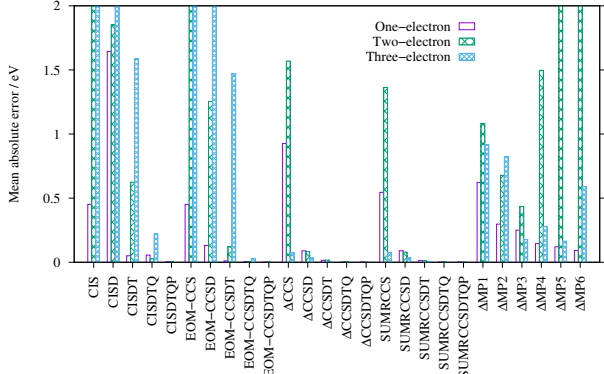


FIG. 35. The mean absolute errors of the CI, EOM-CC, Δ CC, Li-Paldus SUMRCC, and Δ MP methods from the FCI method for predominantly one-, two-, and three-electron excitation, ionization, or electron-attachment transitions. An error of infinity is recorded when the corresponding root does not exist.

ticular problem, the order of performance is Δ CC > Δ MP > EA-EOM-CC > CI.

D. Summary of the numerical tests

The foregoing benchmark calculations' results can be summarized in Fig. 35 in the form of comparison of their mean absolute errors from the FCI data. The minimal-basis-set calculations on the BH molecule are excluded. The order of performance is Δ CC > EOM-CC > CI as well as Δ CC > Δ MP > MBGF corrected for their cost scaling. The last method is not included in Fig. 35, but the order is based on the established fact that for most Koopmans roots, Δ MP \approx MBGF, while for most satellite roots, the Δ MP series are convergent toward the correct FCI limits (unless divergent), but the MBGF series are frequently convergent at wrong limits.¹²⁴ Li-Paldus SUMRCC and Δ CC theories' performance are interchangeable beyond the CCS level, and in this sense, the rather strong restrictions (in the form of projectors) imposed on the Δ CC ansatz by its black-box requirement have the minimal impact on the performance. The practical utility of Δ CCS is limited for general states and transitions, but there are a few pieces of evidence suggesting that it is accurate for core ionizations and high-spin states, where there are large orbital-relaxation and small correlation effects, and possibly for electron affinities also.

In short, Δ CC theory is a viable alternative to the powerful and versatile EOM-CC theory with complementary pros and cons; it may even become a replacement of the latter in many applications.

V. CONCLUSIONS AND OUTLOOK

A systematically converging, size-extensive, and black-box *ab initio* CC theory is introduced, which applies the time-honored exponential ansatz of single-reference CC theory to degenerate as well as nondegenerate reference determinants with any numbers and occupancies of α - and β -spin electrons. This degenerate CC (Δ CC) theory is a natural CC extension of the degenerate Rayleigh–Schrödinger perturbation theory based on the Møller–Plesset partitioning (Δ MP), the former being an infinite diagram resummation of the latter including the folded diagrams of Δ MP theory, which can be further transformed into the renormalization diagrams of finite-temperature MBPT.¹⁵⁵

It can be applied to excited, ionized, and electron-attached states with any number of electrons excited, removed, added, and/or spin-flipped. For a given truncation order of the cluster excitation operator, all of these situations can be handled uniformly by one and the same set of formalisms implemented into a single computer program. Nowhere in the Δ CC formalisms do we need an ionization, double-ionization, electron-attachment, spin-flip, etc. operator; instead, (degenerate) reference determinants are responsible for describing electron rearrangements and the exponential operator is left to concentrate on capturing electron correlation. For instance, Δ CC theory reaps the same benefits as the spin-flip methods of Krylov and coworkers^{162–164} by simply adopting a high-spin determinant as the reference.

For all excitation, ionization, and electron-attachment energies of one-, two-, and three-electron types considered in this study, Δ CC including singles and doubles (Δ CCSD) achieves the mean absolute errors of 0.08, 0.09, and 0.03 eV, respectively. This is compared with non-size-extensive CISD, which has the large errors of 1.6, 1.9, and ∞ eV, with “ ∞ ” meaning that there are no roots. The widely used EOM-CCSD method displays much smaller errors of 0.13, 1.3, and ∞ eV, but its performance falls short of Δ CCSD. The order of performance is, therefore, Δ CC > EOM-CC > CI.

The third-order Δ MP method (Δ MP3) has the same $O(n^6)$ scaling as Δ CCSD, CISD, and EOM-CCSD and has the corresponding errors of 0.25, 0.43, and 0.18 eV, respectively, for one-, two-, and three-electron transitions, which are decent. However, Δ MP4 has the errors of 0.15, 1.5, and 0.28 eV, showing signs of divergence. Δ MP theory is, therefore, hard to use in a predictive calculation that requires a converging series of approximations. Feynman–Dyson MBGF theory is even worse, guaranteed to converge at wrong limits for most satellite ionized or electron-attachment transitions.¹²⁴ The order of performance is Δ CC > Δ MP > MBGF, underscoring the importance of infinite diagram resummation that turns Δ MP into Δ CC.

The Δ CCS method can be viewed as a projection HF theory for degenerate and nondegenerate references. In the general context, however, its practical utility seems limited because its accuracy is low. However, there are pieces of evidence and compelling theoretical arguments suggesting that it is more accurate than CIS, EOM-CCS, or Koopmans theorem for core ionizations and high-spin states, and thus can be a method of

choice for these cases. It may also work well for electron affinities. A more systematic, larger-scale benchmark study is needed to reach a definitive conclusion.

Δ CC theory is a promising alternative to the popular, powerful, versatile EOM-CC theory with complementary pros and cons; it may even be a replacement of the latter in many applications. EOM-CC theory may be ideally suited for simulations of one-photon absorption/emission spectra and various one-particle properties. Its trial-vector algorithms are exceedingly robust and efficient. Δ CC theory seems generally and considerably more accurate for a wide range of electronic configurations and transitions. It should be able to reuse the formalisms for analytical derivatives and properties as well as their optimized algorithms of the well-established single-reference CC methods. Our pilot implementations have revealed only slightly more frequent convergence difficulties of the iterative solution algorithm of the amplitude equations.

Looking ahead, we find it important to develop an efficient, optimal-scaling algorithm of the Δ CC methods through a sufficiently high order (the present Δ CCS and Δ CCSD implementations are optimal scaling, but inefficient). Formulas, algorithms, and computer codes should be developed for their analytical derivatives, transition probabilities between two Δ CC states, noniterative inclusions of higher-order connected excitation operators such as CCSD(T)^{214,215} and CCSD(2),²¹⁶ explicitly correlated ansätze, crystals under periodic boundary conditions, etc. Having roots for all reference determinants, Δ CC theory (but not EOM-CC theory) can serve as a basis for a finite-temperature generalization of CC theory,^{217–223} which should be consistent with and an infinite diagram resummation of finite-temperature MBPT.^{155,224–229} Such a theory may eventually encompass *ab initio* descriptions of electron correlation in a metal at nonzero temperature and of nonideal gases and liquids and their equation of state,^{230,231} an exciting new dimension to CC theory.²³²

Appendix: Equivalence of variational coupled-cluster singles and Hartree–Fock theory

As per Thouless,¹⁹⁰ a Slater determinant acted on by $e^{\hat{T}_1}$ with the single-excitation operator \hat{T}_1 is another Slater determinant. Hence, the VCC method^{191–200} limited to singles (VCCS) is identified as the conventional HF theory, despite its nonterminating energy and amplitude equations. Here, we shall demonstrate how the nonterminating energy equation of VCCS is transformed to the HF energy expression and thus VCCS (if not VCCSD or higher¹⁹⁹) is a viable computational procedure, which may bypass explicit orbital rotations or matrix diagonalization. This conclusion is an obvious consequence of the Thouless theorem, and VCCS is not implemented in this work.

Let $|\Phi\rangle$ be a normalized Slater determinant made of $\{\varphi_i|i=1, \dots, n\}$, where n is the number of electrons. Then,

$$|\Psi\rangle = e^{\hat{T}_1}|\Phi\rangle \quad (\text{A.1})$$

is also another Slater determinant made of a different set of orthogonal spin-orbitals $\{\psi_\alpha|\alpha=1, \dots, n\}$. The $|\Psi\rangle$ is inter-

mediately normalized to $|\Phi\rangle$, i.e., $\langle\Psi|\Phi\rangle = 1$. Its \hat{T}_1 operator is the single-excitation operator,

$$\hat{T}_1 = \sum_i^{\text{occ.}} \sum_a^{\text{vir.}} (t)_i^a \hat{a}^\dagger \hat{i}, \quad (\text{A.2})$$

whose amplitudes are given by¹⁹⁰

$$(t)_i^a = \sum_\alpha O_\alpha^{i*} V_\alpha^a, \quad (\text{A.3})$$

where matrices \mathbf{O} and \mathbf{V} connect ψ 's with φ 's by the relationship,

$$\psi_\alpha = \sum_i^{\text{occ.}} O_\alpha^i \varphi_i + \sum_a^{\text{vir.}} V_\alpha^a \varphi_a. \quad (\text{A.4})$$

We adhere to the convention that i, j, k , and l (a, b, c , and d) refer to occupied (virtual) orbitals in $|\Phi\rangle$, while Greek letters denote occupied orbitals in $|\Psi\rangle$. The $n \times n$ matrix \mathbf{O} above is unitary, satisfying

$$\sum_i O_\alpha^{i*} O_\beta^i = \delta_{\alpha\beta}, \quad (\text{A.5})$$

$$\sum_\alpha O_\alpha^{i*} O_\alpha^j = \delta_{ij}, \quad (\text{A.6})$$

where δ is Kronecker's delta. Since $\{\psi_\alpha\}$ are mutually orthogonal, but not normalized, we can write

$$\langle\psi_\alpha|\psi_\beta\rangle = (1 + S_\alpha)\delta_{\alpha\beta} \quad (\text{A.7})$$

with

$$\sum_a^{\text{vir.}} V_\alpha^{a*} V_\beta^a = S_\alpha \delta_{\alpha\beta}. \quad (\text{A.8})$$

See the original paper by Thouless¹⁹⁰ for a proof of the foregoing statements.

The HF energy expression in the determinant $|\Psi\rangle$ is expanded as

$$E_\psi^{\text{HF}} = \langle\Psi|\hat{H}|\Psi\rangle = \frac{\langle\Psi|\hat{h}|\Psi\rangle}{\langle\Psi|\Psi\rangle} + \frac{\langle\Psi|\hat{v}|\Psi\rangle}{\langle\Psi|\Psi\rangle} \quad (\text{A.9})$$

where \hat{h} is the one-electron part of the Hamiltonian \hat{H} and \hat{v} is the two-electron part. (The zero-electron part can be set to zero without losing generality.) Each term in the right-hand side is further rewritten using \mathbf{O} and \mathbf{V} as

$$\begin{aligned} \frac{\langle\Psi|\hat{h}|\Psi\rangle}{\langle\Psi|\Psi\rangle} &= \frac{\sum(h)_\alpha^\alpha}{1 + S} = \\ &\frac{\sum O_\alpha^{j*}(h)_i^j O_\alpha^i}{1 + S} + \frac{\sum O_\alpha^{i*}(h)_a^i V_\alpha^a}{1 + S} + \frac{\sum V_\alpha^{a*}(h)_i^a O_\alpha^i}{1 + S} + \frac{\sum V_\alpha^{b*}(h)_a^b V_\alpha^a}{1 + S} \end{aligned} \quad (\text{A.10})$$

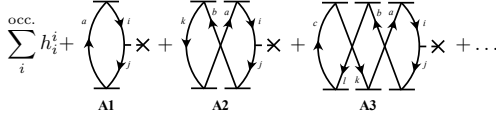


FIG. 36. The nonterminating series of the VCCS accordion diagrams involving $(h)_i^j$ denoted by a cross.

where $(h)_\beta^\alpha = \langle \psi_\alpha | \hat{h} | \psi_\beta \rangle$, $(h)_q^p = \langle \varphi_p | \hat{h} | \varphi_q \rangle$, and $S = \sum_\alpha S_\alpha$, as well as

$$\begin{aligned} \frac{\langle \Psi | \hat{v} | \Psi \rangle}{\langle \Psi | \Psi \rangle} &= \frac{1}{2} \frac{\sum(v)_{\alpha\beta}^{\alpha\beta}}{(1+S)^2} = \\ &\frac{1}{2} \frac{\sum O_\alpha^{k*} O_\beta^{l*} (v)_{ij}^{kl} O_\alpha^i O_\beta^j}{(1+S)^2} + \frac{1}{2} \frac{\sum O_\alpha^{k*} V_\beta^{a*} (v)_{ij}^{ka} O_\alpha^i O_\beta^j}{(1+S)^2} \\ &+ \frac{1}{2} \frac{\sum V_\alpha^{a*} O_\beta^{k*} (v)_{ij}^{ak} O_\alpha^i O_\beta^j}{(1+S)^2} + \frac{1}{2} \frac{\sum V_\alpha^{a*} V_\beta^{b*} (v)_{ij}^{ab} O_\alpha^i O_\beta^j}{(1+S)^2} \\ &+ \dots + \frac{1}{2} \frac{\sum V_\alpha^{a*} V_\beta^{b*} (v)_{cd}^{ab} V_\alpha^c V_\beta^d}{(1+S)^2}, \end{aligned} \quad (\text{A.11})$$

where $(v)_{\gamma\delta}^{\alpha\beta} = \langle \psi_\alpha \psi_\beta | \psi_\gamma \psi_\delta \rangle$ and $(v)_{rs}^{pq} = \langle \varphi_p \varphi_q | \varphi_r \varphi_s \rangle$. There are sixteen terms in the right-hand side, and the indices and ranges of all unrestricted summations are suppressed to save space.

We shall show that the same energy formula can be reached by a transformation of the following nonterminating energy expression of VCCS:

$$\begin{aligned} E^{\text{VCCS}} &= \frac{\langle \Psi | \hat{H} | \Psi \rangle}{\langle \Psi | \Psi \rangle} = \frac{\langle \Phi | e^{\hat{T}_1^\dagger} \hat{H} e^{\hat{T}_1} | \Phi \rangle}{\langle \Phi | e^{\hat{T}_1^\dagger} e^{\hat{T}_1} | \Phi \rangle} = \langle \Phi | e^{\hat{T}_1^\dagger} \hat{H} e^{\hat{T}_1} | \Phi \rangle_C \\ &= E_\varphi^{\text{HF}} + \langle \Phi | \hat{H} \hat{T}_1 | \Phi \rangle_C + \langle \Phi | \hat{T}_1^\dagger \hat{H} | \Phi \rangle_C \\ &\quad + \langle \Phi | \hat{T}_1^\dagger \hat{H} \hat{T}_1 | \Phi \rangle_C + \frac{1}{2} \langle \Phi | \hat{H} (\hat{T}_1)^2 | \Phi \rangle_C \\ &\quad + \frac{1}{2} \langle \Phi | (\hat{T}_1^\dagger)^2 \hat{H} | \Phi \rangle_C + \frac{1}{2} \langle \Phi | \hat{T}_1^\dagger \hat{H} (\hat{T}_1)^2 | \Phi \rangle_C \\ &\quad + \frac{1}{2} \langle \Phi | (\hat{T}_1^\dagger)^2 \hat{H} \hat{T}_1 | \Phi \rangle_C \\ &\quad + \frac{1}{4} \langle \Phi | (\hat{T}_1^\dagger)^2 \hat{H} (\hat{T}_1)^2 | \Phi \rangle_C + \dots, \end{aligned} \quad (\text{A.12})$$

where the first term in the right-hand side is the HF energy of $|\Phi\rangle$,

$$\begin{aligned} E_\varphi^{\text{HF}} &= \langle \Phi | \hat{h} | \Phi \rangle + \langle \Phi | \hat{v} | \Phi \rangle \\ &= \sum (h)_i^i + \frac{1}{2} \sum (v)_{ij}^{ij}, \end{aligned} \quad (\text{A.13})$$

which differs from E_ψ^{HF} of Eq. (A.9) both formally and numerically. Here, “ $\langle \dots \rangle_C$ ” means diagrammatically connected. Despite this strong restriction on the diagram topology, an infinite number of valid diagrams arise because of the simultaneous and repeated appearances of the \hat{T}_1^\dagger deexcitation and \hat{T}_1 excitation operators. They feature successive contractions of \hat{T}_1^\dagger and \hat{T}_1 vertexes, and may be called “accordion” diagrams.¹⁹⁹

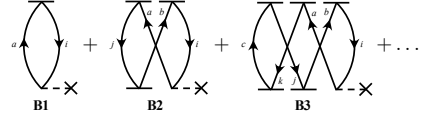


FIG. 37. The nonterminating series of the VCCS accordion diagrams involving $(h)_i^a$ denoted by a cross.

Collecting diagrams containing an $(h)_i^j$ vertex, we obtain Fig. 36. Here, a Fock-operator vertex is split into one with an h vertex (cross) and the other with a v vertex (circle; see below) because the Fock operator depends on the orbitals in the manner that unduly complicates the following analysis.

The interpretation of these diagrams into algebraic formulas obeys the same rules documented in Shavitt and Bartlett.⁸ For example, diagram **A1** is interpreted as

$$\begin{aligned} \mathbf{A1} &= (-1)^{\text{holes}+1} \text{loop} \sum (t)_i^{a*} (t)_j^a (h)_i^j \\ &= - \sum O_\alpha^i V_\alpha^{a*} O_\beta^{j*} V_\beta^a (h)_i^j \\ &= -S \sum (h)_i^i, \end{aligned} \quad (\text{A.14})$$

where Eqs. (A.6) and (A.8) are used in the last equality. Likewise, accordion diagrams **A2** and **A3** are transformed as

$$\begin{aligned} \mathbf{A2} &= (-1)^{3+1} \sum (t)_i^{a*} (t)_j^b (t)_k^{b*} (t)_k^a (h)_i^j \\ &= \sum O_\alpha^i V_\alpha^{a*} O_\beta^{j*} V_\beta^b O_\gamma^k V_\gamma^{b*} O_\delta^k V_\delta^{a*} O_\epsilon^i V_\epsilon^{a*} O_\zeta^{j*} V_\zeta^b (h)_i^j \\ &= S^2 \sum (h)_i^i, \end{aligned} \quad (\text{A.15})$$

and

$$\begin{aligned} \mathbf{A3} &= (-1)^{4+1} \sum (t)_i^{c*} (t)_l^c (t)_l^{b*} (t)_k^a (t)_i^{a*} (t)_j^b (h)_i^j \\ &= - \sum O_\alpha^k V_\alpha^{c*} O_\beta^{l*} V_\beta^c O_\gamma^l V_\gamma^{b*} O_\delta^k V_\delta^a O_\epsilon^i V_\epsilon^{a*} O_\zeta^{j*} V_\zeta^b (h)_i^j \\ &= -S^3 \sum (h)_i^i, \end{aligned} \quad (\text{A.16})$$

where Eqs. (A.5)–(A.8) are repeatedly used. Generally, each addition of a \hat{T}_1^\dagger - \hat{T}_1 pair multiplies $(-S)$ to the algebraic interpretation of the parent diagram, although care must be exercised to the diagram symmetry. Summing them together, we have

$$\begin{aligned} \sum (h)_i^i + \mathbf{A1} + \mathbf{A2} + \mathbf{A3} + \dots &= \\ \sum (h)_i^i (1 - S + S^2 - S^3 + \dots) &= \frac{\sum (h)_i^i}{1+S} = \frac{\sum O_\alpha^{j*} (h)_i^j O_\alpha^i}{1+S}, \end{aligned} \quad (\text{A.17})$$

which agrees with the first term in the right-hand side of Eq. (A.10).

Turning to diagrams with an $(h)_i^a$ vertex, we obtain Fig. 37. Expanding the i th hole line into accordions leads to the identical series of diagrams, and is thus unnecessary. Their alge-

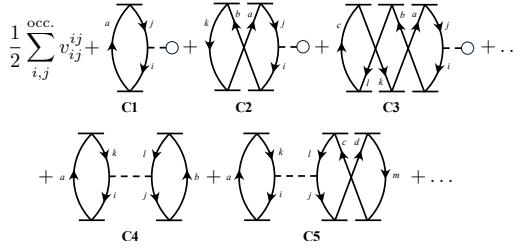


FIG. 38. The nonterminating series of the VCCS accordion diagrams involving $(v)_{ij}^{kl}$ denoted by a dashed line and $\sum_k (v)_{jk}^{ik}$ denoted by a circle.

braic interpretation reads

$$\begin{aligned}
 & \mathbf{B1} + \mathbf{B2} + \mathbf{B3} + \dots \\
 &= (-1)^{1+1} \sum (t)_i^{a*} (h)_i^a + (-1)^{2+1} \sum (t)_j^{a*} (t)_j^b (t)_i^{b*} (h)_i^a \\
 &+ (-1)^{3+1} \sum (t)_j^{c*} (t)_k^c (t)_k^{a*} (t)_j^b (t)_i^{b*} (h)_i^a + \dots \\
 &= \sum O_\alpha^i V_\alpha^{a*} (h)_i^a - \sum O_\alpha^j V_\alpha^{a*} O_\beta^{j*} V_\beta^b O_\gamma^i V_\gamma^{b*} (h)_i^a \\
 &+ \sum O_\alpha^j V_\alpha^{c*} O_\beta^{k*} V_\beta^c O_\gamma^{k*} V_\gamma^a O_\delta^{j*} V_\delta^b O_\epsilon^i V_\epsilon^{b*} (h)_i^a + \dots \\
 &= \sum V_\alpha^{a*} (h)_i^a O_\alpha^i (1 - S + S^2 - \dots) \\
 &= \frac{\sum V_\alpha^{a*} (h)_i^a O_\alpha^i}{1 + S}, \tag{A.18}
 \end{aligned}$$

which is equal to the third term in the right-hand side of Eq. (A.10). Clearly, similar procedures account for the second and fourth terms, and thus for the whole one-electron part of E_ψ^{HF} [Eq. (A.9)].

The infinite series of the VCCS accordion diagrams containing a $(v)_{ij}^{kl}$ vertex is drawn in Fig. 38. It consists of a constant (the first algebraic term), diagrams originating from the ones with a Fock-operator vertex (**C1**, **C2**, and **C3**), and the rest (**C4** and **C5**). They are algebraically interpreted as

$$\begin{aligned}
 & \frac{1}{2} \sum (v)_{ij}^{ij} + \mathbf{C1} + \mathbf{C2} + \mathbf{C3} + \dots + \mathbf{C4} + \mathbf{C5} + \dots \\
 &= \frac{1}{2} \sum (v)_{ij}^{ij} - S \sum (v)_{ij}^{ij} + S^2 \sum (v)_{ij}^{ij} - S^3 \sum (v)_{ij}^{ij} + \dots \\
 &+ \frac{1}{2} S^2 \sum (v)_{ij}^{ij} - S^3 \sum (v)_{ij}^{ij} + \dots \\
 &= \frac{1}{2} \sum (v)_{ij}^{ij} (1 - 2S + 3S^2 - 4S^3 + \dots) \\
 &= \frac{1}{2} \frac{\sum O_\alpha^{k*} O_\beta^{l*} (v)_{ij}^{kl} O_\alpha^i O_\beta^j}{(1 + S)^2}, \tag{A.19}
 \end{aligned}$$

thus accounting for the $(v)_{ij}^{kl}$ contribution to the E_ψ^{HF} in its entirety, i.e., the first term in the right-hand side of Eq. (A.11).

Likewise, the VCCS accordion diagrams containing a $(v)_{ij}^{ab}$

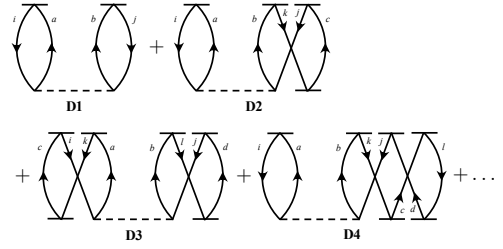


FIG. 39. The nonterminating series of the VCCS accordion diagrams involving $(v)_{ij}^{ab}$ denoted by a dashed line.

vertex (Fig. 39) are interpreted algebraically as

$$\begin{aligned}
 & \mathbf{D1} + \mathbf{D2} + \mathbf{D3} + \mathbf{D4} + \dots \\
 &= \frac{1}{2} \sum V_\alpha^{a*} V_\beta^{b*} (v)_{ij}^{ab} O_\alpha^i O_\beta^j - S \sum V_\alpha^{a*} V_\beta^{b*} (v)_{ij}^{ab} O_\alpha^i O_\beta^j \\
 &+ \frac{1}{2} S^2 \sum V_\alpha^{a*} V_\beta^{b*} (v)_{ij}^{ab} O_\alpha^i O_\beta^j \\
 &+ S^2 \sum V_\alpha^{a*} V_\beta^{b*} (v)_{ij}^{ab} O_\alpha^i O_\beta^j + \dots \\
 &= \frac{1}{2} \sum V_\alpha^{a*} V_\beta^{b*} (v)_{ij}^{ab} O_\alpha^i O_\beta^j (1 - 2S + 3S^2 - \dots) \\
 &= \frac{1}{2} \frac{\sum V_\alpha^{a*} V_\beta^{b*} (v)_{ij}^{ab} O_\alpha^i O_\beta^j}{(1 + S)^2}, \tag{A.20}
 \end{aligned}$$

which agrees with the whole $(v)_{ij}^{ab}$ contribution to the E_ψ^{HF} , i.e., the fourth term in the right-hand side of Eq. (A.11). Clearly, all sixteen terms of the latter are generated in the same way. This completes the proof that the sum of the nonterminating series of the VCCS accordion diagrams is equal to the HF energy expression.

Note that linear response theory applied to CCS with a HF reference is EOM-CCS, and it is equivalent to CIS (see Sec. IV), but not to time-dependent HF (TDHF), which is the linear response of HF theory. This is because ‘CCS’ here is based on the projection ansatz. If linear response theory were applied to VCCS instead, the result would be TDHF (and not CIS).

SUPPLEMENTARY MATERIAL

Numerical data used to generate the figures are made available as supplementary material.

ACKNOWLEDGMENTS

The author expresses the deepest gratitude to Late Professor John F. Stanton for his continuous encouragement and friendship over the years. He also thanks Professors Rodney J. Bartlett, Martín Mosquera, and Piotr Piecuch for their interest in this study, technical advice, and stimulating discussions. This work has been supported by the U.S. Department of Energy (DoE), Office of Science, Office of Basic Energy Sciences under Grant No. DE-SC0006028 and also by the Center for Scalable Predictive methods for Excitations and Correlated phenomena (SPEC), which is funded by the U.S. DoE,

Office of Science, Office of Basic Energy Sciences, Division of Chemical Sciences, Geosciences and Biosciences as part of the Computational Chemical Sciences (CCS) program at Pacific Northwest National Laboratory (PNNL) under FWP 70942. PNNL is a multi-program national laboratory operated by Battelle Memorial Institute for the U.S. DoE.

DATA AVAILABILITY

The data that support the findings of this study are available within the article and its supplementary material.

- ¹F. Coester, "Bound states of a many-particle system," *Nucl. Phys.* **7**, 421–424 (1958).
- ²F. Coester and H. Kümmel, "Short-range correlations in nuclear wave functions," *Nucl. Phys.* **17**, 477–485 (1960).
- ³J. Čížek, "On correlation problem in atomic and molecular systems. Calculation of wavefunction components in Ursell-type expansion using quantum-field theoretical methods," *J. Chem. Phys.* **45**, 4256–4266 (1966).
- ⁴J. Čížek, "On the use of the cluster expansion and the technique of diagrams in calculations of correlation effects in atoms and molecules," *Adv. Chem. Phys.* **14**, 35–89 (1969).
- ⁵J. Paldus, I. Shavitt, and J. Čížek, "Correlation problems in atomic and molecular systems. IV. Extended coupled-pair many-electron theory and its application to BH_3 molecule," *Phys. Rev. A* **5**, 50–67 (1972).
- ⁶H. Kümmel, K. H. Lührmann, and J. G. Zabolitzky, "Many-fermion theory in $\text{exp}S$ (or coupled cluster) form," *Phys. Rep.* **36**, 1–63 (1978).
- ⁷R. J. Bartlett and M. Musiał, "Coupled-cluster theory in quantum chemistry," *Rev. Mod. Phys.* **79**, 291–352 (2007).
- ⁸I. Shavitt and R. J. Bartlett, *Many-Body Methods in Chemistry and Physics* (Cambridge University Press, Cambridge, 2009).
- ⁹R. J. Bartlett, "The coupled-cluster revolution," *Mol. Phys.* **108**, 2905–2920 (2010).
- ¹⁰R. J. Bartlett, "Coupled-cluster theory and its equation-of-motion extensions," *WIREs Comput. Mol. Sci.* **2**, 126–138 (2012).
- ¹¹J. A. Pople, "Nobel Lecture: Quantum chemical models," *Rev. Mod. Phys.* **71**, 1267–1274 (1999).
- ¹²R. J. Bartlett, "Coupled-cluster approach to molecular structure and spectra: A step toward predictive quantum chemistry," *J. Phys. Chem.* **93**, 1697–1708 (1989).
- ¹³S. Hirata and K. Yagi, "Predictive electronic and vibrational many-body methods for molecules and macromolecules," *Chem. Phys. Lett.* **464**, 123–134 (2008).
- ¹⁴G. D. Purvis III and R. J. Bartlett, "A full coupled-cluster singles and doubles model: The inclusion of disconnected triples," *J. Chem. Phys.* **76**, 1910–1918 (1982).
- ¹⁵J. A. Pople, R. Krishnan, H. B. Schlegel, and J. S. Binkley, "Electron correlation theories and their application to study of simple reaction potential surfaces," *Int. J. Quantum Chem.* **14**, 545–560 (1978).
- ¹⁶R. J. Bartlett and G. D. Purvis III, "Many-body perturbation theory, coupled-pair many-electron theory, and importance of quadruple excitations for correlation problem," *Int. J. Quantum Chem.* **14**, 561–581 (1978).
- ¹⁷J. Noga and R. J. Bartlett, "The full CCSDT model for molecular electronic structure," *J. Chem. Phys.* **86**, 7041–7050 (1987).
- ¹⁸G. E. Scuseria and H. F. Schaefer III, "A new implementation of the full CCSDT model for molecular electronic structure," *Chem. Phys. Lett.* **152**, 382–386 (1988).
- ¹⁹S. A. Kucharski and R. J. Bartlett, "The coupled-cluster single, double, triple, and quadruple excitation method," *J. Chem. Phys.* **97**, 4282–4288 (1992).
- ²⁰M. Musiał, S. A. Kucharski, and R. J. Bartlett, "Formulation and implementation of the full coupled-cluster method through pentuple excitations," *J. Chem. Phys.* **116**, 4382–4388 (2002).
- ²¹S. Hirata and R. J. Bartlett, "High-order coupled-cluster calculations through connected octuple excitations," *Chem. Phys. Lett.* **321**, 216–224 (2000).
- ²²M. Kállay and P. R. Surján, "Computing coupled-cluster wave functions with arbitrary excitations," *J. Chem. Phys.* **113**, 1359–1365 (2000).
- ²³J. Olsen, "The initial implementation and applications of a general active space coupled cluster method," *J. Chem. Phys.* **113**, 7140–7148 (2000).
- ²⁴Both Greek and Latin numerical prefixes are used in these acronyms to minimize repeated initial letters.
- ²⁵R. J. Bartlett, "Many-body perturbation theory and coupled cluster theory for electron correlation in molecules," *Annu. Rev. Phys. Chem.* **32**, 359–401 (1981).
- ²⁶L. Adamowicz, W. D. Laidig, and R. J. Bartlett, "Analytical gradients for the coupled-cluster method," *Int. J. Quantum Chem.* **S18**, 245–254 (1984).
- ²⁷A. C. Scheiner, G. E. Scuseria, J. E. Rice, T. J. Lee, and H. F. Schaefer III, "Analytic evaluation of energy gradients for the single and double excitation coupled cluster (CCSD) wave function: Theory and application," *J. Chem. Phys.* **87**, 5361–5373 (1987).
- ²⁸G. E. Scuseria, A. C. Scheiner, J. E. Rice, T. J. Lee, and H. F. Schaefer III, "Analytic evaluation of energy gradients for the single and double excitation coupled cluster (CCSD) wave function. A comparison with configuration-interaction (CISD, CISDT, and CISDTQ) results for the harmonic vibrational frequencies, infrared intensities, dipole moment, and inversion barrier of ammonia," *Int. J. Quantum Chem.* **S21**, 495–501 (1987).
- ²⁹E. A. Salter, G. W. Trucks, and R. J. Bartlett, "Analytic energy derivatives in many-body methods. I. First derivatives," *J. Chem. Phys.* **90**, 1752–1766 (1989).
- ³⁰H. Koch, H. J. A. Jensen, P. Jørgensen, T. Helgaker, G. E. Scuseria, and H. F. Schaefer III, "Coupled cluster energy derivatives. Analytic Hessian for the closed-shell coupled cluster singles and doubles wave function: Theory and applications," *J. Chem. Phys.* **92**, 4924–4940 (1990).
- ³¹J. Gauss, J. F. Stanton, and R. J. Bartlett, "Coupled-cluster open-shell analytic gradients: Implementation of the direct-product decomposition approach in energy gradient calculations," *J. Chem. Phys.* **95**, 2623–2638 (1991).
- ³²J. Gauss, J. F. Stanton, and R. J. Bartlett, "Analytic evaluation of energy gradients at the coupled-cluster singles and doubles level using quasi-restricted Hartree–Fock open-shell reference functions," *J. Chem. Phys.* **95**, 2639–2645 (1991).
- ³³J. F. Stanton and J. Gauss, "Analytic second derivatives in high-order many-body perturbation and coupled-cluster theories: Computational considerations and applications," *Int. Rev. Phys. Chem.* **19**, 61–95 (2000).
- ³⁴J. Gauss and J. F. Stanton, "Analytic gradients for the coupled-cluster singles, doubles, and triples (CCSDT) model," *J. Chem. Phys.* **116**, 1773–1782 (2002).
- ³⁵M. Kállay, J. Gauss, and P. G. Szalay, "Analytic first derivatives for general coupled-cluster and configuration interaction models," *J. Chem. Phys.* **119**, 2991–3004 (2003).
- ³⁶M. Kállay and J. Gauss, "Analytic second derivatives for general coupled-cluster and configuration-interaction models," *J. Chem. Phys.* **120**, 6841–6848 (2004).
- ³⁷S. A. Perera and R. J. Bartlett, "Coupled-cluster calculations of Raman intensities and their application to N_4 and N_5^- ," *Chem. Phys. Lett.* **314**, 381–387 (1999).
- ³⁸D. P. O'Neill, M. Kállay, and J. Gauss, "Analytic evaluation of Raman intensities in coupled-cluster theory," *Mol. Phys.* **105**, 2447–2453 (2007).
- ³⁹T.-C. Jagau, J. Gauss, and K. Ruud, "Analytic evaluation of the dipole hessian matrix in coupled-cluster theory," *J. Chem. Phys.* **139**, 154106 (2013).
- ⁴⁰J. F. Stanton and R. J. Bartlett, "A coupled-cluster based effective Hamiltonian method for dynamic electric polarizabilities," *J. Chem. Phys.* **99**, 5178–5183 (1993).
- ⁴¹R. Kobayashi, H. Koch, and P. Jørgensen, "Static polarizabilities and dipole moment derivatives for the closed-shell coupled-cluster singles and doubles wave function," *J. Chem. Phys.* **101**, 4956–4963 (1994).
- ⁴²P. B. Rozyczko, S. A. Perera, M. Nooijen, and R. J. Bartlett, "Correlated calculations of molecular dynamic polarizabilities," *J. Chem. Phys.* **107**, 6736–6747 (1997).
- ⁴³C. Hättig, O. Christiansen, H. Koch, and P. Jørgensen, "Frequency-dependent first hyperpolarizabilities using coupled cluster quadratic response theory," *Chem. Phys. Lett.* **269**, 428–434 (1997).
- ⁴⁴D. P. O'Neill, M. Kállay, and J. Gauss, "Calculation of frequency-dependent hyperpolarizabilities using general coupled-cluster models," *J. Chem. Phys.* **127**, 134109 (2007).

⁴⁵S. A. Perera, H. Sekino, and R. J. Bartlett, "Coupled-cluster calculations of indirect nuclear coupling constants. The importance of non-Fermi contact contributions," *J. Chem. Phys.* **101**, 2186–2191 (1994).

⁴⁶J. Gauss and J. F. Stanton, "Gauge-invariant calculation of nuclear magnetic shielding constants at the coupled-cluster singles and doubles level," *J. Chem. Phys.* **102**, 251–253 (1995).

⁴⁷J. Gauss and J. F. Stanton, "Coupled-cluster calculations of nuclear magnetic resonance chemical shifts," *J. Chem. Phys.* **103**, 3561–3577 (1995).

⁴⁸S. A. Perera, M. Nooijen, and R. J. Bartlett, "Electron correlation effects on the theoretical calculation of nuclear magnetic resonance spin-spin coupling constants," *J. Chem. Phys.* **104**, 3290–3305 (1996).

⁴⁹T. Helgaker, S. Coriani, P. Jørgensen, K. Kristensen, J. Olsen, and K. Ruud, "Recent advances in wave function-based methods of molecular-property calculations," *Chem. Rev.* **112**, 543–631 (2012).

⁵⁰S. Hirata, I. Grabowski, M. Tobita, and R. J. Bartlett, "Highly accurate treatment of electron correlation in polymers: Coupled-cluster and many-body perturbation theories," *Chem. Phys. Lett.* **345**, 475–480 (2001).

⁵¹S. Hirata, R. Podeszwa, M. Tobita, and R. J. Bartlett, "Coupled-cluster singles and doubles for extended systems," *J. Chem. Phys.* **120**, 2581–2592 (2004).

⁵²W. Kutzelnigg, "R12-dependent terms in the wave functions as closed sums of partial wave amplitudes for large l ," *Theor. Chim. Acta* **68**, 445–469 (1985).

⁵³S. Ten-no, "Initiation of explicitly correlated Slater-type geminal theory," *Chem. Phys. Lett.* **398**, 56–61 (2004).

⁵⁴S. Ten-no, "Explicitly correlated second order perturbation theory: Introduction of a rational generator and numerical quadratures," *J. Chem. Phys.* **121**, 117 (2004).

⁵⁵W. Klopper, F. R. Manby, S. Ten-no, and E. F. Valeev, "R12 methods in explicitly correlated molecular electronic structure theory," *Int. Rev. Phys. Chem.* **25**, 427–468 (2006).

⁵⁶T. Shiozaki, E. F. Valeev, and S. Hirata, "Explicitly correlated coupled-cluster methods," *Ann. Rep. Comp. Chem.* **5**, 131–148 (2009).

⁵⁷L. Kong, F. A. Bischoff, and E. F. Valeev, "Explicitly correlated R12/F12 methods for electronic structure," *Chem. Rev.* **112**, 75–107 (2012).

⁵⁸A. Grüneis, S. Hirata, Y.-y. Ohnishi, and S. Ten-no, "Perspective: Explicitly correlated electronic structure theory for complex systems," *J. Chem. Phys.* **146**, 080901 (2017).

⁵⁹T. Shiozaki, M. Kamiya, S. Hirata, and E. F. Valeev, "Explicitly correlated coupled-cluster singles and doubles method based on complete diagrammatic equations," *J. Chem. Phys.* **129**, 071101 (2008).

⁶⁰A. Köhn, G. W. Richings, and D. P. Tew, "Implementation of the full explicitly correlated coupled-cluster singles and doubles model CCSD-F12 with optimally reduced auxiliary basis dependence," *J. Chem. Phys.* **129**, 201103 (2008).

⁶¹T. Shiozaki, M. Kamiya, S. Hirata, and E. F. Valeev, "Higher-order explicitly correlated coupled-cluster methods," *J. Chem. Phys.* **130**, 054101 (2009).

⁶²R. J. Bartlett, "A scientific autobiography for Rodney J. Bartlett: From Elvis Presley Boulevard to the Quantum Theory Project," *J. Phys. Chem. A* **129**, 5213–5219 (2025).

⁶³J. B. Foresman, M. Head-Gordon, J. A. Pople, and M. J. Frisch, "Toward a systematic molecular-orbital theory for excited states," *J. Phys. Chem.* **96**, 135–149 (1992).

⁶⁴T. P. Živković and H. J. Monkhorst, "Analytic connection between configuration-interaction and coupled-cluster solutions," *J. Math. Phys.* **19**, 1007–1022 (1978).

⁶⁵K. Kowalski and K. Jankowski, "Towards complete solutions to systems of nonlinear equations of many-electron theories," *Phys. Rev. Lett.* **81**, 1195–1198 (1998).

⁶⁶K. Kowalski and P. Piecuch, "Complete set of solutions of the generalized Bloch equation," *Int. J. Quantum Chem.* **80**, 757–781 (2000).

⁶⁷K. Kowalski and P. Piecuch, "Complete set of solutions of multireference coupled-cluster equations: The state-universal formalism," *Phys. Rev. A* **61**, 052506 (2000).

⁶⁸S. Sverrisdóttir and F. M. Faulstich, "Exploring ground and excited states via single reference coupled-cluster theory and algebraic geometry," *J. Chem. Theory Comput.* **20**, 8517–8528 (2024).

⁶⁹F. E. Harris, "Coupled-cluster method for excitation energies," *Int. J. Quantum Chem.* **S11**, 403–411 (1977).

⁷⁰K. Emrich, "An extension of the coupled cluster formalism to excited states. I," *Nucl. Phys. A* **351**, 379–396 (1981).

⁷¹K. Emrich, "An extension of the coupled cluster formalism to excited states. II. Approximations and tests," *Nucl. Phys. A* **351**, 397–438 (1981).

⁷²H. Sekino and R. J. Bartlett, "A linear response, coupled-cluster theory for excitation energy," *Int. J. Quantum Chem.* **S18**, 255–265 (1984).

⁷³J. Geertsen, M. Rittby, and R. J. Bartlett, "The equation-of-motion coupled-cluster method: Excitation energies of Be and CO," *Chem. Phys. Lett.* **164**, 57–62 (1989).

⁷⁴D. C. Comeau and R. J. Bartlett, "The equation-of-motion coupled-cluster method: Applications to open-shell and closed-shell reference states," *Chem. Phys. Lett.* **207**, 414–423 (1993).

⁷⁵J. F. Stanton and R. J. Bartlett, "The equation of motion coupled-cluster method. A systematic biorthogonal approach to molecular excitation energies, transition probabilities, and excited-state properties," *J. Chem. Phys.* **98**, 7029–7039 (1993).

⁷⁶S. Hirata, "Higher-order equation-of-motion coupled-cluster methods," *J. Chem. Phys.* **121**, 51–59 (2004).

⁷⁷H. J. Monkhorst, "Calculation of properties with coupled-cluster method," *Int. J. Quantum Chem.* **S11**, 421–432 (1977).

⁷⁸S. Ghosh, D. Mukherjee, and S. Bhattacharyya, "Application of linear response theory in a coupled cluster framework for the calculation of ionization potentials," *Mol. Phys.* **43**, 173–179 (1981).

⁷⁹E. Dalgaard and H. J. Monkhorst, "Some aspects of the time-dependent coupled-cluster approach to dynamic response functions," *Phys. Rev. A* **28**, 1217–1222 (1983).

⁸⁰M. Takahashi and J. Paldus, "Time-dependent coupled cluster approach: Excitation-energy calculation using an orthogonally spin-adapted formalism," *J. Chem. Phys.* **85**, 1486–1501 (1986).

⁸¹H. Koch and P. Jørgensen, "Coupled cluster response functions," *J. Chem. Phys.* **93**, 3333–3344 (1990).

⁸²H. Koch, H. J. A. Jensen, P. Jørgensen, and T. Helgaker, "Excitation-energies from the coupled cluster singles and doubles linear response function (CCSDLR): Applications to be, CH⁺, CO, and H₂O," *J. Chem. Phys.* **93**, 3345–3350 (1990).

⁸³R. J. Rico and M. Head-Gordon, "Single-reference theories of molecular excited states with single and double substitutions," *Chem. Phys. Lett.* **213**, 224–232 (1993).

⁸⁴H. Nakatsuji, "Cluster expansion of the wavefunction. Electron correlations in ground and excited-states by SAC (symmetry-adapted-cluster) and SAC CI theories," *Chem. Phys. Lett.* **67**, 329–333 (1979).

⁸⁵H. Nakatsuji, "Cluster expansion of the wavefunction. Calculation of electron correlations in ground and excited-states by SAC and SAC CI theories," *Chem. Phys. Lett.* **67**, 334–342 (1979).

⁸⁶H. Nakatsuji and K. Hirao, "Cluster expansion of the wavefunction: Electron correlations in singlet and triplet excited states, ionized states, and electron attached states by SAC and SAC-CI theories," *Int. J. Quantum Chem.* **20**, 1301–1313 (1981).

⁸⁷H. Nakatsuji, K. Ohta, and K. Hirao, "Cluster expansion of the wavefunction: Electron correlations in the ground state, valence and Rydberg excited states, ionized states, and electron attached states of formaldehyde by SAC and SAC-CI theories," *J. Chem. Phys.* **75**, 2952–2958 (1981).

⁸⁸S. Hirata, M. Nooijen, and R. J. Bartlett, "High-order determinantal equation-of-motion coupled-cluster calculations for electronic excited states," *Chem. Phys. Lett.* **326**, 255–262 (2000).

⁸⁹M. A. Mosquera, "Time-dependent coupled-cluster theory of multireference systems," *Phys. Rev. A* **112**, 012825 (2025).

⁹⁰J. F. Stanton and J. Gauss, "Analytic energy derivatives for ionized states described by the equation-of-motion coupled-cluster method," *J. Chem. Phys.* **101**, 8938–8944 (1994).

⁹¹R. J. Bartlett, J. E. DelBene, S. A. Perera, and R. P. Mattie, "Ammonia: The prototypical lone pair molecule," *J. Mol. Struct. Theochem* **400**, 157–168 (1997).

⁹²J. F. Stanton and J. Gauss, "A simple scheme for the direct calculation of ionization potentials with coupled-cluster theory that exploits established excitation energy methods," *J. Chem. Phys.* **111**, 8785–8788 (1999).

⁹³M. Musial, S. A. Kucharski, and R. J. Bartlett, "Equation-of-motion coupled cluster method with full inclusion of the connected triple excitations for ionized states: IP-EOM-CCSDT," *J. Chem. Phys.* **118**, 1128–1136 (2003).

⁹⁴M. Kamiya and S. Hirata, "Higher-order equation-of-motion coupled-cluster methods for ionization processes," *J. Chem. Phys.* **125**, 074111 (2006).

⁹⁵M. Nooijen and R. J. Bartlett, "Equation-of-motion coupled-cluster method for electron attachment," *J. Chem. Phys.* **102**, 3629–3647 (1995).

⁹⁶M. Musiał and R. J. Bartlett, "Equation-of-motion coupled cluster method with full inclusion of connected triple excitations for electron-attached states: EA-EOM-CCSDT," *J. Chem. Phys.* **119**, 1901–1908 (2003).

⁹⁷M. Kamiya and S. Hirata, "Higher-order equation-of-motion coupled-cluster methods for electron attachment," *J. Chem. Phys.* **126**, 134112 (2007).

⁹⁸K. Schönhammer and O. Gunnarsson, "Time-dependent approach to the calculation of spectral functions," *Phys. Rev. B* **18**, 6606–6614 (1978).

⁹⁹M. Nooijen and J. G. Snijders, "Coupled cluster approach to the single-particle Green function," *Int. J. Quantum Chem.* **S26**, 55–83 (1992).

¹⁰⁰M. Nooijen and J. G. Snijders, "Coupled-cluster Green function method: Working equations and applications," *Int. J. Quantum Chem.* **48**, 15–48 (1993).

¹⁰¹L. Meissner and R. J. Bartlett, "Electron propagator theory with the ground-state correlated by the coupled-cluster method," *Int. J. Quantum Chem.* **S27**, 67–80 (1993).

¹⁰²K. Kowalski, K. Bhaskaran-Nair, and W. A. Shelton, "Coupled-cluster representation of Green function employing modified spectral resolutions of similarity transformed Hamiltonians," *J. Chem. Phys.* **141**, 094102 (2014).

¹⁰³B. Peng and K. Kowalski, "Coupled-cluster Green's function: Analysis of properties originating in the exponential parametrization of the ground-state wave function," *Phys. Rev. A* **94**, 062512 (2016).

¹⁰⁴K. Bhaskaran-Nair, K. Kowalski, and W. A. Shelton, "Coupled cluster Green function: Model involving single and double excitations," *J. Chem. Phys.* **144**, 144101 (2016).

¹⁰⁵J. Lee, D. W. Small, and M. Head-Gordon, "Excited states via coupled cluster theory without equation-of-motion methods: Seeking higher roots with application to doubly excited states and double core hole states," *J. Chem. Phys.* **151**, 214103 (2019).

¹⁰⁶Y. Damour, A. Scemama, D. Jacquemin, F. Koskoski, and P. F. Loos, "State-specific coupled-cluster methods for excited states," *J. Chem. Theory Comput.* **20**, 4129–4145 (2024).

¹⁰⁷A. Balková, S. A. Kucharski, L. Meissner, and R. J. Bartlett, "The multireference coupled-cluster method in Hilbert-space: An incomplete model space application to the LiH molecule," *J. Chem. Phys.* **95**, 4311–4316 (1991).

¹⁰⁸A. Balková and R. J. Bartlett, "Coupled-cluster method for open-shell singlet states," *Chem. Phys. Lett.* **193**, 364–372 (1992).

¹⁰⁹A. Balková and R. J. Bartlett, "The two-determinant coupled-cluster method for electric properties of excited electronic states: The lowest 1B_1 and 3B_1 states of the water molecule," *J. Chem. Phys.* **99**, 7907–7915 (1993).

¹¹⁰A. Balková and R. J. Bartlett, "A multireference coupled-cluster study of the ground-state and lowest excited-states of cyclobutadiene," *J. Chem. Phys.* **101**, 8972–8987 (1994).

¹¹¹P. G. Szalay and R. J. Bartlett, "Analytic energy gradients for the two-determinant coupled-cluster method with application to singlet excited states of butadiene and ozone," *J. Chem. Phys.* **101**, 4936–4944 (1994).

¹¹²J. Lutz, M. Nooijen, A. Perera, and R. J. Bartlett, "Reference dependence of the two-determinant coupled-cluster method for triplet and open-shell singlet states of biradical molecules," *J. Chem. Phys.* **148**, 164102 (2018).

¹¹³B. H. Brandow, "Linked-cluster expansions for nuclear many-body problem," *Rev. Mod. Phys.* **39**, 771 (1967).

¹¹⁴P. G. H. Sandars, "A linked diagram treatment of configuration interaction in open-shell atoms," *Adv. Chem. Phys.* **14**, 365–419 (1969).

¹¹⁵M. B. Johnson and M. Baranger, "Folded diagrams," *Ann. Phys. (N.Y.)* **62**, 172–226 (1971).

¹¹⁶T. T. S. Kuo, S. Y. Lee, and K. F. Ratcliff, "Folded-diagram expansion of model-space effective Hamiltonian," *Nucl. Phys. A* **A176**, 65–88 (1971).

¹¹⁷I. Lindgren, "Rayleigh–Schrödinger perturbation and linked-diagram theorem for a multi-configuration model space," *J. Phys. B* **7**, 2441–2470 (1974).

¹¹⁸J. O. Hirschfelder and P. R. Certain, "Degenerate RS perturbation theory," *J. Chem. Phys.* **60**, 1118–1137 (1974).

¹¹⁹J. Paldus and X.-Z. Li, "Analysis of the multireference state-universal coupled-cluster," *J. Chem. Phys.* **118**, 6769–6783 (2003).

¹²⁰X.-Z. Li and J. Paldus, "General-model-space state-universal coupled-cluster theory: Connectivity conditions and explicit equations," *J. Chem. Phys.* **119**, 5320–5333 (2003).

¹²¹X. Z. Li and J. Paldus, "The general-model-space state-universal coupled-cluster method exemplified by the LiH molecule," *J. Chem. Phys.* **119**, 5346–5357 (2003).

¹²²J. Paldus, X.-Z. Li, and N. D. K. Petracó, "General-model-space state-universal coupled-cluster method: Diagrammatic approach," *J. Math. Chem.* **35**, 215–251 (2004).

¹²³X.-Z. Li and J. Paldus, "Size extensivity of a general-model-space state-universal coupled-cluster method," *Int. J. Quantum Chem.* **99**, 914–924 (2004).

¹²⁴S. Hirata, I. Grabowski, J. V. Ortiz, and R. J. Bartlett, "Nonconvergence of the Feynman–Dyson diagrammatic perturbation expansion of propagators," *Phys. Rev. A* **109**, 052220 (2024).

¹²⁵S. Hirata, M. R. Hermes, J. Simons, and J. V. Ortiz, "General-order many-body Green's function method," *J. Chem. Theory Comput.* **11**, 1595–1606 (2015).

¹²⁶S. Hirata, A. E. Doran, P. J. Knowles, and J. V. Ortiz, "One-particle many-body Green's function theory: Algebraic recursive definitions, linked-diagram theorem, irreducible-diagram theorem, and general-order algorithms," *J. Chem. Phys.* **147**, 044108 (2017).

¹²⁷S. Hirata, "Symbolic algebra in quantum chemistry," *Theor. Chem. Acc.* **116**, 2–17 (2006).

¹²⁸S. Hirata, "Tensor Contraction Engine: Abstraction and automated parallel implementation of configuration-interaction, coupled-cluster, and many-body perturbation theories," *J. Phys. Chem. A* **107**, 9887–9897 (2003).

¹²⁹S. Hirata, "tce," <https://github.com/sohirata/tce> (2026).

¹³⁰P. J. Knowles and N. C. Handy, "A new determinant-based full configuration-interaction method," *Chem. Phys. Lett.* **111**, 315–321 (1984).

¹³¹S. Hirata, M. Nooijen, and R. J. Bartlett, "High-order determinantal equation-of-motion coupled-cluster calculations for ionized and electron-attached states," *Chem. Phys. Lett.* **328**, 459–468 (2000), the two entries of "19.794" in the rows of CI(1,1h) and IP-EOM-CC(1,1h) should correctly read "17.427".

¹³²P. J. Knowles, K. Somasundram, N. C. Handy, and K. Hirao, "The calculation of higher-order energies in the many-body perturbation theory series," *Chem. Phys. Lett.* **113**, 8–12 (1985).

¹³³S. Hirata, "Thermodynamic limit and size-consistent design," *Theor. Chem. Acc.* **129**, 727–746 (2011).

¹³⁴B. Jezierski and H. J. Monkhorst, "Coupled-cluster method for multideterminantal reference states," *Phys. Rev. A* **24**, 1668–1681 (1981).

¹³⁵I. Hubač and P. Neogrády, "Size-consistent Brillouin–Wigner perturbation theory with an exponentially parametrized wave function: Brillouin–Wigner coupled-cluster theory," *Phys. Rev. A* **50**, 4558–4564 (1994).

¹³⁶J. Mášik, I. Hubač, and P. Mach, "Single-root multireference Brillouin–Wigner coupled-cluster theory: Applicability to the F₂ molecule," *J. Chem. Phys.* **108**, 6571–6579 (1998).

¹³⁷J. Pittner, P. Nachtigall, P. Čársky, J. Mášik, and I. Hubač, "Assessment of the single-root multireference Brillouin–Wigner coupled-cluster method: Test calculations on CH, SiH, and twisted ethylene," *J. Chem. Phys.* **110**, 10275–10282 (1999).

¹³⁸J. Pittner, "Continuous transition between Brillouin–Wigner and Rayleigh–Schrödinger perturbation theory, generalized Bloch equation, and Hilbert space multireference coupled cluster," *J. Chem. Phys.* **118**, 10876–10889 (2003).

¹³⁹J. Pittner and O. Demel, "Towards the multireference Brillouin–Wigner coupled-clusters method with iterative connected triples: MR BWCCSDT- α approximation," *J. Chem. Phys.* **122**, 181101 (2005).

¹⁴⁰U. S. Mahapatra, B. Datta, B. Bandyopadhyay, and D. Mukherjee, "State-specific multi-reference coupled cluster formulations: Two paradigms," *Adv. Quantum Chem.* **30**, 163–193 (1998).

¹⁴¹U. S. Mahapatra, B. Datta, and D. Mukherjee, "Molecular applications of a size-consistent state-specific multireference perturbation theory with relaxed model-space coefficients," *J. Phys. Chem. A* **103**, 1822–1830 (1999).

¹⁴²U. S. Mahapatra, B. Datta, and D. Mukherjee, "A size-consistent state-specific multireference coupled cluster theory: Formal developments and

molecular applications," *J. Chem. Phys.* **110**, 6171–6188 (1999).

¹⁴³S. Chattopadhyay, U. S. Mahapatra, and D. Mukherjee, "Development of a linear response theory based on a state-specific multireference coupled cluster formalism," *J. Chem. Phys.* **112**, 7939–7952 (2000).

¹⁴⁴S. Chattopadhyay, D. Pahari, D. Mukherjee, and U. S. Mahapatra, "A state-specific approach to multireference coupled electron-pair approximation-like methods: Development and applications," *J. Chem. Phys.* **120**, 5968–5986 (2004).

¹⁴⁵F. A. Evangelista, W. D. Allen, and H. F. Schaefer III, "High-order excitations in state-universal and state-specific multireference coupled cluster theories: Model systems," *J. Chem. Phys.* **125**, 154113 (2006).

¹⁴⁶L. Meissner, S. A. Kucharski, and R. J. Bartlett, "A multireference coupled-cluster method for special classes of incomplete model spaces," *J. Chem. Phys.* **91**, 6187–6194 (1989).

¹⁴⁷C. Møller and M. S. Plesset, "Note on an approximation treatment for many-electron systems," *Phys. Rev.* **46**, 0618–0622 (1934).

¹⁴⁸M. Gellmann and F. Low, "Bound states in quantum field theory," *Phys. Rev.* **84**, 350–354 (1951).

¹⁴⁹K. A. Brueckner, "Many-body problem for strongly interacting particles. II. Linked cluster expansion," *Phys. Rev.* **100**, 36–45 (1955).

¹⁵⁰J. Goldstone, "Derivation of the Brueckner many-body theory," *Proc. Roy. Soc. A (London)* **239**, 267–279 (1957).

¹⁵¹N. M. Hugenholtz, "Perturbation theory of large quantum systems," *Physica* **23**, 481–532 (1957).

¹⁵²L. M. Frantz and R. L. Mills, "Many-body basis for the optical model," *Nucl. Phys.* **15**, 16–32 (1960).

¹⁵³R. Manne, "Linked-diagram expansion of ground-state of a many-electron system. Time-independent derivation," *Int. J. Quantum Chem.* **S11**, 175–192 (1977).

¹⁵⁴D. J. Klein, "Degenerate perturbation theory," *J. Chem. Phys.* **61**, 786–798 (1974).

¹⁵⁵S. Hirata, "Finite-temperature many-body perturbation theory for electrons: Algebraic recursive definitions, second-quantized derivation, linked-diagram theorem, general-order algorithms, and grand canonical and canonical ensembles," *J. Chem. Phys.* **155**, 094106 (2021).

¹⁵⁶K. W. Sattelmeyer, H. F. Schaefer III, and J. F. Stanton, "Use of 2h and 3h-p-like coupled-cluster Tamm–Dancoff approaches for the equilibrium properties of ozone," *Chem. Phys. Lett.* **378**, 42–46 (2003).

¹⁵⁷T. Kuš and A. I. Krylov, "Using the charge-stabilization technique in the double ionization potential equation-of-motion calculations with dianion references," *J. Chem. Phys.* **135**, 084109 (2011).

¹⁵⁸J. Shen and P. Piecuch, "Doubly electron-attached and doubly ionized equation-of-motion coupled-cluster methods with 4-particle-2-hole and 4-hole-2-particle excitations and their active-space extensions," *J. Chem. Phys.* **138**, 194102 (2013).

¹⁵⁹K. Gururangan, A. K. Dutta, and P. Piecuch, "Double ionization potential equation-of-motion coupled-cluster approach with full inclusion of 4-hole-2-particle excitations and three-body clusters," *J. Chem. Phys.* **162**, 061101 (2025).

¹⁶⁰M. Musiał, S. A. Kucharski, and R. J. Bartlett, "Multireference double electron attached coupled cluster method with full inclusion of the connected triple excitations: MR-DA-CCSDT," *J. Chem. Theory Comput.* **7**, 3088–3096 (2011).

¹⁶¹S. Gulania, E. F. Kjønstad, J. F. Stanton, H. Koch, and A. I. Krylov, "Equation-of-motion coupled-cluster method with double electron-attaching operators: Theory, implementation, and benchmarks," *J. Chem. Phys.* **154**, 114115 (2021).

¹⁶²A. I. Krylov, "Size-consistent wave functions for bond-breaking: The equation-of-motion spin-flip model," *Chem. Phys. Lett.* **338**, 375–384 (2001).

¹⁶³L. V. Slipchenko and A. I. Krylov, "Singlet-triplet gaps in diradicals by the spin-flip approach: A benchmark study," *J. Chem. Phys.* **117**, 4694–4708 (2002).

¹⁶⁴Manisha and P. U. Manohar, "Spin-flip equation-of-motion coupled cluster method with singles, doubles and (full) triples: Computational implementation and some pilot applications," *Phys. Chem. Chem. Phys.* **26**, 21204–21212 (2024).

¹⁶⁵J. Paldus, P. Piecuch, L. Pylypow, and B. Jezierski, "Application of Hilbert-space coupled-cluster theory to simple (H₂)₂ model systems: Planar models," *Phys. Rev. A* **47**, 2738–2782 (1993).

¹⁶⁶P. Piecuch and J. Paldus, "Application of Hilbert-space coupled-cluster theory to simple (H₂)₂ model systems. II. Nonplanar models," *Phys. Rev. A* **49**, 3479–3514 (1994).

¹⁶⁷R. J. Bartlett and E. J. Brändas, "Reduced partitioning procedure in configuration interaction studies. I. Ground states," *J. Chem. Phys.* **56**, 5467 (1972).

¹⁶⁸R. J. Bartlett and E. J. Brändas, "Reduced partitioning procedure in configuration interaction studies. II. Excited states," *J. Chem. Phys.* **59**, 2032–2042 (1973).

¹⁶⁹E. R. Davidson, "Iterative calculation of a few of lowest eigenvalues and corresponding eigenvectors of large real symmetric matrices," *J. Comput. Phys.* **17**, 87–94 (1975).

¹⁷⁰K. Hirao and H. Nakatsuji, "A generalization of the Davidson method to large nonsymmetric eigenvalue problems," *J. Comput. Phys.* **45**, 246–254 (1982).

¹⁷¹J. Linderberg and Y. Öhrn, "Improved single-particle propagators in theory of conjugated systems," *Proc. Roy. Soc. (London) A* **285**, 445 (1965).

¹⁷²L. Hedin, "New method for calculating one-particle Green's function with application to electron-gas problem," *Phys. Rev.* **139**, A796 (1965).

¹⁷³J. Linderberg and Y. Öhrn, *Propagators in Quantum Chemistry* (Academic Press, London, 1973).

¹⁷⁴B. T. Pickup and O. Goscinski, "Direct calculation of ionization energies. I. Closed shells," *Mol. Phys.* **26**, 1013–1035 (1973).

¹⁷⁵J. Paldus and J. Čížek, "Time-independent diagrammatic approach to perturbation theory of Fermion systems," *Adv. Quantum Chem.* **9**, 105–197 (1975).

¹⁷⁶L. S. Cederbaum and W. Domcke, *Adv. Chem. Phys.* **36**, 205–344 (1977).

¹⁷⁷J. Simons, "Theoretical studies of negative molecular-ions," *Annu. Rev. Phys. Chem.* **28**, 15–45 (1977).

¹⁷⁸J. Schirmer, "Beyond the random-phase approximation: A new approximation scheme for the polarization propagator," *Phys. Rev. A* **26**, 2395–2416 (1982).

¹⁷⁹Y. Öhrn and G. Born, "Molecular electron propagator theory and calculations," *Adv. Quantum Chem.* **13**, 1–88 (1981).

¹⁸⁰J. Oddershede, *Adv. Chem. Phys.* **69**, 201–239 (1987).

¹⁸¹J. V. Ortiz, "Toward an exact one-electron picture of chemical bonding," *Adv. Quantum Chem.* **35**, 33–52 (1999).

¹⁸²Y. Öhrn and J. Linderberg, "Propagators and their implications," *Mol. Phys.* **108**, 2899–2904 (2010).

¹⁸³J. V. Ortiz, "Electron propagator theory: An approach to prediction and interpretation in quantum chemistry," *WIREs Comput. Mol. Sci.* **3**, 123–142 (2013).

¹⁸⁴J. V. Ortiz, "Dyson-orbital concepts for description of electrons in molecules," *J. Chem. Phys.* **153**, 070902 (2020).

¹⁸⁵J. V. Ortiz, "Recent progress in electron-propagator, extended-Koopmans-theorem and self-consistent-field approaches to the interpretation and prediction of electron binding energies," *Adv. Quantum Chem.* **85**, 109–155 (2022).

¹⁸⁶A. Szabo and N. S. Ostlund, *Modern Quantum Chemistry* (MacMillan, New York, 1982).

¹⁸⁷R. J. Bartlett and I. Shavitt, "Comparison of high-order many-body perturbation theory and configuration interaction for H₂O," *Chem. Phys. Lett.* **50**, 190–198 (1977).

¹⁸⁸R. J. Bartlett and I. Shavitt, "Erratum: Comparison of high-order many-body perturbation theory and configuration interaction for H₂O," *Chem. Phys. Lett.* **57**, 157 (1978).

¹⁸⁹L. P. Kadanoff and G. Baym, *Quantum Statistical Mechanics* (CRC Press, Boca Raton, 2018).

¹⁹⁰D. J. Thouless, "Stability conditions and nuclear rotations in the Hartree–Fock theory," *Nucl. Phys.* **21** (1960).

¹⁹¹J. Arponen, "Variational principles and linked-cluster exp S expansions for static and dynamic many-body problems," *Ann. Phys.* **151**, 311–382 (1983).

¹⁹²S. Pal, M. D. Prasad, and D. Mukherjee, "Use of a size-consistent energy functional in many-electron theory for closed shells," *Theor. Chim. Acta* **62**, 523–536 (1983).

¹⁹³A. Haque and U. Kaldor, "Open-shell coupled-cluster method: Variational and nonvariational calculation of ionization potentials," *Int. J. Quantum Chem.* **29**, 425–433 (1986).

¹⁹⁴R. J. Bartlett and J. Noga, "The expectation value coupled-cluster method and analytical energy derivatives," *Chem. Phys. Lett.* **150**, 29–36 (1988).

¹⁹⁵W. Kutzelnigg, "Almost variational coupled cluster theory," *Mol. Phys.* **94**, 65–71 (1998).

¹⁹⁶Y. Xian, "Diagrammatic approach in the variational coupled-cluster method," *Phys. Rev. B* **72**, 224438 (2005).

¹⁹⁷B. Cooper and P. J. Knowles, "Benchmark studies of variational, unitary and extended coupled cluster methods," *J. Chem. Phys.* **133**, 234102 (2010).

¹⁹⁸J. B. Robinson and P. J. Knowles, "Approximate variational coupled cluster theory," *J. Chem. Phys.* **135**, 044113 (2011).

¹⁹⁹S. Hirata and I. Grabowski, "On the mutual exclusion of variationality and size consistency," *Theor. Chem. Acc.* **133**, 1440 (2014).

²⁰⁰J. A. Black and P. J. Knowles, "Quasi-variational coupled-cluster theory: Performance of perturbative treatments of connected triple excitations," *J. Chem. Phys.* **148**, 194102 (2018).

²⁰¹H. Nakatsuji and K. Hirao, "Cluster expansion of wavefunction. Pseudoorbital theory applied to spin correlation," *Chem. Phys. Lett.* **47**, 569–571 (1977).

²⁰²H. Nakatsuji and K. Hirao, "Cluster expansion of wavefunction. Pseudoorbital theory based on SAC expansion and its application to spin-density of open-shell systems," *J. Chem. Phys.* **68**, 4279–4291 (1978).

²⁰³C. L. Janssen and H. F. Schaefer III, "The automated solution of second quantization equations with applications to the coupled cluster approach," *Theor. Chim. Acta* **79**, 1–42 (1991).

²⁰⁴X.-Z. Li and J. Paldus, "Automation of the implementation of spin-adapted open-shell coupled-cluster theories relying on the unitary group formalism," *J. Chem. Phys.* **101**, 8812–8826 (1994).

²⁰⁵M. L. Abrams and C. D. Sherrill, "General-order single- and multi-reference configuration interaction and coupled-cluster theory: Symmetric dissociation of water," *Chem. Phys. Lett.* **404**, 284–288 (2005).

²⁰⁶D. I. Lyakh, V. V. Ivanov, and L. Adamowicz, "Automated generation of coupled-cluster diagrams: Implementation in the multireference state-specific coupled-cluster approach with the complete-active-space reference," *J. Chem. Phys.* **122**, 024108 (2005).

²⁰⁷S. Hirata, "POLYMER," <https://github.com/sohirata/polymer> (2026).

²⁰⁸P. Pulay, "Convergence acceleration of iterative sequences: The case of SCF iteration," *Chem. Phys. Lett.* **73**, 393–398 (1980).

²⁰⁹E. Aprà, E. J. Bylaska, W. A. de Jong, N. Govind, K. Kowalski, T. P. Straatsma, M. Valiev, H. J. J. van Dam, Y. Alexeev, J. Anchell, V. Anisimov, F. W. Aquino, R. Atta-Fynn, J. Autschbach, N. P. Bauman, J. C. Becca, D. E. Bernholdt, K. Bhaskaran-Nair, S. Bogatko, P. Borowski, J. Boschen, J. Brabec, A. Bruner, E. Cauet, Y. Chen, G. N. Chuev, C. J. Cramer, J. Daily, M. J. O. Deegan, T. H. Dunning, M. Dupuis, K. G. Dyall, G. I. Fann, S. A. Fischer, A. Fonari, H. Früchtli, L. Gagliardi, J. Garza, N. Gawande, S. Ghosh, K. Glaesemann, A. W. Götz, J. Hammond, V. Helms, E. D. Hermes, K. Hirao, S. Hirata, M. Jacquelin, L. Jensen, B. G. Johnson, H. Jonsson, R. A. Kendall, M. Klemm, R. Kobayashi, V. Konkov, S. Krishnamoorthy, M. Krishnan, Z. Lin, R. D. Lins, R. J. Littlefield, A. J. Logsdail, K. Lopata, W. Ma, A. V. Marenich, J. M. del Campo, D. Mejia-Rodriguez, J. E. Moore, J. M. Mullin, T. Nakajima, D. R. Nascimento, J. A. Nichols, P. J. Nichols, J. Nieplocha, A. Otero-de-la Roza, B. Palmer, A. Panyala, T. Pirojsirikul, B. Peng, R. Peverati, J. Pittner, L. Pollack, R. M. Richard, P. Sadayappan, G. C. Schatz, W. A. Shelton, D. W. Silverstein, D. M. A. Smith, T. A. Soares, D. Song, M. Swart, H. L. Taylor, G. S. Thomas, V. Tippuraj, D. G. Truhlar, K. Tsemekhman, T. Van Voorhis, A. Vázquez-Mayagoitia, P. Verma, O. Villa, A. Vishnu, *et al.*, "NWChem: Past, present, and future," *J. Chem. Phys.* **152**, 184102 (2020).

²¹⁰A. I. Krylov, "Spin-flip configuration interaction: An electronic structure model that is both variational and size-consistent," *Chem. Phys. Lett.* **350**, 522–530 (2001).

²¹¹Y. H. Shao, M. Head-Gordon, and A. I. Krylov, "The spin-flip approach within time-dependent density functional theory: Theory and applications to diradicals," *J. Chem. Phys.* **118**, 4807–4818 (2003).

²¹²J. Olsen, O. Christiansen, H. Koch, and P. Jørgensen, "Surprising cases of divergent behavior in Møller–Plesset perturbation theory," *J. Chem. Phys.* **105**, 5082–5090 (1996).

²¹³J. Vura-Weis, "Femtosecond extreme ultraviolet absorption spectroscopy of transition metal complexes," *Annu. Rev. Phys. Chem.* **76**, 455–470 (2025).

²¹⁴K. Raghavachari, G. W. Trucks, J. A. Pople, and M. Head-Gordon, "A fifth-order perturbation comparison of electron correlation theories," *Chem. Phys. Lett.* **157**, 479–483 (1989).

²¹⁵R. J. Bartlett, J. D. Watts, S. A. Kucharski, and J. Noga, "Noniterative fifth-order triple and quadruple excitation-energy corrections in correlated methods," *Chem. Phys. Lett.* **165**, 513–522 (1990).

²¹⁶S. Hirata, P. D. Fan, A. A. Auer, M. Nooijen, and P. Piecuch, "Combined coupled-cluster and many-body perturbation theories," *J. Chem. Phys.* **121**, 12197–12207 (2004).

²¹⁷G. Sanyal, S. H. Mandal, S. Guha, and D. Mukherjee, "Systematic non-perturbative approach for thermal averages in quantum many-body systems: The thermal-cluster-cumulant method," *Phys. Rev. E* **48**, 3373–3389 (1993).

²¹⁸S. H. Mandal, R. Ghosh, G. Sanyal, and D. Mukherjee, in *Recent Progress in Many-Body Theories*, edited by R. Bishop, T. Brandes, K. A. Gernoth, N. R. Walet, and Y. Xian (World Scientific, Singapore, 2002) pp. 383–392.

²¹⁹S. H. Mandal, R. Ghosh, and D. Mukherjee, "A non-perturbative cumulant expansion method for the grand partition function of quantum systems," *Chem. Phys. Lett.* **335**, 281–288 (2001).

²²⁰A. F. White and G. K.-L. Chan, "A time-dependent formulation of coupled-cluster theory for many-fermion systems at finite temperature," *J. Chem. Theory Comput.* **14**, 5690–5700 (2018).

²²¹G. Harsha, T. M. Henderson, and G. E. Scuseria, "Thermofield theory for finite-temperature quantum chemistry," *J. Chem. Phys.* **150**, 154109 (2019).

²²²G. Harsha, T. M. Henderson, and G. E. Scuseria, "Thermofield theory for finite-temperature coupled cluster," *J. Chem. Theory Comput.* **15**, 6127–6136 (2019).

²²³G. Harsha, T. M. Henderson, and G. E. Scuseria, "Thermofield theory for finite-temperature electronic structure," *J. Phys. Chem. A* **127**, 3063–3071 (2023).

²²⁴P. K. Jha and S. Hirata, "Numerical evidence invalidating finite-temperature many-body perturbation theory," *Annu. Rep. Comput. Chem.* **15**, 3–15 (2019).

²²⁵S. Hirata and P. K. Jha, "Converging finite-temperature many-body perturbation theory in the grand canonical ensemble that conserves the average number of electrons," *Annu. Rep. Comput. Chem.* **15**, 17–37 (2019).

²²⁶P. K. Jha and S. Hirata, "Finite-temperature many-body perturbation theory in the canonical ensemble," *Phys. Rev. E* **101**, 022106 (2020).

²²⁷S. Hirata and P. K. Jha, "Finite-temperature many-body perturbation theory in the grand canonical ensemble," *J. Chem. Phys.* **153**, 014103 (2020).

²²⁸S. Hirata, "Low-temperature breakdown of many-body perturbation theory for thermodynamics," *Phys. Rev. A* **103**, 012223 (2021).

²²⁹S. Hirata, "General solution to the Kohn–Luttinger nonconvergence problem," *Chem. Phys. Lett.* **800**, 139668 (2022).

²³⁰H. D. Ursell, "The evaluation of Gibbs' phase-integral for imperfect gases," *P. Camb. Philos. Soc.* **23**, 685–697 (1927).

²³¹J. E. Mayer and E. Montroll, "Molecular distribution," *J. Chem. Phys.* **9**, 2–16 (1941).

²³²S. Hirata, "New dimension in electronic structure theory: Temperature, pressure, and chemical potential," *J. Phys. Chem. Lett.* **16**, 3632–3645 (2025).